# MARINE GEOPHYSICAL AND GEOMORPHIC SURVEY OF SUBMERGED BRONZE AGE SHORELINES AND ANCHORAGE SITES AT KALAMIANOS (KORPHOS, GREECE)

By
PETER DAO, B.Sc. (HONS.)

A Thesis

Submitted to the School of Graduate Studies
in Partial Fulfillment of the Requirements
for the Degree

Master of Science

McMaster University

MASTER OF SCIENCE (2011) McMaster University
(Geology) Hamilton, Ontario

TITLE: Marine Geophysical and Geomorphic Survey of Submerged Bronze Age Shorelines and Anchorage sites at Kalamianos (Korphos, Greece)

AUTHOR: Peter Dao, B.Sc. (Hons.) (McMaster University)

SUPERVISOR: Dr. J.I. Boyce

NUMBER OF PAGES: xiii + 127

## ABSTRACT

Rapid changes in relative sea level (RSL) dramatically altered the position and configuration of the Aegean coast since it was first settled by prehistoric peoples. In the Saronic Gulf of southern Greece, differential vertical tectonic displacement of the coast has resulted in the variable uplift of some prehistoric sites and inundation of a number of ancient harbours and coastal settlements. An improved knowledge of RSL change and the paleogeography of the ancient Aegean coast are essential for predicting the location of these sites and for understanding their environmental context.

In this study, RSL changes and the paleogeography of Bronze Age coastlines were investigated at Kalamianos, a newly discovered Mycenaean (Late Helladic IIIB; ca 1300-1190 BC) coastal settlement on the western Saronic Gulf, near Korphos, Greece. The settlement's coastal context and site plan indicate its function as a port but the location its harbour was unknown. The modern coastline provides few clues as to the harbour location as the site has been partially inundated by > 6 m RSL rise since the Early Bronze Age. A detailed marine geophysical survey and geomorphological study was conducted in the inshore waters to reconstruct the coastal paleoenvironments and to identify potential anchorage. More than 400-line km of single-beam bathymetry and magnetic gradiometer data were acquired across a 10-$km^2$ area using a 200 kHz echosounder and marine tri-axial gradiometer. Underwater geological mapping and sampling of beachrock platforms was conducted by diver survey over a 2-$km^2$ shallow inshore area.

Bathymetric mapping and diver reconnaissance revealed two submerged beachrock platforms (BR-1, BR-2) paralleling the modern shoreline and a submerged promontory connecting the mainland with small island 200 m offshore. The BR-1 platform (3.5-3.7 m depth)

consisted of a well-cemented calcarenite containing abundant Late Helladic (LH; 1400-1200 BC) pottery shards (30-50%) and wood charcoal fragments. The pottery showed little reworking or bioencrustation, consistent with rapid burial in a low energy beach environment. 14C dating of the extracted charcoal yielded a 2-sigma calibrated age of ca. 1600-1400 BC, slightly older than the LH ceramics. The BR-2 platform (5.8-5.9 m depth) contained less pottery (<20%) and included well preserved fragments of Early Helladic (EH; 2700-2200 BC) jars.

The beachrock elevations and $^{14}C$ and pottery ages were used to reconstruct a sea level curve and paleogeographic maps of the EH to LH shorelines. During the initial EH phase of site occupation the mainland was connected to the island by a narrow isthmus with well-sheltered natural harbour basins to the east and west. During the subsequent Mycenaean phase, sea level had risen by about 1.5 m, inundating the promontory. The presence of abundant pottery and wood charcoal in the BR-1 beachrock indicates that shipping activity during the LH was focused at the south end of the site in a western harbour basin. This is supported by magnetic gradiometer results, which identify magnetic anomalies in the western and eastern harbour basin associated with ballast and pottery sherds in beachrock. Other linear magnetic lineaments in magnetic residual maps were interpreted as fractures infilled with high magnetic susceptibility terra rosa soils.

## ACKNOWLEDGEMENTS

This project was supported through a NSERC Discovery Grant to J. Boyce and a National Science Foundation Grant (no. 0810096) Grant to D. Pullen and T. Tartaron. Thanks to the Canadian Institute in Greece (CIG) and the Greek Ephorate of Underwater Antiquities for support of the project and assistance with field logistics.

First and foremost, I would like to personally thank my project supervisor Dr. Joe Boyce who provided me with the great opportunity to work on this project. Joe has been everything, a supervisor, a teacher, a mentor, a leader, a colleague and a friend. The journey to the completion of this project has been smooth due to his patience and guidance. Thank you!

I would also like to thank Dr. Eduard Reinhardt, Dr. William Morris and Dr. Hernan Ugalde. I really appreciate Ed and Bill for lending me the use of their equipment and lab space for beachrock analysis. I am also grateful to Hernan for answering geophysics related questions I had when I was having difficulty with my data.

A thanks to my friends and colleagues Lisa Sonnenburg, Andrew Brennan and Nicole Fallon in the Environmental and Archaeological Geophysics Lab at McMaster University for the great times and jokes we shared to pass some of the more dreary days working in the office.

A special thanks to my mother, for her love and support for me and my interests in the Earth Sciences. I truly would have not been able to come so far without her support.

I have learned numerous things and matured greatly as an academic and as a person during the duration of this project. The time spent in graduate studies has been fun and enjoyable and I will surely miss these times when I look back on them in the future. It has been an inspiring and memorable experience and I have changed for the better. I thank everyone who has shared time with me in Greece and McMaster for making it a wonderful journey.

# TABLE OF CONTENTS

ABSTRACT.....iv

ACKNOWLEDGEMENTS.....vi

TABLE OF CONTENTS.....vii

LIST OF FIGURES.....viii

LIST OF TABLES.....xii

PREFACE.....xiii

Chapter 1: INTRODUCTION

1.1. Background.....1
1.2. Objectives.....5
1.3. Study Site.....7
1.4. Methods.....14
1.5. Shoreline Reconstruction.....17
1.6. References.....20

Chapter 2: RECONSTRUCTION OF BRONZE-AGE (MYCENAEAN) COASTAL ENVIRONMENTS AND ANCHORAGE SITES AT KALAMIANOS (KORPHOS, GREECE)

Abstract.....27
2.1. Introduction.....29
2.2. Study Area.....35
2.3. Methods.....40
2.4. Results.....43
2.5. Discussion.....56

2.6. Summary.....65
2.7. References.....65

Chapter 3: TRI-AXIAL GRADIOMETER SURVEY OF A BRONZE AGE ANCHORAGE AT KALAMIANOS (KORPHOS, GREECE)

Abstract.....78
3.1. Introduction.....79
3.2. Study Area and Archaeology.....81
3.3. Methods.....85
3.4. Results.....92
3.5. Discussion.....99
3.6. Summary.....114
3.7. References.....115

Chapter 4: CONCLUSIONS

4.1. Research Findings and Archaeological Implications.....121
4.2. Improvements to Geophysical Survey Methods.....123
4.3 Future Work.....124

# LIST OF FIGURES

## Chapter 1:

**Figure 1.1:** Predicted eustatic sea level (ESL) and glacio-hydro-eustatic relative sea level (RSL) curves for the Greek Peloponnesus compared with observed sea levels from four sites in the Aegean (modified from Lambeck, 2002; Lambeck and Purcell, 2005). Archaeological time periods also shown. Note > 2 m difference in two curves due to glacio-hydrostatic component of SL rise. During the Early to Late Neolithic (ca. 10-6 ka BP) sea levels rose rapidly (10-12 mmyr$^{-1}$) more than 45 m, inundating shallow shelf areas. By the Chalcolithic and Bronze Age period (ca. 5.5-3.2 ka BP) sea level rise had decelerated (< 5 mm yr$^{-1}$) but levels rose a further 2.5 to 3 m completely or partially inundating prehistoric coastal settlements (e.g. Pavlo Petri, Argolid Gulf; Kraft et al., 1978).....3

**Figure 1.2:** Predicted relative sea level (RSL) in the Aegean at A) 10 ka BP, B) 6 ka BP and C) 2 ka BP (modified from Lambeck, 1996). RSL decelerated rapidly after 6-7 ka BP due the end of glacial melting and stabilization in ice volumes. Continued glacio-hydrostatic adjustment of the lithosphere resulted in a further 4-5 m rise in SL between 6-2 ka BP and transgression of the coastline across much of the Aegean during the mid- to late Holocene.....4

**Figure 1.3:** A) Study area location (Korphos-Kalamianos region) in the western Saronic Gulf showing location of regional fault systems (modified from Nixon et al. 2009). B) Combined digital elevation model and digital bathymetric model of the Korphos study area.....6

**Figure 1.4:** A) Satellite photograph of Korphos study area on the western Saronic Gulf (modified from Google Earth Ltd., 2010). B) Aerial photograph of Kalamianos taken by kite-mounted camera (courtesy T. Tartaron). Note partially submerged architectural features on modern shoreline and submerged beach rock platforms in the shallow inshore area.....9

**Figure 1.5:** A) Architectural features mapped during survey of Kalamianos landsite by the Saronic Harbours Archaeological Project (SHARP) 2009-2011 (Tartaron et al., *In Press*). B) Well preserved wall and foundation structures at Kalamianos showing 'cyclopean' masonry style typical of the Mycenaean palatial period. Scale stick is 1 m in height.....12

**Figure 1.6:** Comparison of relative sea level (RSL) curve for Korphos Bay (after Nixon et al., 2009) with predicted glacio-hydro-eustatic curve for Aegean (from Lambeck and Purcell, 2005). Korphos RSL envelope (grey shaded) is derived from elevation and probability distributions of calibrated radiocarbon dates on salt marsh deposits. Note all points (with the exception of one) lie within < 1 m of the predicted Aegean RSL curve. Several transgression events (T1-T5) were interpreted by Nixon et al. (2009) based on the marsh sediment and corresponding record from tidal notches from Korphos Bay.....13

**Figure 1.7:** A) Survey boat (6 m zodiac) and geophysical equipment in water. B) Catamaran with Trimble RTK 4600 D-GPS receiver and Knudsen 200 kHz echosounder. C) Catamaran equipped with Humminbird 200 kHz echosounder system. (D) SeaQuest$^{TM}$ tri-axial magnetic gradiometer. E) Schematic of SeaQuest$^{TM}$ tri-axial gradiometer platform.....15

**Figure 1.8:** A) Typical dipole anomaly in total magnetic intensity data. B) Analytic signal transform of dipole anomaly. Note dipole collapses to a single peak over located over source body.....18

**Chapter 2:**

**Figure 2.1.** Predicted relative sea level (RSL) in the Aegean at A) 10 ka BP, B) 6 ka BP and C) 2 ka BP (modified from Lambeck, 1996). RSL decelerated rapidly after 6-7 ka BP due the end of glacial melting and stabilization in ice volumes. Continued glacio-hydrostatic adjustment of the lithosphere resulted in a further 4-5 m rise in SL between 6-2 ka BP and transgression of the coastline.....31

**Figure 2.2.** Predicted eustatic sea level (ESL) and glacio-hydro-eustatic relative sea level (RSL) curves for the Greek Peloponnesus compared with observed sea levels from four sites in the Aegean (modified from Lambeck, 2002; Lambeck and Purcell, 2005). Archaeological time periods also shown. Note > 2 m difference in two curves due to glacio-hydrostatic component of SL rise. During the Early to Late Neolithic (ca. 10-6 ka BP) sea levels rose rapidly (10-12 $mmyr^{-1}$) more than 45 m, inundating shallow shelf areas. By the Chalcolithic and Bronze Age period (ca. 5.5-3.2 ka BP) sea level rise had decelerated (< 5 mm yr-1) but levels rose a further 2.5 to 3 m completely or partially inundating prehistoric coastal settlements (e.g. Pavlo Petri, Argolid Gulf; Kraft et al., 1978).....32

**Figure 2.3:** A. Location of study area in the western Saronic Gulf showing mapped regional fault structures, modified from Nixon et al. (2009). B. Digital elevation model showing location of Kalamianos near Korphos, Greece.....34

**Figure 2.4:** Aerial photograph of Kalamianos taken by kite-mounted camera showing Mycenaean settlement (courtesy T. Tartaron). Note partially submerged architectural features on modern shoreline and submerged beach rock platforms in the shallow inshore area.....36

**Figure 2.5:** Mycenaean architectural features mapped at Kalamianos by Saronic Harbours Archaeological Project (from Tartaron et al., in press). Note some partially inundated architectural features on shoreline at southern end of site.....38

**Figure 2.6:** Survey area showing 200 kHz bathymetry survey track lines. Detailed survey over harbour basin (2-5 m line spacing) conducted with swimmer propelled catamaran.....41

**Figure 2.7:** A. Equipment setup for regional bathymetric survey. B. Setup for high resolution shallow water bathymetric surveying swimmer propelled catamaran.....42

**Figure 2.8:** Regional colour-shaded digital bathymetry map at Kalamianos. Submerged isthmus identified southeast of Kalamianos. Note extension of normal faults visible in aerial photograph in bathymetric data.....44

**Figure 2.9A:** Colour-shaded digital bathymetry map of the inshore area south of Kalamianos showing locations of beach rock ridges (BR-1, BR-2) potential harbour basins.....46

**Figure 2.9B:** Bathymetric model showing reconstructed paleoshoreline configuration during Mycenaean occupation (Late Helladic; 1300-1190 BC).....47

**Figure 2.9C:** Bathymetric model showing paleoshoreline configuration during Early Helladic (3100-2150 BC) occupation at Kalamianos.....48

**Figure 2.10:** A 2.5-D colour-shaded digital bathymetric model of the inshore area at Kalamianos showing inundated promontory and potential anchorage sites during Late Helladic and Early Helladic lower phases of relative sea-level.....49

**Figure 2.11:** Underwater photographs of A) of beachrock platform BR-1 at 3.7-4.5 m water depth. B) Beachrock platform BR-2 at 5.8 m water depth. C) Mycenaean jug handle embedded and extracted from BR-1 beachrock. D) Charcoal fragments embedded within BR-1 beachrock.....51

**Figure 2.12:** Underwater photographs of A) beachrock platform BR-2 in 5.8 m water depth. B) Well-preserved Early Helladic bowl fragment cemented in BR-2 beachrock.....52

**Figure 2.13:** Underwater photograph of small ballast deposit consisting of limestone and andesitic cobbles and boulders.....53

**Figure 2.14:** Sea-level curve for Korphos Bay from Nixon et al. (2009) with beachrock sea-level indicator from this study for comparison. Beachrock elevations lie well below the predicted RSL curve (Lambeck and Purcell, 2005) indicating active tectonic subsidence of the coastline at Kalamianos since the Early Helladic occupation.....55

**Figure 2.15:** A) Steeply dipping fault scarp defining northeastern hanging wall block of normal fault to northeast of Kalamianos. B) Slickenside striations on fault plane pitching 83. , indicating oblique slip motions.....57

**Figure 2.16:** Aerial photo of the Korphos-Kalamianos region with inferred faults based on topographic lineaments.....58

**Chapter 3:**

**Figure 3.1:** A) Location of Kalamianos in north-eastern Peloponnesus with mapped regional faults, modified from Nixon et al. (2009). B) Contoured topographic map of the Korphos-Kalamianos region (contour interval 20m)….....83

**Figure 3.2:** Colour-shaded digital bathymetric map of the coastal region adjacent to Kalamianos. Contours at 3.7 m and 5.8 m below modern sea level show paleoshoreline configuration during the Mycenaean (Late Helladic; ca. 1300-1190 BC) and Early Helladic (ca. 3100-2150 BC) occupation respectively.....86

**Figure 3.3:** Survey area showing magnetic gradient survey track lines.....87

**Figure 3.4:** A) Survey boat and equipment configuration. B) Schematic of the SeaQuest$^{TM}$ magnetic gradiometer system. Total magnetic fields are measured by 4 Overhauser sensors and gradients calculated along three axes.....88

**Figure 3.5:** Colour-shaded total magnetic intensity map obtained with single sensor. Northwest-southeast and west-east linear magnetic anomalies are interpreted as fault planes and fracture zones. Note southeastward extension of normal faults into small embayment to east of Kalamianos.....93

**Figure 3.6A:** Colour-shaded horizontal (x) magnetic gradient map.....94

**Figure 3.6B:** Colour-shaded longitudinal (y) magnetic gradient map.....95

**Figure 3.6C:** Colour-shaded vertical (z) magnetic gradient.....96

**Figure 3.7:** Colour-shaded analytic signal (total gradient) map. Note clustering of magnetic anomalies in shallow embayments to south of Kalamianos landsite. Magnetic anomaly around fish farm is due to ferrometallic debris and dock infrastructure.....97

**Figure 3.8A:** Semi-transparent overlay of the analytic signal map on the digital bathymetry model of the inshore harbour basin at Kalamianos. Location of the Early Helladic paleoshoreline (5.8 m) and Late Helladic paleoshoreline (3.7 m) also shown. The submerged promontory connecting the island to mainland was emergent during the Early Helladic period, providing two well-sheltered anchorage areas.....102

**Figure 3.8B:** Colour-shaded residual magnetic intensity map of the harbour area. Note west-east magnetic lineaments indicating presence of fractures in limestone bedrock underlying harbour areas. Isolated dipole anomalies are likely the result of ballast mounds.....103

**Figure 3.8C:** Map showing interpreted magnetic lineaments.....104

**Figure 3.8D:** 1) Conceptual model for formation of beachrock and fracture system at Kalamianos. During phase of lowered sea level (-5.8 m) solutionally widened fractures (grikes)

are sub-aerially exposed and infilled with high magnetic susceptibility terra rosa soil. 2) During subsequent shoreline transgression, infilled grikes are inundated and beachrock and marine sediments are deposited over submerged terrestrial surface. Infilled grikes have a much greater magnetic susceptibility than the surrounding bedrock and are responsible for observed west-east magnetic lineaments in Figure 3.8B. .....105

**Figure 3.9:** Bathymetry and magnetic profiles across inshore area (location on Fig. 3.8B). A) Water depth. B) Total magnetic intensity. C) Vertical gradient. D) Analytic signal. High-frequency magnetic anomalies in C and D are related to local concentrations of pottery and ballast materials. .....106

**Figure 3.10:** A) Solutionally-widened fracture (grike) on shoreline at Kalamianos. B) Terra rosa soil and limestone breccia, formed by collapse in filling of fractures. C) Terra rosa soil with brecciated clast in 1 m wide grike.....108

**Figure 3.11:** GM-SYS forward magnetic model showing hypothetical total field anomaly generated by various cultural materials (ballast, pottery rich beachrock).....109

**Figure 3.12:** Underwater photographs showing A) Beachrock platform BR-1 at 3.7-4.5 m water depth. B) Mycenaean pottery sherds extracted from BR-1 beachrock samples. C) Small ballast deposit containing limestone and andesite cobbles.....111

## LIST OF TABLES

### Chapter 3:

**Table 3.1:** Results of volume magnetic susceptibility measurements of beachrock, ballast stones, pottery and limestone bedrock.....100

## PREFACE

Chapter 2 and 3 of this thesis have been prepared for publication in various academic journals. As per McMaster University regulations, the following section outlines what work was performed by the author and the contributions of the co-authors.

Chapter 2, **Reconstruction of Bronze-age (Mycenaean) coastal environments and anchorage sites at Kalamianos (Korphos, Greece),** will be submitted in condensed form to the *Journal of Archaeological Science*. The author was involved in all data collection, processing and interpretation. Co-author, Dr. J.I. Boyce, provided funding through a NSERC Discovery Grant, assisted in data collection, processing, interpretation and provided leadership and critical review of the manuscript in the role of M.Sc. supervisor. Co-author, D. Koutsoumba, provided support for the project and assistance in data collection and field logistics. Co-author, Dr. D. Pullen and Dr. T. Tartaron, provided funding through National Science Foundation Grant (no. 0810096). Co-author, Dr. R. Rothaus, provided assistance in field logistics and data collection.

Chapter 3, **Tri-Axial Gradiometer Survey of Bronze Age Anchorage at Kalamianos (Korphos, Greece)**, will be submitted to the *Journal of Archaeological Science*. The author was involved in all data collection, processing and interpretation. Co-author, Dr. J.I. Boyce, provided funding through a NSERC Discovery Grant, assisted in data collection, processing, interpretation and provided leadership and critical review of the manuscript in the role of M.Sc. supervisor. Co-author, D. Koutsoumba, provided support for the project and assistance in data collection and field logistics. Co-author, Dr. D. Pullen and Dr. T. Tartaron, provided funding through National Science Foundation Grant (no. 0810096).

# CHAPTER 1: INTRODUCTION

## 1.1 Background

Post-glacial relative sea level (RSL) change has dramatically altered the paleogeography of coastlines worldwide (Lambeck, 1996; Flemming, 1999; Lambeck and Purcell 2005). At the end of the last glacial maximum (ca. 25-18 ka BP) global sea levels were more than 120 m below present and large areas of the world's continental shelves were exposed terrestrial landscapes (Flemming, 1999). As the continental ice retreated sea levels rose rapidly (15-20 $mmyr^{-1}$) between 16-8 ka BP, as a result of glacial meltwater inputs to the oceans (Lambeck and Purcell, 2005). The eustatic component of sea level rise decelerated rapidly after 7 ka BP and sea level recovery continued at a much-reduced rate during the Mid- to Late Holocene (Lambeck, 1996; Lambeck and Purcell, 2005). In many shallow shelf regions postglacial shorelines transgressed rapidly at rates of up to 1 $kmyr^{-1}$, inundating large tracts of coastal terrestrial environments. These 'drowned' coastal landscapes were inhabited by prehistoric peoples and are now a major focus of archaeological exploration, as they preserve an important record of prehistoric human settlement and cultural development (Flemming, 1999; Fedje and Christensen, 1999; Bailey and Flemming, 2008). Growing archaeological interest in drowned landscapes has also been a major stimulus for the study of coastal paleoenvironments and changes in the configuration of paleoshorelines by geoarchaeologists (e.g. O'Shea et al., 2009; Sonnenburg et al., 2011; Sonnenburg et al., In Review). Much recent work has focussed on the exploration of Late Pleistocene drowned shorelines for Palaeolithic and Mesolithic sites (Fischer, 2004; Gron and Skarup, 2004) but there has been a growing recognition that Holocene RSL change had a major impact on Neolithic and Bronze age cultures (Rothaus et al., 2008; Nixon et al., 2009).

In the archaeologically-rich Aegean region, sea levels rose more than 40 m during the Neolithic and Chalcolithic-Bronze Age periods (10-3.2 ka BP)(Fig. 1.1), inundating and dramatically altering the configuration of the coastline (Lambeck, 1996). Submerged or partially inundated prehistoric sites have been documented at a number of coastal and underwater prehistoric sites around the Aegean. These include Neolithic Early Bronze Age sites in Antiparos (Morrison, 1968) at Pavlopetri in Laconia (Harding et al., 1969; Mahon et al., 2011; Henderson et al., in press) and a number of Neolithic and Bronze Age sites on the Attic coast and Cycladic Islands as summarized by Baika (2008). These submerged sites accord with numerical sea-level models and paleogeographic maps (Fig. 1.2), which predict that shallow shelf areas and embayments became flooded and many coastal headlands formed during the maximum lowstand (e.g. Cycladic peninsula; van Andel and Shackleton, 1982) became detached from the mainland forming new islands during the Neolithic period (Lambeck, 1996; Lambeck and Purcell, 2005). Changes in shoreline positions during the Chalcolithic/Bronze Age period were less extensive (Fig. 1.2) but would have been an important environmental determinant in the choice of settlement and harbour locations (Tartaron et al., 2006).

Changes in RSL have important implications for understanding the archaeological record of coastal prehistoric sites in the Aegean. Rapid RSL rise during the early Holocene was likely a major environmental determinant for Neolithic peoples (ca. 10-8 ka BP), as Early Holocene shorelines transgressed rapidly (Fig. 1.2) submerging coastal habitats within the span of a few generations. Changes in the coastline following 6 Ka BP were less dramatic but were significant, as many Bronze-age prehistoric harbour sites and settlements were inundated by gradually rising sea levels (Lambeck, 1996; Marriner and Morhange, 2007; Baika, 2008). An important archaeological implication is that the modern configuration of the coast (e.g. pattern of bays and

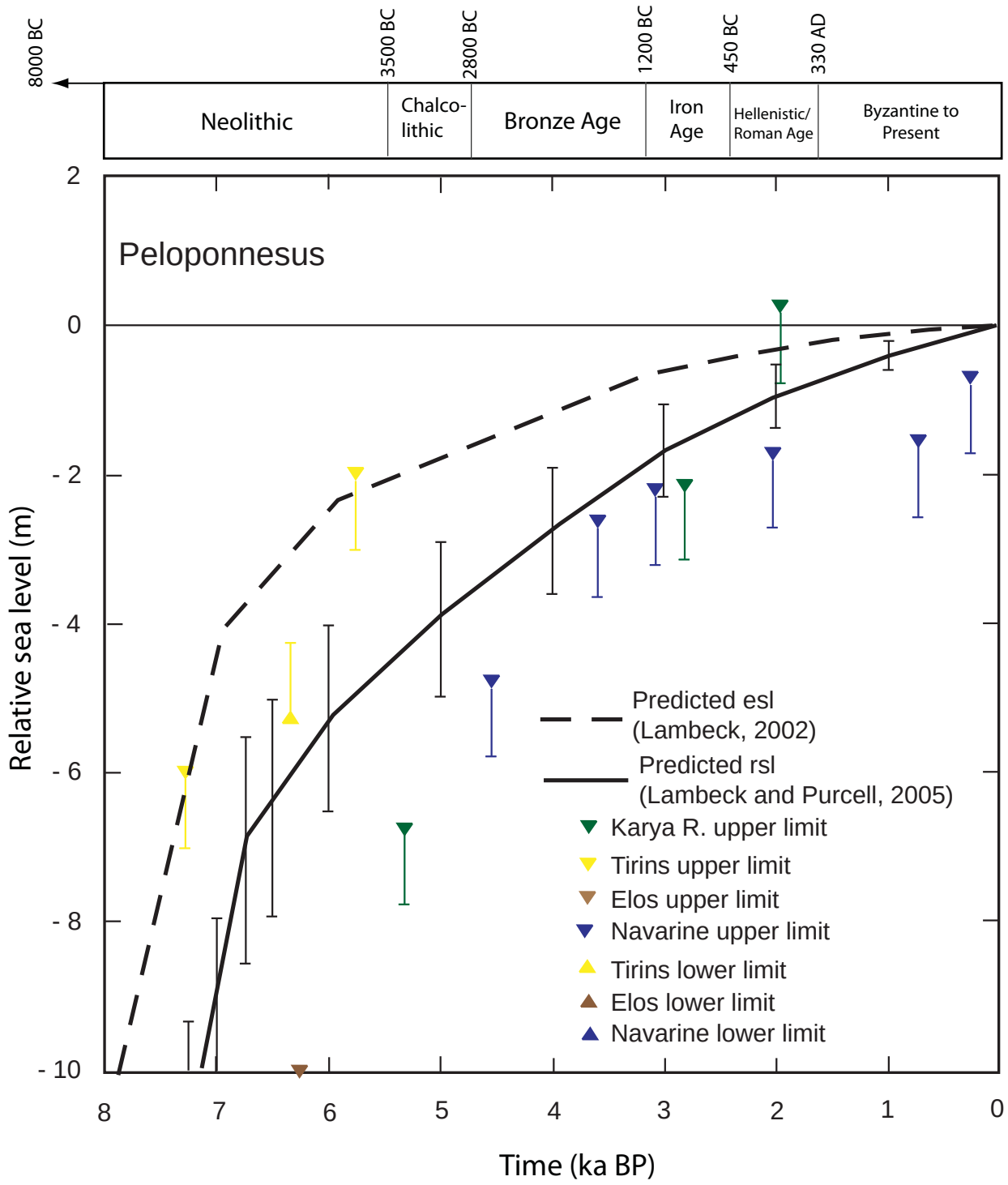


Figure 1.1: Predicted eustatic sea level (ESL) and glacio-hydro-eustatic relative sea level (RSL) curves for the Greek Peloponnesus compared with observed sea levels from four sites in the Aegean (modified from Lambeck, 2002; Lambeck and Purcell, 2005). Archaeological time periods also shown. Note > 2 m difference in two curves due to glacio-hydrostatic component of SL rise. During the Early to Late Neolithic (ca. 10-6 ka BP) sea levels rose rapidly (10-12 mmyr-1) more than 45 m, inundating shallow shelf areas. By the Chalcolithic and Bronze Age period (ca. 5.5-3.2 ka BP) sea level rise had decelerated (< 5 mm yr-1) but levels rose a further 2.5 to 3 m completely or partially inundating prehistoric coastal settlements (e.g. Pavlo Petri, Argolid Gulf; Kraft et al., 1978).

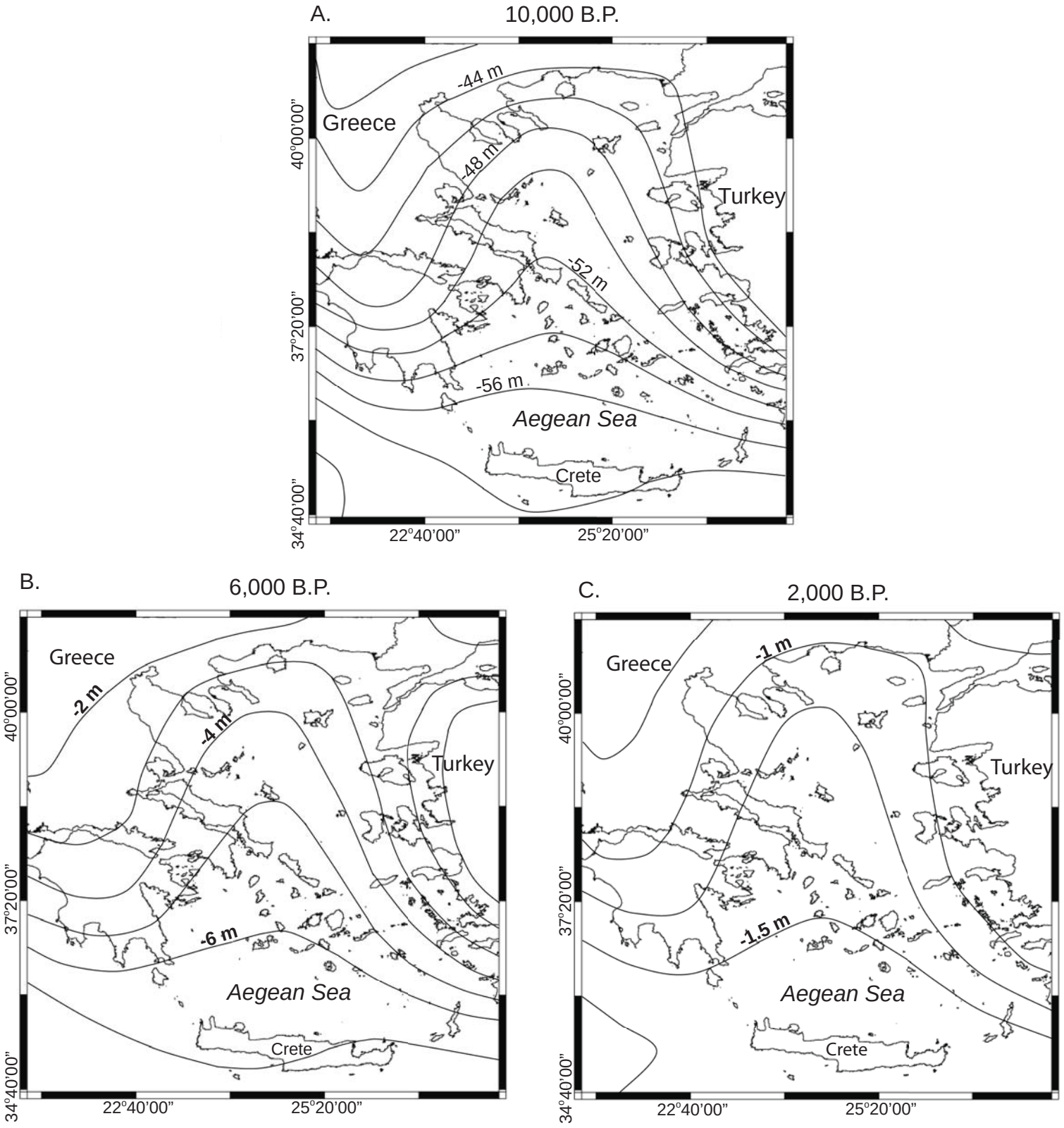


Figure 1.2: Predicted relative sea level (RSL) in the Aegean at A) 10 ka BP, B) 6 ka BP and C) 2 ka BP (modified from Lambeck, 1996). RSL decelerated rapidly after 6-7 ka BP due the end of glacial melting and stabilization in ice volumes. Continued glacio-hydrostatic adjustment of the lithosphere resulted in a further 4-5 m rise in SL between 6-2 ka BP and transgression of the coastline across much of the Aegean during the mid- to late Holocene.

headlands) could be quite different from the prehistoric shoreline, and is likely a poor predictor of the location of coastal settlements and harbour basins. Geographical and geomorphological data for modern coasts must therefore be used with caution in predictive mapping studies (e.g. Tartaron et al., 2003).

Knowledge of past RSL changes and the configuration (geometry) of ancient coastlines are critical to the study of prehistoric settlements and the exploration for new underwater archaeological sites. The available paleogeographic maps for the Aegean (e.g. Lambeck, 1996) are useful for large regional-scale studies but are insufficiently detailed for reconstruction of ancient coastlines at local to site-scales. The purpose of this thesis is to document RSL changes and the configuration of prehistoric shorelines at Kalamianos, a newly discovered Bronze Age coastal settlement located on the western Saronic Gulf in Greece (Fig. 1.3). Kalamianios was first occupied during the Late Neolithic to Early Helladic period and may have played and important role as a Mycenaean harbour or possibly a naval base during the Late Bronze period (Tartaron et al., in press). As a result of Holocene transgression, the settlement has been partially-inundated and the location of the harbour basin was unknown prior to this study. A major objective was to reconstruct the configuration of the Bronze Age coast during the Helladic settlement to main Mycenaean phase of occupation and to locate potential harbour basins and anchorages sites.

### 1.2. Objectives

The overall objective of this study was to document changes in the configuration of Bronze Age shorelines and coastal environments at Kalamianos using geophysical and geomorphological data acquired during a detailed marine survey conducted in 2009. The survey included

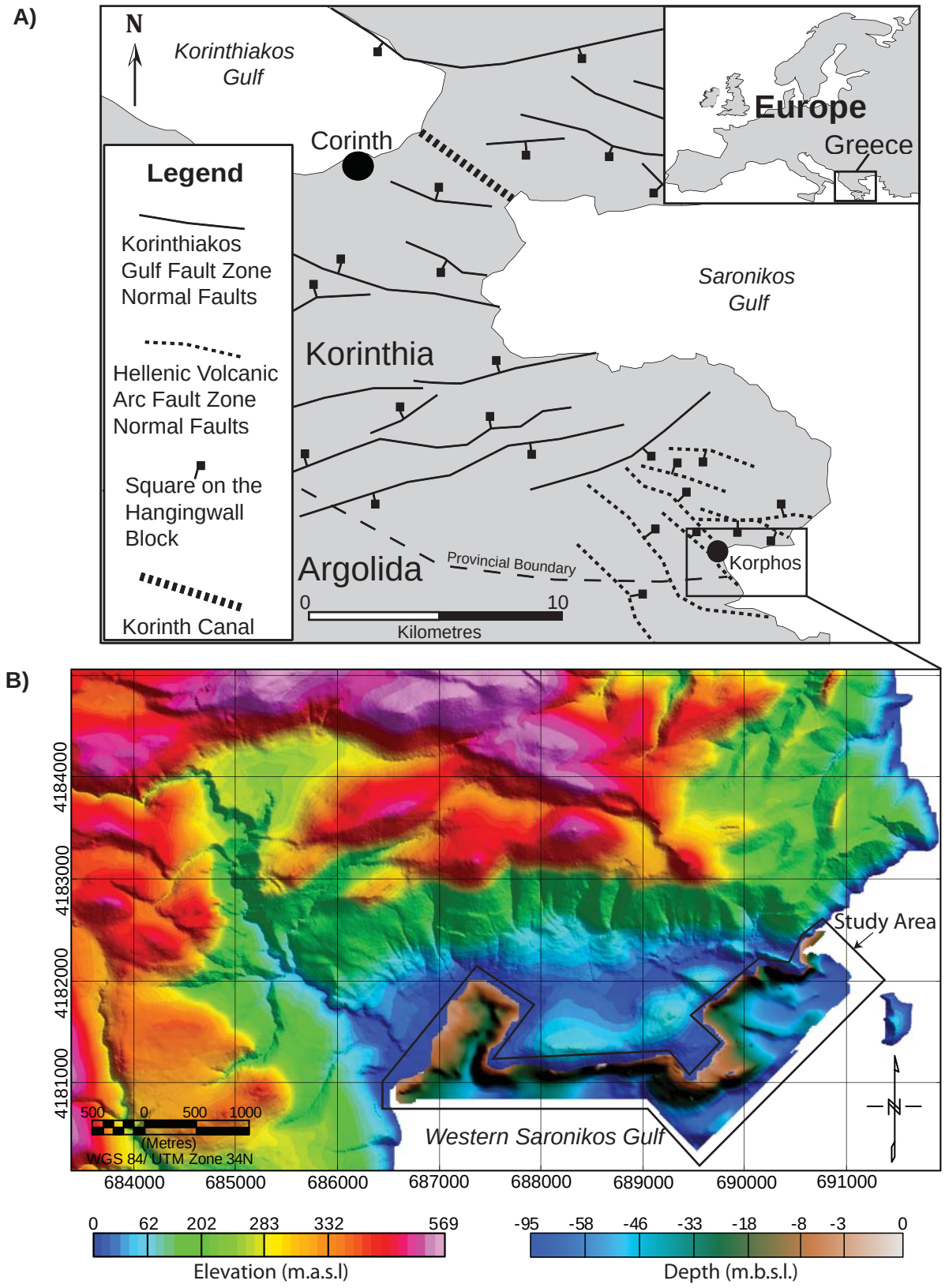


Figure 1.3: A) Study area location (Korphos-Kalamianos region) in the western Saronic Gulf showing location of regional fault systems (modified from Nixon et al. 2009). B) Combined digital elevation model and digital bathymetric model of the Korphos study area.

bathymetric and diver surveys across a 10-km$^2$ area of the inshore waters to the south of the land archaeological site with the purpose of mapping submerged shorelines and cultural features. The specific objectives of the thesis were to:

1) to map the position of the Early to Late Bronze shoreline, including the location of submerged beachrock ridges and other geomorphic features that can be used to reconstruct the former coastline,
2) to identify the location of potential harbour basins and anchorage sites using geomorphic an geophysical data,
3) to investigate the potential for buried architectural features and to evaluate the use of magnetic gradiometry for mapping pottery and ballast materials in the harbour sediments,
4) to inventory and ground-truth all geomorphic and archaeological features identified in geophysical data through systematic diver searches of the seabed.

The results of are presented as two separate papers that have been prepared for publication in the Journal of Archaeological Sciences. The first paper (Chapter 2) reports on the mapping of Bronze Age shorelines and anchorages sites using detailed bathymetric survey data and geomorphic analysis of beachrock ridges. The second paper (Chapter 3) reports on the results of a magnetic gradiometer survey and its application to mapping of anchorage sites and delineation of fault and fracture systems at Kalamianos.

## 1.3. Study Site

### 1.3.1. Physical and Geologic Setting

Kalamianos is located approximately 2.5 km southeast of the modern town of Korphos on the western Saronic Gulf of the Greek Peloponnesus (Fig. 1.4). The site is located on a small promontory that projects southward from a narrow coastal plain on the north shore of Korphos Bay. The coastal plain is backed by rugged hills and mountains of southeastern Korinthia (Fig. 1.3). The bedrock below the study area consists of Mesozoic-age fossiliferous limestone (Clift and Robertson, 1990) that strikes 260° westward and dips northward at 20-25° degrees. The bedrock surface is highly weathered and overlain locally by colluvium eroded from the surrounding slopes and terra rosa soils. The terra rosa soil is very thin (< 10-20 cm) or absent over much of the archaeological site, and in many places the Late Bronze foundations have been exposed, indicating widespread denudation of soil across the site (Tartaron et al., in press). The exposed bedrock surfaces are heavily fractured with extensive development of karst features (e.g. rillenkaren, solution pits) on limestone surfaces. In many places fractures have been widened by dissolution forming grikes and are either open or infilled by a collapse breccia consisting of sparry calcite. The collapse breccia is intermixed in many locations with red terra rosa soil, which has been interpreted as evidence for cave ceiling collapse (Tartaron et al., in press). The bedrock fractures are host to a bedrock aquifer system with artesian springs, which discharge groundwater to fractures onsite and as submarine springs in the shallow inshore area along the coastline (Collins and Dunn, 2008). The groundwater have low total dissolved solids and excellent water quality and would have provided an attractive freshwater resource for the prehistoric settlement at Kalamianos.

The study area lies within the northern Peloponnesus, an area of active seismicity and neotectonics. The study area has been subjected to normal and right-lateral oblique slip faulting resulting from north-south crustal extension and the retreat of Hellenic Arc Trench (Armijo et al.,

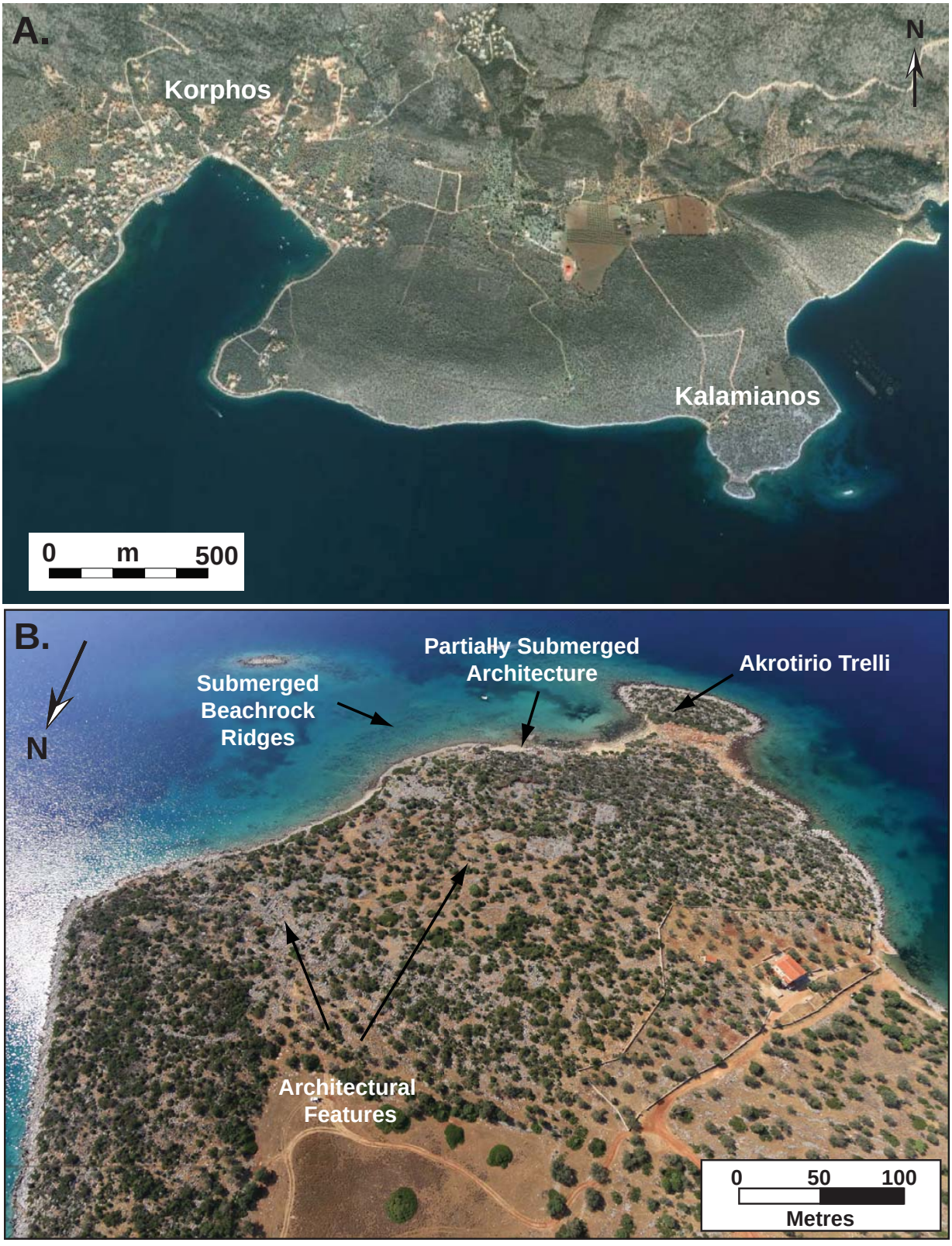


Figure 1.4: A) Satellite photograph of Korphos study area on the western Saronic Gulf (modified from Google Earth Ltd., 2010). B) Aerial photograph of Kalamianos taken by kite-mounted camera (courtesy T. Tartaron). Note partially submerged architectural features on modern shoreline and submerged beach rock platforms in the shallow inshore area.

1996; Burchfiel et al., 2003). The Korphos-Kalamianos region lies within a graben-horst system lying to the southeast of the Corinth Rift zone (Fig. 1.3A). The coastline in Korphos Bay is cut by several northwest-southeast trending normal faults, which have been subject to differential fault motions during the Holocene. , Kalamianos is located on a footwall block, that has experienced recent (post-Bronze Age) near vertical movement that has dropped the block several metres relative to the hanging wall block to the northeast (Tartaron et al., in press). Evidence for the fault displacement can be observed in submerged beachrock horizons and a well-developed normal fault scarp 400 m northeast of the archaeological site. The fault is marked by a well-defined scarp which striking 116° and dipping 76-80° to the southwest. As a result of the north-dipping limestone beds and northwest-southeast fault-fracture pattern, the south slope of Kalamianos has natural stair-step topography.

The coastline of Korphos Bay has a rugged rocky shoreline that terminates in low coastal bluffs or promontories separated by a number of small embayments that contain small gravelly or sandy beaches. The shelf area around the bay is generally narrow, dropping off very rapidly to more than 100 m water depth within a few hundred metres of the shoreline. The inshore area to the south of the archaeological site has low bathymetric relief, is shallow (<5-10 m depth) and gently slopes seaward until a steep drop-off into deeper waters (>70 m depth) within 100-250 m from the modern shoreline. The Mesozoic limestone bedrock crops out extensively along the modern shoreline and is overlain by a variable thickness of marine sediments and locally, a well-cemented calcarenite beachrock unit. The beachrock crop out in several flat-topped platforms at that extend 50-60 m seaward from the modern shoreline. The beachrock contains abundant Mycenaean and Early Bronze pottery and records at least two phases of lower sea levels at Kalamianos that were documented in this study.

### 1.3.2. Site Archaeology

Kalamianos was first discovered in 2001 during a regional archaeological survey conducted as part of the Eastern Korinthia Archaeological Survey (EKAS)(Tartaron et al., 2006). A systematic archaeological inventory of the site was conducted between 2009-2011 by an American team in collaboration with the Greek Ephorate of Prehistoric and Classical Antiquities (Saronic Harbours Research Project – SHARP) (Tartaron et al., in press). The site is unique because the foundations and walls have been exposed by soil erosion, which has allowed for the detailed documentation of the layout of the settlement without the need for excavation. A detailed archaeological inventory conducted by SHARP revealed the remains of 50 buildings and 120 rooms, including monumental architecture belonging to the Mycenaean Palatial Period (Fig. 1.5) (Tartaron et al., in press). Based on pottery evidence, the architectural remains date from the Late Helladic (LH) IIIB period (ca. 1300-1190 B.C.), indicating the site was occupied prior to the construction of the Mycenaean settlement. The sites coastal context and its proximity to Mycenae suggest its role as the primary harbour for the ancient capital on the Saronic Gulf (Tartaron et al., in press).

### 1.3.3. Sea Level History

The RSL history of the Korphos region was recently examined by Nixon et al. (2009) using tidal notches and dating of transgressive salt marsh deposits. Figure 1.6 shows the RSL curve developed by Nixon et al. (2009) compared with the glacio-hydro-isostatic and eustatic RSL model of Lambeck and Purcell (2005). The RSL curve for Korphos Bay indicates > 5 m of RSL rise since 6 ka BP. The differences between the RSL derived for Korphos bay and the glacio-hydro eustatic sea level model of Lambeck and Purcell (2005) were attributed to punctuated co-

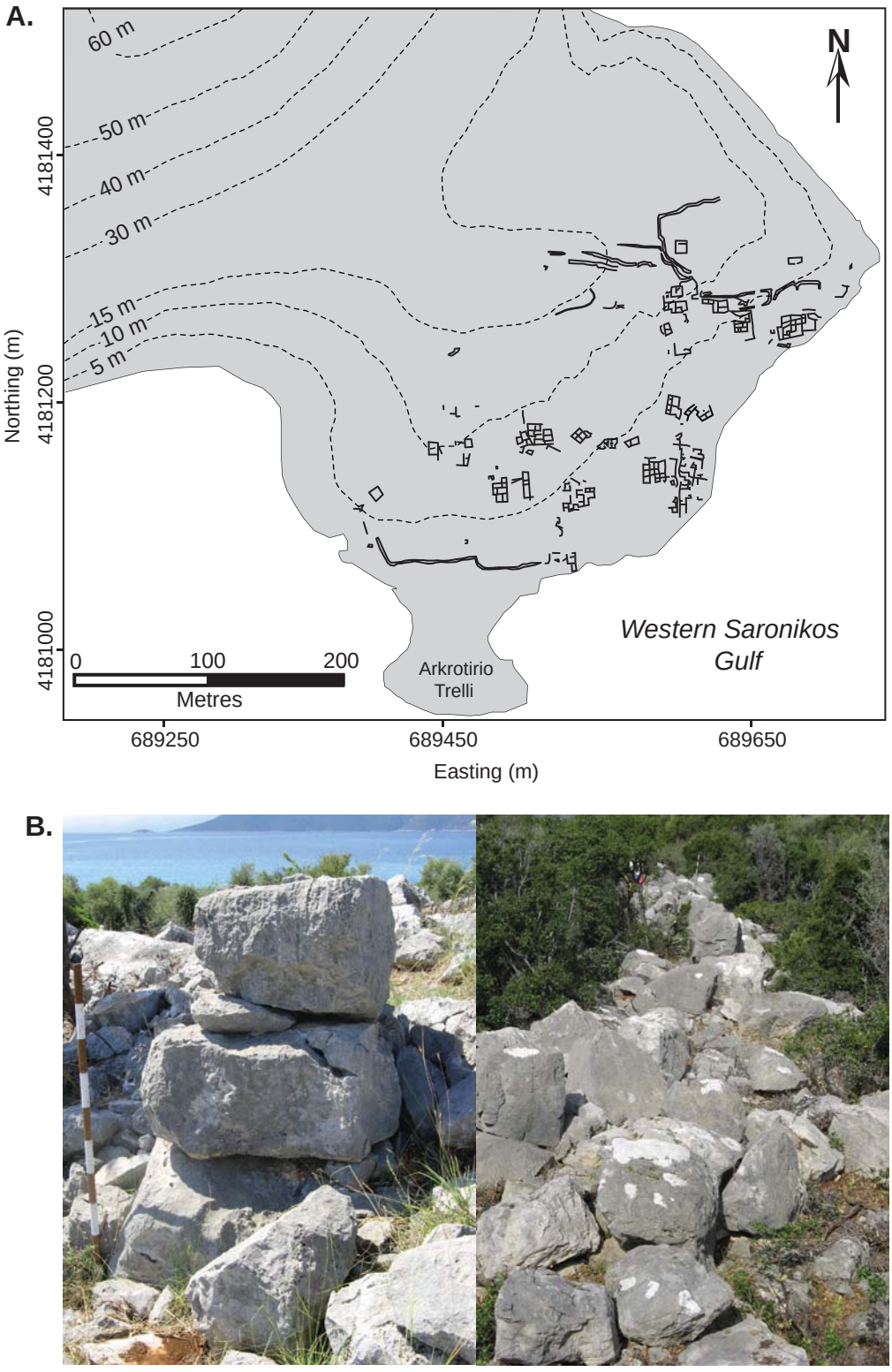


Figure 1.5: A) Architectural features mapped during survey of Kalamianos landsite by the Saronic Harbours Archaeological Project (SHARP) 2009-2011 (Tartaron et al., In Press). B) Well preserved wall and foundation structures at Kalamianos showing 'cyclopean' masonry style typical of the Mycenaean palatial period. Scale stick is 1 m in height.

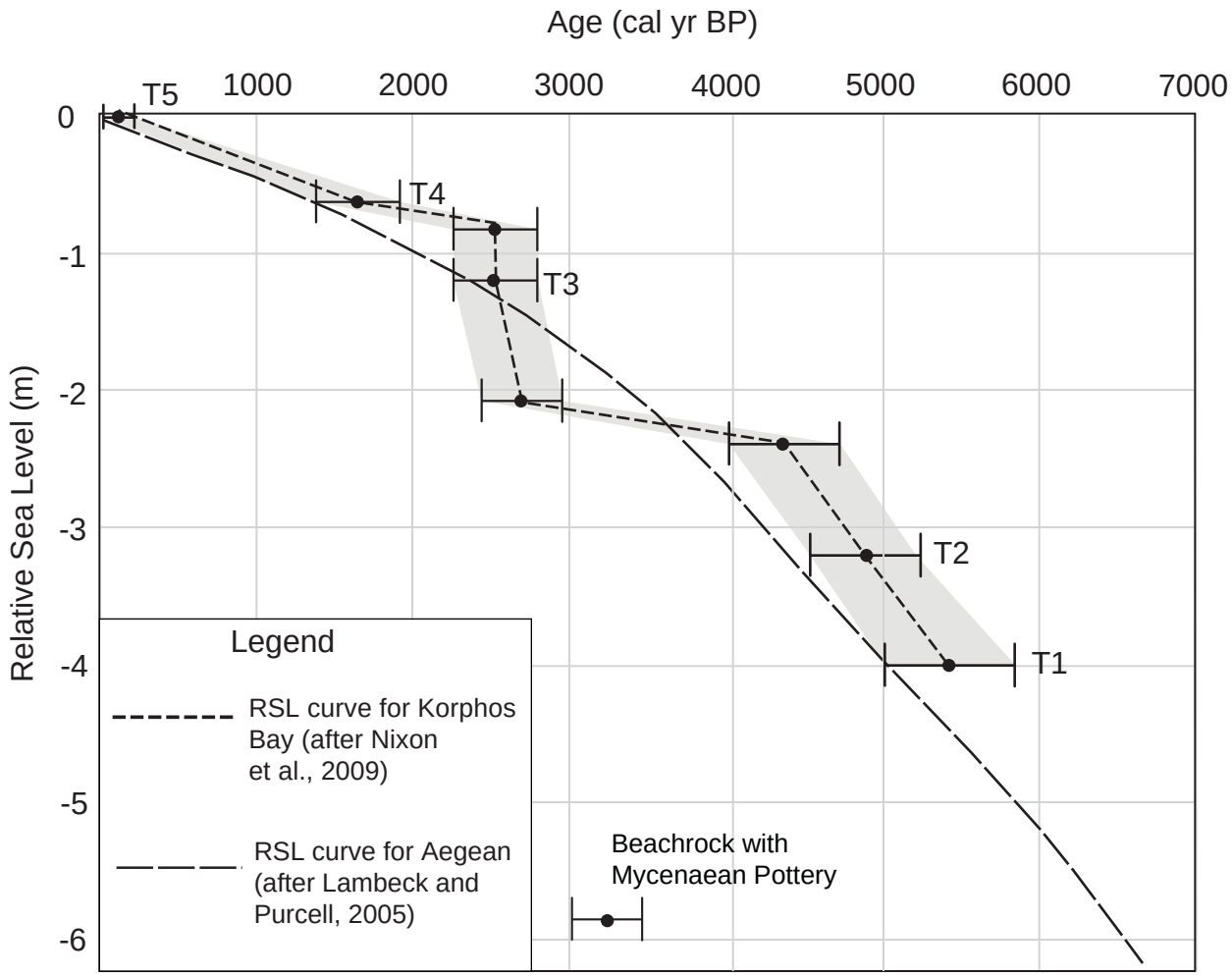


Figure 1.6: Comparison of relative sea level (RSL) curve for Korphos Bay (after Nixon et al., 2009) with predicted glacio-hydro-eustatic curve for Aegean (from Lambeck and Purcell, 2005). Korphos RSL envelope (grey shaded) is derived from elevation and probability distributions of calibrated radiocarbon dates on salt marsh deposits. Note all points (with the exception of one) lie within < 1 m of the predicted Aegean RSL curve. Several transgression events (T1-T5) were interpreted by Nixon et al. (2009) based on the marsh sediment and corresponding record from tidal notches from Korphos Bay.

seismic subsidence on several mapped faults in the Korphos area (Nixon et al., 2009).. While Kalamianos is located a short 2.5 km southeast of the Korphos Bay study site, it is also situated on a separate fault block, which has undergone differential displacement. The RSL history at Kalamianos must first be determined to understand the paleoenvironmental context of the shoreline during Mycenaean occupation.

## 1.4. Methods

### 1.4.1. Geophysical Surveys

A systematic marine geophysical survey was conducted over a 10-km$^2$ area at Kalamianos (Fig. 1.3). More than 150 line km of magnetic and bathymetry data was collected using a Marine Magnetics SeaQuest$^{TM}$ (Overhauser) marine tri-axial gradiometer system and a Knudsen 320BP 200 kHz echosounder (Fig 1.7). The gradiometer was towed 45 m behind a boat at an average speed of 10 km/h and at a depth of 0-1 m below the water surface. The echosounder was mounted on a catamaran and towed 10 m behind the survey vessel at the same cruising speed of 10 km/h for data acquisition.

### 1.4.2. Bathymetry

Echosounder data were acquired with a line spacing of 5-20 m and an inline sample rate of 20 Hz. The survey lines were oriented perpendicular to the shoreline with tie lines orthogonal to the primary line direction. The sonar records were post-processed in Oasis Montaj$^{TM}$ software and interpolated to produce a digital bathymetric model (DBM) of the inshore area. The high-resolution DBM provided significant information on the submerged landscape, which was an important initial step in the process of paleoenvironmental reconstruction.

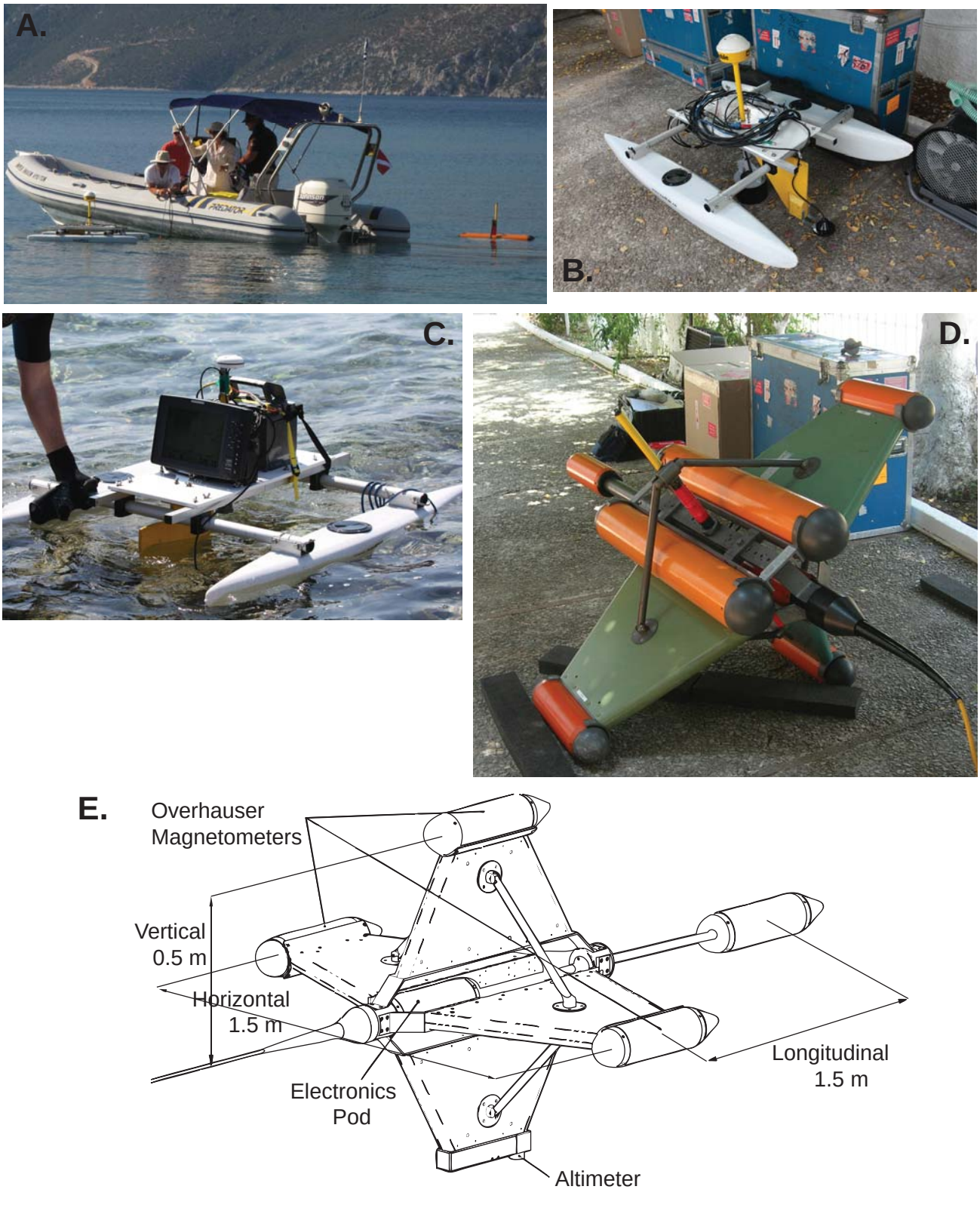


Figure 1.7: A) Survey boat (6 m zodiac) and geophysical equipment in water. B) Catamaran with Trimble RTK 4600 D-GPS receiver and Knudsen 200 kHz echosounder. C) Catamaran equipped with Humminbird 200 kHz echosounder system. (D) SeaQuestTM tri-axial magnetic gradiometer. E) Schematic of SeaQuestTM tri-axial gradiometer platform.

A Knudsen 320BP single-beam echosounder with a 200 kHz transducer (8˚ conical beam) was mounted on a catamaran and towed 10 m behind the survey vessel. A sonar acoustic pulse is emitted from a transducer on the echosounder and the reflected pulse from the rock/sediment interface of the seafloor is measured. Depth to bottom was calculated as:

$D = \frac{1}{2} T_t * V_w$

where $T_t$ = two-way travel time (seconds)

$V_w$ = velocity of acoustic pulse in water column (ca. 1500 $ms^{-1}$)

1.4.3. Marine Gradiometer Survey

Cultural material deposits (i.e. clay pottery, andesitic ballast mounds) often have contrasting magnetic susceptibility with the surrounding sediment and bedrock, allowing for possible detection by magnetic geophysical methods (Boyce et al., 2009). In this study, we employed a SeaQuest$^{TM}$ tri-axial marine gradiometer system instead of the traditional single sensor magnetometer that has been commonly used in archaeological studies. Gradiometers, which measure the change in magnetic field intensity with respect to vertical or horizontal distance (units $nTm^{-1}$), have several advantages over single (total field) magnetometers: 1) they are immune to time-varying shifts in the geomagnetic field strength and do not require diurnal corrections, 2) they have a much greater sensitivity for detection of small magnetic anomalies, 3) gradient measurement acts as a low-pass spatial filter, rejecting contributions from deep magnetic source bodies. A gradiometer thus has the ability to resolve much smaller near-surface magnetic targets, which benefits archaeological applications.

The SeaQuest$^{TM}$ collected real magnetic gradients in the vertical, horizontal and vertical directions which allowed for the calculation of the real total gradient or analytic signal. The absolute value of the amplitude of the 3-D analytic signal (AAS) or total gradient at (x,y) is derived from the three orthogonal gradients of the total magnetic field:

$$|A(x,y)| = \sqrt{\left(\partial M/\partial x\right)^2 + \left(\partial M/\partial y\right)^2 + \left(\partial M/\partial z\right)^2}$$

where $|A(x,y)|$=the absolute value of the 3-D analytic signal ($nTm^{-1}$), and $M$=field strength (nT), is directly measured by a tri-axial gradiometer system (Roest et al. 1992). The 3-D Analytic signal produces a simple bell shaped function anomaly with localized maxima over magnetic contacts (Fig. 1.8). It is independent of the inclination of the Earth's field and of anomaly distortions caused by strong remnant magnetization vectors (Roest et al. 1992 and MacLeod et al. 1993). Also, high frequency anomalies from induced ferrous targets are more enhanced than relatively low frequency anomalies produced by large deep seated magnetic sources. It has proven to be accurate and useful for improving magnetic source location interpretations (Roest et al. 1992; Salem et al., 2002).

## 1.5. Shoreline Reconstruction

### 1.5.1. Beachrock Mapping

Beachrocks are a type of coastal sedimentary deposit consisting of lithified beach sediments (i.e. gravel and sands of biogenic or detrital origin). Beachrocks are rapidly lithified through the precipitation of carbonate cements of mainly high-magnesian calcite or aragonite

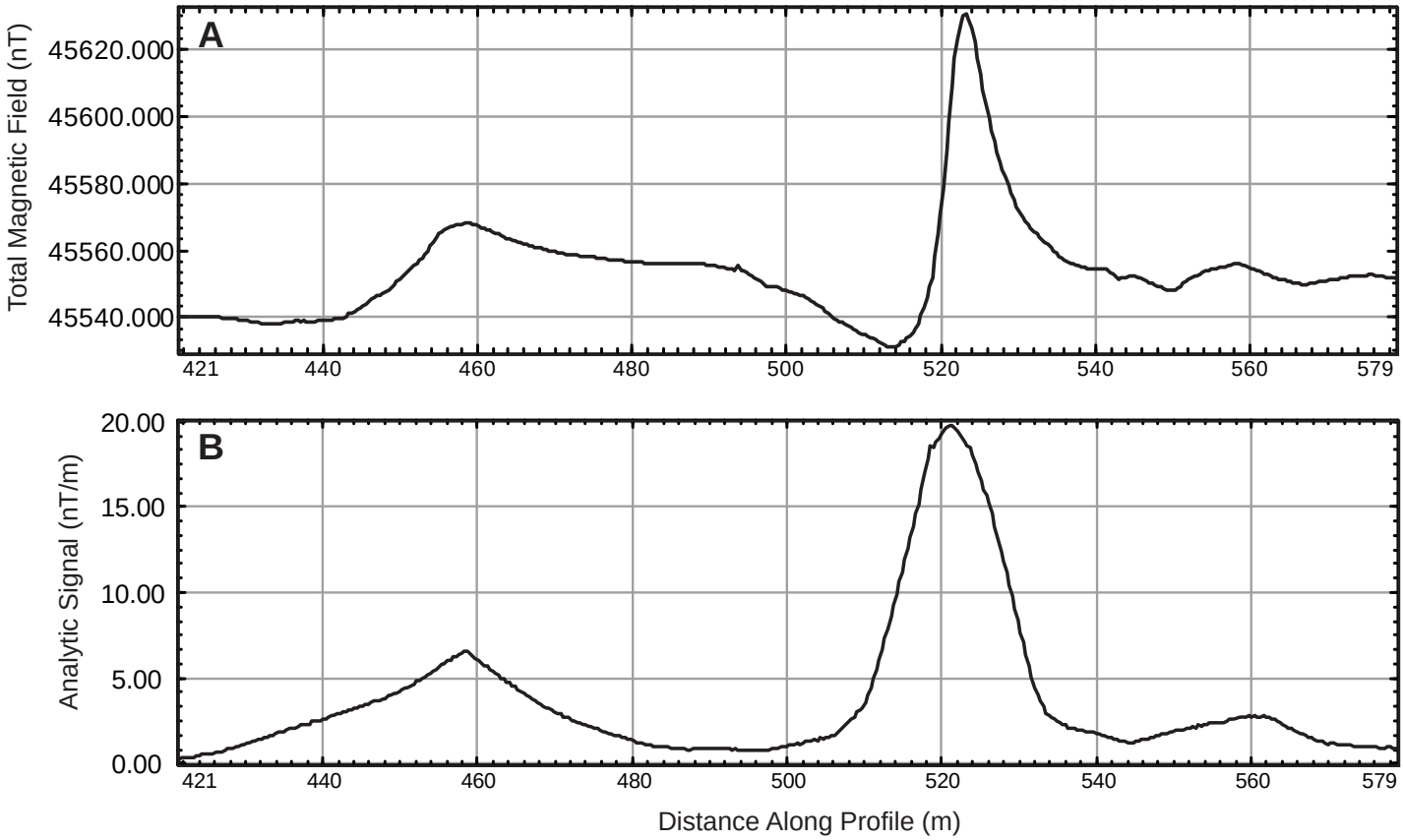


Figure 1.8: A) Typical dipole anomaly in total magnetic intensity data. B) Analytic signal transform of dipole anomaly. Note dipole collapses to a single peak over located over source body.

(Vousdoukas, 2007). The formation of beachrock is a diagenetic process with time scales in the order of a few years to a few decades (Chivas et al., 1986; Vousdoukas, 2007). The lithification of beachrock occurs exclusively in the intertidal zone along coastlines, which makes relict beachrock platforms a suitable proxy for an upper limit estimation of Quaternary sea level (Tatsumi 2003; Kelletat, 2006).

Scuba reconnaissance, conducted to photo document and collected samples over the inshore area at Kalamianos, discovered two inundated beachrock platforms that contained a significant concentration of pottery material. Samples of the beachrock were collected and transported to McMaster University for analysis. The anthropogenic materials discovered in the beachrock (i.e. pottery fragments, charcoal) were dated to determine the age of the beachrock deposits. The beachrock age and elevation provide an indicator of Mid-Holocene sea level fluctuations at Kalamianos.

### 1.5.2. Radiocarbon Dating

Embedded charcoal fragments were discovered within the matrix of beachrock samples obtained at Kalamianos. The fragments of charcoal were small (<5 mm in size) and required the use of a micro drill to remove the surrounding rock matrix for extraction with a thin needle. Samples were packaged in aluminum foil and sent for AMS radiocarbon analysis at Beta Analytic Inc.

Reported AMS radiocarbon ages are in conventional radiocarbon years and calibration is required to convert the results to calendar years. Conventional radiocarbon age results assume that atmospheric carbon 14 has remained constant over time but this assumption is false. Atmospheric carbon 14 is in constant flux and could be associated with but not limited to the

advent of fossil fuel burning, nuclear testing, Earth's magnetosphere fluctuations, climate change etc. For this thesis, the calibration of radiocarbon results to calendar years was done using the CALIB 6.0 software with the INTCAL09 calibration database.

## 1.6. References

Armijo, R., Meyer, B., King, G.C.P., Rigo, A., Papanastassiou, D., 1996. Quaternary Evolution of the Corinth Rift and its Implications for the Late Cenozoic Evolution of the Aegean. Geophysical Journal International 126(1), 11-53.

Baika, K., 2008, Archaeological indicators of relative sea level changes in the Attico-Cycladic massif: preliminary results. Bulletin of the Geological Society of Greece 42, 33-48.

Bailey, G.N., and Flemming, N.C., 2008. Archaeology of the continental shelf: Marine resources, submerged landscapes and underwater archaeology. Quaternary Science Reviews 27(23-24), 2153-2165.

Boyce, J.I., Reinhardt, E.G., Raban, A., Pozza, M.R., 2004. Marine magnetic survey of a submerged Roman harbour, Caesarea Maritima, Israel. International Journal of Nautical Archaeology 33(1), 122-136.

Boyce, J.I., Krezoski, G.M., Reinhardt, E.G., Goodman, B.N., Artzy, M., 2006. Marine Geophysical Mapping of Bronze-Age Harbor Structures, Liman Tepe, Turkey. Geological Society of America Abstracts with Programs 38(7), 150.

Boyce, J.I., Reinhardt, E.G., Goodman, B.N., 2009. Magnetic detection of ship ballast deposits and anchorage sites in King Herod's Roman harbour, Caesarea Maritima, Israel. Journal of Archaeological Science 36(7), 1516-1526.

Chivas, A., Chappell, J., Polach, H., Pillans, B., Flood, P., 1986. Radiocarbon evidence for the timing and rate of island development, beach-rock formation and hosphatization at Lady Elliot Island, Queensland, Australia. Mar. Geol. 69, 273–287.

Clift, P.D., Robertson, A.H.F., 1990. Deep-water basins within the Mesozoic carbonate platform of Argolis, Greece. Journal of the Geological Society 147, 825-836.

Collins, D., Dunn, R.K., 2008. Using Late Bronze Age Walls at Kalamianos, Greece, to Determine a Minimum Rate of Rillenkarren Formation. Geological Society of America Abstracts with Programs 40(2), 66.

Erginal, A., Kıyak, N.G., and Öztürk, B., 2010, Investigation of beachrock using microanalyses and OSL dating: A case study from Bozcaada Island, Turkey. Journal of Coastal Research, 27,350-358.

Fedje, D.W. and Christensen, 1999. Modeling Paleoshorelines and Locating Early Holocene Coastal sites in Haida Gwaii. American Antiquity 64(4), 635-652.

Fischer, A., 2004. Submerged Stone Age - Danish examples and North Sea potential. CBA Research Report 141, 21-36.

Flemming, N.C., 1999, Archaeological evidence for vertical movement on the continental shelf during the Palaeolithic, Neolithic and Bronze Age periods. Geological Society, London, Special Publications 1999, v. 146, p. 129-146.

Galili, E., Weinstein-Evron, M., Hershkovitz, I., Gopher, A., Kislev, M., Lernau, O., Kolska-Horwitz, L., Lernau, H., 1993. Atlit-Yam: a prehistoric site on the sea floor off the Israeli coast. Journal of Field Archaeology 20, 133–157.

Gron, O., and Skaarup, J., 2004. Submerged Stone Age Coastal Zones in Denmark: investigation strategies and results. CBA Research Report 141, 53-56.

Harding, A., Cadogan, G. and Howell, R., 1969, Pavlopetri, an underwater Bronze Age town in Laconia, Annual of the British School at Athens, 64, pp. 112-142

Henderson, J.C., Gallou, C., Flemming, N.C. and Spondylis, E., in press, The Pavlopetri Underwater Archaeology Project: investigating an ancient submerged town, J. Benjamin and C. Bonsall, Eds. Oxbow Books, Oxford.

Kelletat, D., 2006. Beachrock as sea level indicator? Remarks from a geomorphological point of view. Journal of Coastal Research 22 (6), 1555–1564.

Lambeck, K., 1996, Sea level change and shoreline evolution in Aegean Greece since Upper Paleolithic time. Antiquity, 70, 588-611.

Lambeck, K., and Purcell, A., 2005. Sea level change in the Mediterranean Sea since the LGM, model predictions for tectonically stable areas. Quaternary Science Reviews 24, 1969-1988.

MacLeod, I.N., Jones, K., Dai, T.F., 1993. 3-D Analytic Signal in the Interpretation of Total Magnetic Field Data at Low Magnetic Latitudes: Exploration Geophysics 24, 679-688.

Mahon, I., Pizarro, O., Johnson-Roberson, J., Friedman, A., Williams, S.B., Henderson, J.C., 2011. Reconstructing Pavlopetri: Mapping the World's Oldest Submerged Town using Stereo-vision. IEEE International Conference on Robotics Automation 9-13 May 2011, 2315-2321.

Marriner, N. Morhange, C. and Doumet-Serhal, C., 2006. Geoarchaeology of Sidon's ancient harbours, Phoenicia. Journal of Archaeological Science..

Marriner, N. and Morhange, C., 2007. Geoscience of ancient Mediterranean harbours. Earth Science Reviews, 80, 137-194.

Morrison, I.A., 1968. Appendix I. Relative sea level change in the Saliagos area since Neolithic times, in Evans J.D. and Renfrew, C., (ed.), Excavations at Saliagos near Antiparos: 92-8. London: Thames & Hudson.

O'Shea, J.M., and Meadows, G.A., Evidence for early hunters beneath the Great Lakes. PNAS 106(25), 10120-10123.

Papageorgiou, D., 2008. The marine environment and its influence on seafaring and maritime routes in the Prehistoric Aegean. European Journal of Archaeology 11, 199-222.

Roest, W.R., Verhoef, J., Pilkington, M., 1992. Magnetic interpretation using the 3-D analytic signal. Geophysics 57 (1), 116-125.

Rothaus, R., Reinhardt E.G., and Noller, J., 2008. Earthquakes and subsidence at Kenchreai: using recent earthquakes to reconsider the archaeological and literary evidence. Archaeology and History in Medieval and Post-Medieval Greece, Carraher, W. Hall, L., Moore Aldershot, R.S. (eds) Ashgate Publishing, UK., pp. 53-66.

Salem A., Ravat, D., Gamey, T.J., Ushijima, K., 2002. Analytic signal approach and its applicability in environmental magnetic investigations. Journal of Applied Geophysics 49, 231-244.

Shackleton, J., van Andel, T., Runnels, C., 1984. Coastal paleogeography of the central and western Mediterranean during the last 125,000 years and its archaeological implications. Journal of Field Archaeology 11, 307–314.

Sonnenburg, E.P., Boyce, J.I. and Reinhardt, E.G., 2011. Quartz flakes in lakes: microdebitage evidence for submerged Great Lakes prehistoric (Late Paleoindian-Early Archaic) tool-making sites. Geology 11, 631-634.

Sonnenburg, E.P., Boyce, J.I. and Suttak, P., In Review, Holocene paleoshorelines, water levels and submerged prehistoric site archaeological potential of Rice Lake (Ontario, Canada). J. of Archaeological Sciences.

Tartaron, T. F., Rothaus, R. M., and Pullen, D. J., 2003. Searching for prehistoric Aegean harbors with GIS, geomorphology, and archaeology. Athena Review 3(4): 27–36.

Tartaron, T.F., Gregory, T.E., Pullen, D.J., Noller, J.S., Rothaus, R.M., Rifle, J.L., Tzortzopoulou-Gregory, L., Schon, R., Caraher, W.R., Pettegrew, D.K., Nakassis, D., 2006. The Eastern Korinthia Archaeological Survey - Integrated Methods for a Dynamic Landscape. Hesperia 75, 453-523.

Tartaron, T.F., Pullen, D.J., Dunn, R.K., Dill., A. and Boyce, J.I., *In Press.* The Saronic Harbors Archaeological Research Project (SHARP): Investigations at Mycenaean Kalamianos, 2007-2009. Hesperia.

Tatsumi, S.H., Kowata, E.A., Gozzi, G., Kassab, L.R.P., Suguio, K., Barreto, A.M.F., Bezerra, F.H.R., 2003. Optical dating results of beachrock, eolic dunes and sediments applied to sea level changes study. J. Lumin. 102–103, 562–565.

van Andel, T., Shackleton, J.C., 1982. Late Paleolithic and Mesolithic Coastlines of Greece and the Aegean. Journal of Field Archaeology 9, 445-454.

Vousdoukas, M.I., Velegrakis, A.F., Plomaritis, T.A., 2007. Beachrock occurance, characteristics, formation mechanism and impacts. Earth-Science Reviews 85, 23-46.

# CHAPTER 2: RECONSTRUCTION OF BRONZE-AGE COASTAL ENVIRONMENTS AND ANCHORAGE SITES AT KALAMIANOS (KORPHOS, GREECE)


## Abstract

Kalamianos is a recently discovered fortified Early to Late Bronze (Mycenaean) coastal archaeological site, located on the Saronic Gulf near the modern town of Korphos, Greece. The settlement's coastal context and site plan indicate its function as a port but the location of the harbour basin was unknown. The modern coastline provides few clues as to the harbour configuration as the site has been partially submerged by > 5 m of relative sea level rise since the Early Helladic (EH; ca. 3100-2150 BC) site occupation. In 2009, a detailed marine geophysical survey and underwater diver search was conducted in the inshore waters to identify potential anchorage sites and to examine submerged shoreline features. More than 400-line km of single-beam bathymetry was acquired across a 10-km$^2$ area to produce a detailed digital bathymetric model (DBM). Underwater geological mapping and sampling of submerged beachrock platforms was conducted by diver survey over a 2-km$^2$ area.

Bathymetric mapping revealed two submerged beachrock platforms (BR-1, BR-2) paralleling the modern shoreline and a submerged isthmus connecting the mainland with a small island 200 m offshore. The BR-1 beachrock (3.5-3.7 m depth) consisted of a well-cemented calcarenite containing abundant Late Helladic (LH; 1300-1190 BC) pottery sherds (30-50%) and wood charcoal fragments. The pottery showed little reworking or bioencrustation, consistent with rapid burial in a low energy supratidal environment. $^{14}$C dating of the extracted charcoal yielded an AMS $^{14}$C age of 3250±40 BP (1640-1400 cal BC), consistent with the LH ceramics.

The BR-2 beachrock (5.8-5.9 m depth) contained less pottery (<20%) and included well-preserved fragments of Early Helladic jars.

The beachrock elevations and $^{14}C$ and pottery ages were used to reconstruct a relative sea level (RSL) curve and paleogeographic maps of the EH to LH shorelines. These data were augmented with sea level indicators from a previous study in nearby Korphos Bay. The RSL curves indicate that water levels have risen ~ 5.8 m since EH site occupation. In contrast, a regional glacio-hydro isostatic model, predicted ~ 4 m rise since 3000 BC. The difference in the local and regional RSL curves (1.8 m) is attributed coastal subsidence on several normal faults that displace the modern shoreline. Paleogeographic maps show that during the initial EH phase of site occupation the mainland was connected to the island by a narrow isthmus, forming two well-sheltered natural harbour basins. During the subsequent Mycenaean phase, sea level had risen by about 1.5 m, submerging the promontory. The presence of abundant pottery and wood charcoal in the BR-1 beachrock indicates that shipping activity during the LH was focused at the south end with an anchorage area located on the eastern side of a small headland. No evidence was found for a constructed harbour at Kalamianos but three well-protected natural embayments formed in lee of coastal headlands would have provided Bronze Age seafarers with options for safe anchorage under varying wind and wave conditions.

**Keywords:** Kalamianos, Mycenaean harbour, Bronze Age, beachrock, underwater survey, coastal subsidence

## 2.1. Introduction

The study of coastal paleoenvironmental change has become an increasing focus for geoarchaeological research in the Mediterranean, as it is now recognized that changes in Holocene relative sea level (RSL) and coastal habitats had far-reaching impacts on prehistoric cultures who settled in the coastal zone (Lambeck et al., 1996; Baika, 2008; Marriner et al., 2010). The available record of Holocene RSL in the Mediterranean comes from a variety of geological and archaeological sea level indicators (Bailey and Flemming, 2008). Archaeological indicators include architectural features (e.g. foundations, harbour structures) and other man-made structures (e.g. water wells) that have a known relation to the coastline and could therefore be used to estimate the sea level at the time of their construction (Flemming, 1999; Marinner and Morhange, 2007; Gallili et al., 1988). Geological evidence comes from a variety of sources, including measurements of the depth-age relationships of submerged tidal notches (Pirazzoli et al., 1994; Nixon et al., 2009), submerged marsh and terrestrial sediments (Kraft et al., 1980; Nixon et al., 2009) and from shoreline features imaged in seismic and bathymetry data (Flemming, 1987). The elevations of submerged beachrock ridges can also provide a useful sea level indicator, as beachrock forms rapidly, often over a span of decades, in the supratidal and intertidal zone close to sea level. Few studies, however, have attempted to use beachrock for this purpose due to the difficulties in dating of beachrock deposits (e.g. Nixon et al., 2009; Erginal et al., 2010). Important archives of changes in sea level and coastal environments can also be obtained from the study of ancient harbour sediments (Marriner and Morhange, 2007; Marriner et al., 2010). Harbour basins act as ‘depocentres’ for the accumulation of continuous sediment records and often contain cultural materials (e.g. pottery) that can provide high-resolution chronologies for dating of environmental changes (Marriner and Morhange, 2007).

In the archaeologically rich Aegean coastline of Greece, RSL rise during the Early to Mid-Holocene was an important environmental constraint on the settlement of the coast by Neolithic and Bronze Age peoples (Lambeck, 1996). Underwater prehistoric sites have been documented at a number sites (Flemming, 1987; Baika, 2008), including well-documented submerged Neolithic sites on the Argolis Peninsula (Jacobsen and Farrand, 1987), Early Bronze Age sites in Antiparos (Morrison, 1968) at Pavlopetri in Laconia (Harding et al., 1969; Mahon et al., 2011; Henderson et al., in press) and a number of Neolithic and Bronze Age sites in the Attica and Cycladic Islands summarized by Baika (2008). Numerical predictions of Aegean sea levels accord with these data, showing that sea levels rose more 45 m during the Mid- to Late Neolithic (ca. 10-6 ka BP) and a further 3-4 m during the Chalcolithic and Bronze Age periods (ca. 5.5-3.2 ka BP) (Figs. 2.1, 2.2). Paleogeographic maps based on these predictions suggest that Neolithic shorelines were dramatically reconfigured as shallow shelf areas and embayments became flooded (Lambeck, 1996; Lambeck and Purcell, 2005). The changes in shoreline positions during the Chalcolithic/Bronze Age period were less extensive (Figs. 2.1, 2.2) but would have been an important environmental determinant in the choice of settlement and harbour locations (Tartaron et al., 2006). A further complicating factor that needs to be considered is vertical crustal motions associated with Hellenic Arc subduction and faulting (Flemming, 1999). Many areas of the Aegean coast have been tectonically stable during the Holocene (e.g. Attica; Baika, 2008) while other areas have been subject to large rates of uplift or subsidence associated with Hellenic Arc compressional and extensional faulting. In the Greek Peloponnesus for example, the ancient port of Lechaion located at the western end of the Gulf of Corinth has undergone tectonic uplift whereas the harbour at Kenchreai, some 10 km to the southwest has subsided in association with co-seismic fault motions (Rothaus et al., 2008)

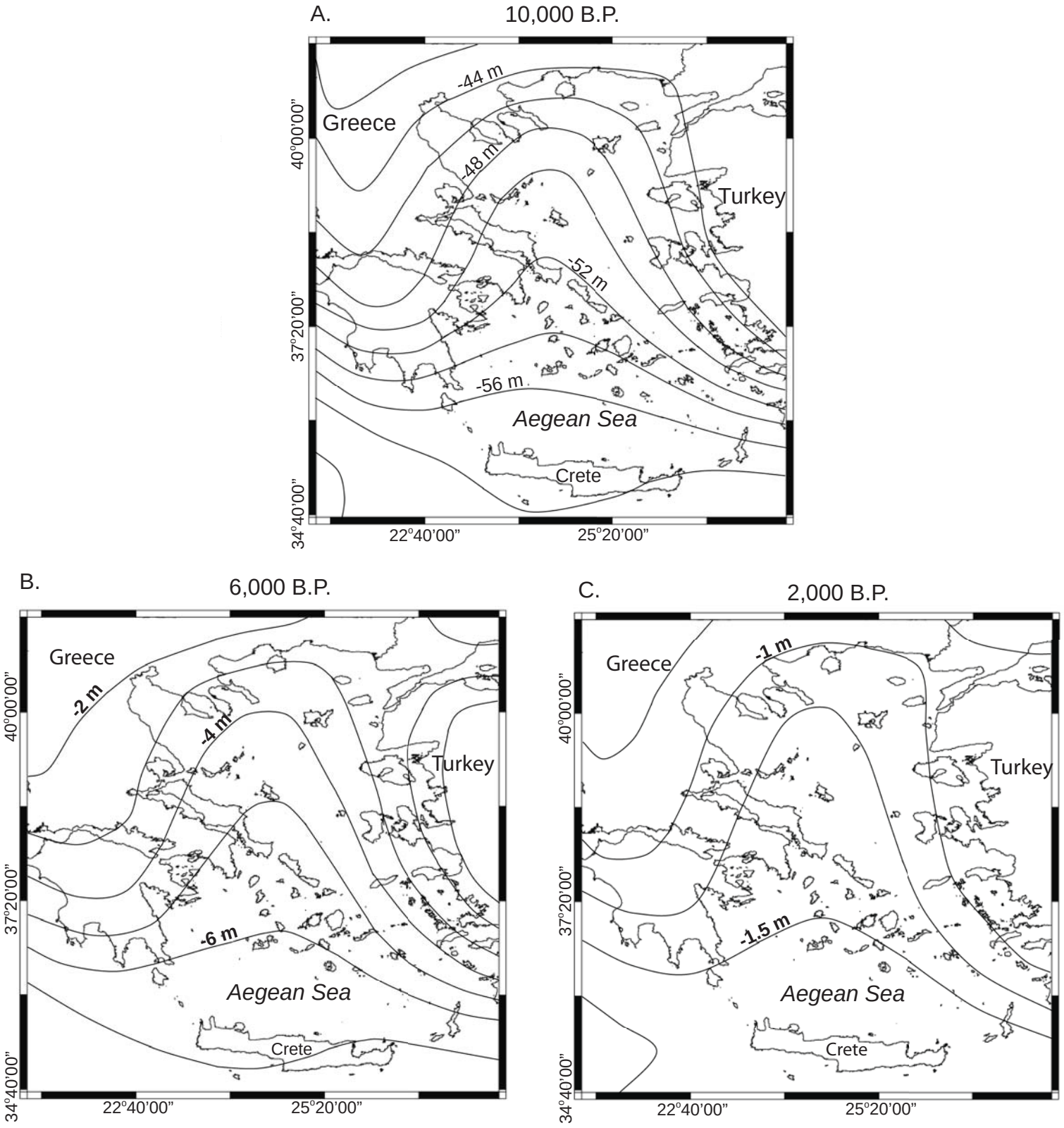


Figure 2.1: Predicted relative sea level (RSL) in the Aegean at A) 10 ka BP, B) 6 ka BP and C) 2 ka BP (modified from Lambeck, 1996). RSL decelerated rapidly after 6-7 ka BP due the end of glacial melting and stabilization in ice volumes. Continued glacio-hydrostatic adjustment of the lithosphere resulted in a further 4-5 m rise in SL between 6-2 ka BP and transgression of the coastline across much of the Aegean during the mid- to late Holocene.

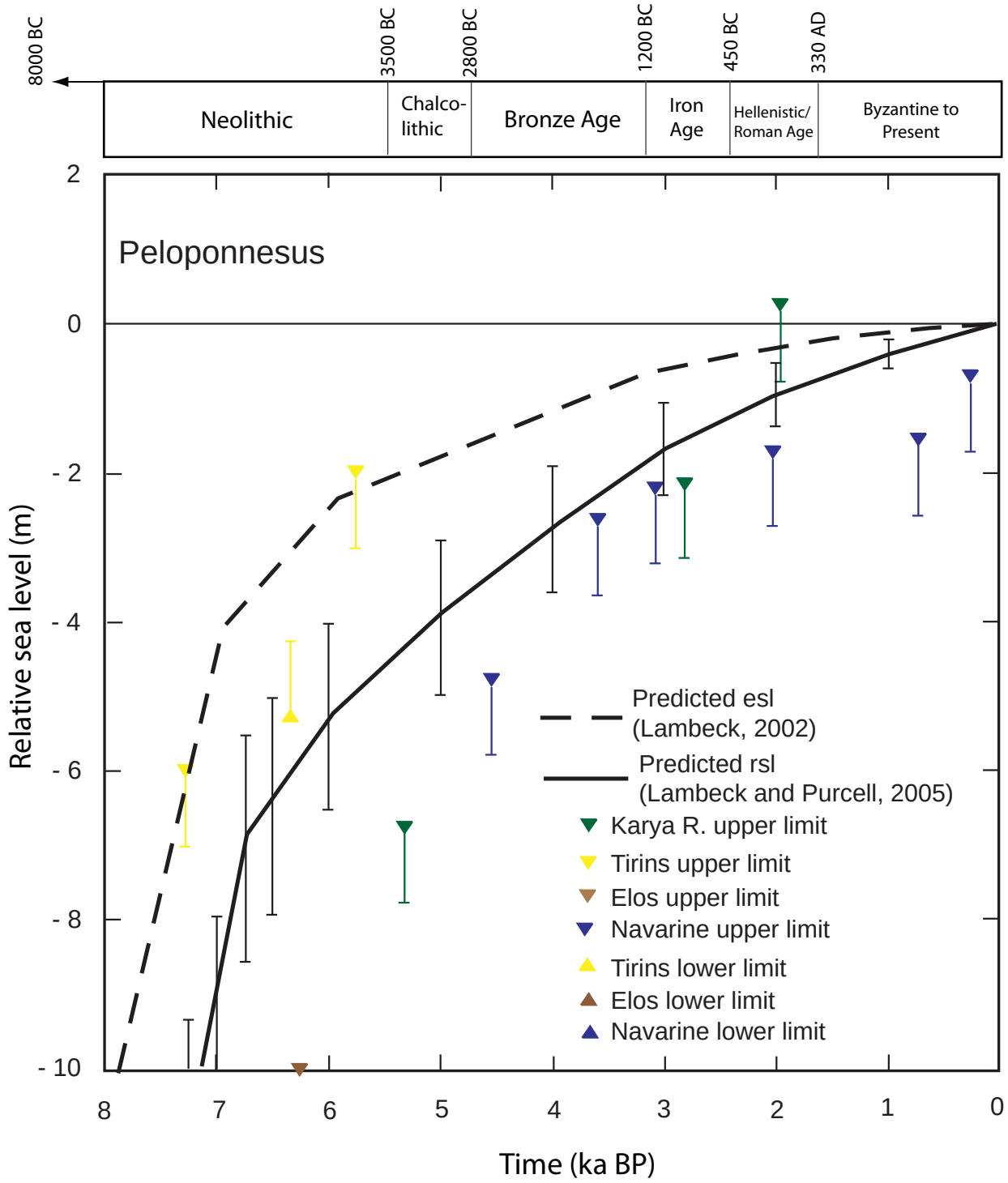


Figure 2.2: Predicted eustatic sea level (ESL) and glacio-hydro-eustatic relative sea level (RSL) curves for the Greek Peloponnesus compared with observed sea levels from four sites in the Aegean (modified from Lambeck, 2002; Lambeck and Purcell, 2005). Archaeological time periods also shown. Note > 2 m difference in two curves due to glacio-hydrostatic component of SL rise. During the Early to Late Neolithic (ca. 10-6 ka BP) sea levels rose rapidly (10-12 mmyr-1) more than 45 m, inundating shallow shelf areas. By the Chalcolithic and Bronze Age period (ca. 5.5-3.2 ka BP) sea level rise had decelerated (< 5 mm yr-1) but levels rose a further 2.5 to 3 m completely or partially inundating prehistoric coastal settlements (e.g. Pavlo Petri, Argolid Gulf; Kraft et al., 1978).

An important archaeological implication of Holocene RSL change is that the geomorphology and configuration of the modern Aegean coastline is likely a poor indicator of the location of harbours and anchorage sites in antiquity (Tartaron et al., in press). Regional paleogeographic reconstructions show that the Early to Mid-Holocene rise in RSL (~ 40-50 m) cut off headlands from the mainland and flooded shallow coastal embayments (Fig. 2.2) (Lambeck, 1996). The headlands would have provided natural sheltered harbours (e.g. Raban, 1985; Shaw, 1999) but over time these sites may have become less favourable anchorage locations as water depths increased and they became less effective barriers to wind and waves. The available palaeographic reconstructions for the Aegean and Mediterranean (e.g. Lambeck, 1996; Lambeck and Purcell, 2005) are useful for large regional-scale studies but provide insufficient details for predictive mapping of prehistoric sites at local to site-scales. As demonstrated by Tartaron et al. (2006), predictive models that incorporate geomorphic constraints such as the modern shoreline configuration and bathymetry can be successful in regional-scale modelling of prehistoric site locations. In their study of the Eastern Korinthos, they used a GIS model that queried a range of environmental and cultural site constraints (e.g. modern shoreline configuration, water depth, terrain slope and stability, wind fetch distance, wave height etc.) to identify coastal areas with high probability for Bronze Age sites. A model identified a number of potential harbour sites which were investigated with field surveys leading to the discovery of the an Early Bronze Age site at Vayia and an extensive, fortified Early to Late Bronze Age coastal settlement at Korphos (Fig. 2.3). The newly discovered site at Korphos, known as Kalamianos, was subsequently investigated as part of the Saronic Harbours Archaeological Research Project (SHARP; Tartaron et al., in press) and as part of this study.

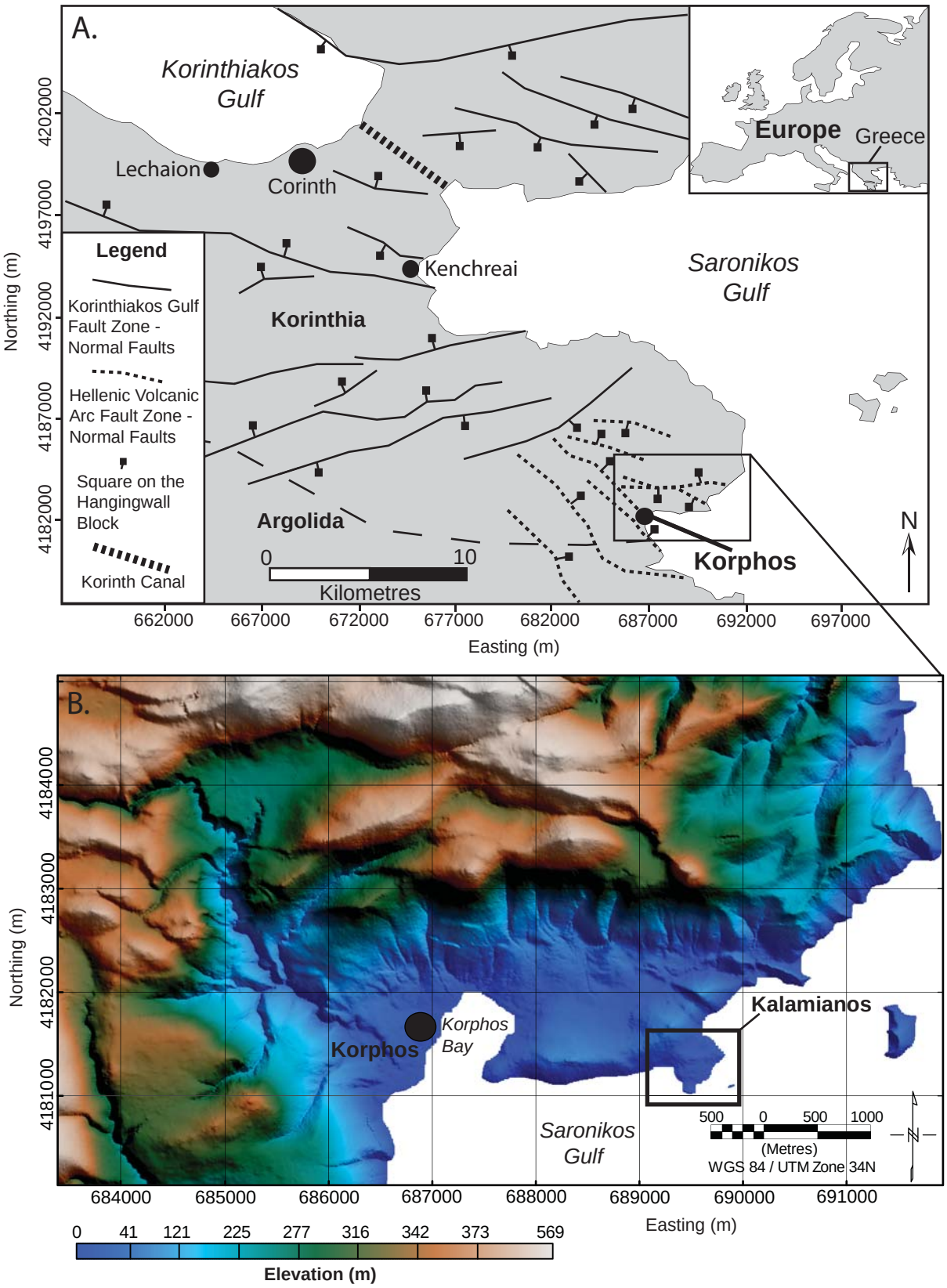


Figure 2.3: A) Location of study area in the western Saronic Gulf showing mapped regional fault structures, modified from Nixon et al. (2009). B) Digital elevation model showing location of Kalamianos near Korphos, Greece.

The exploration for new prehistoric underwater sites in the Aegean requires an improved knowledge of Holocene sea level, including changes in the position and configuration of the shoreline and changes in the coastal environments. In this study, changes in paleogeography of the coastline during the settlement of the Bronze Age site at Kalamianos, Greece were reconstructed using bathymetric survey data and geomorphic evidence from submerged beachrock ridges. Our results show that sea levels were up to ~ 6 m below present during the initial (Early Helladic) occupation of the site and that the coastline provided a number of well sheltered embayment that would have provided natural harbours and anchorage sites.

## 2.2. Study Area

### 2.2.1. Site Location and Archaeology

Kalamianos is Late Bronze Age fortified coastal settlement belonging to the Mycenaean palatial period (Tartaron et al., 2006; Tartaron et al., in press). The site is located on the Western Saronic Gulf about 2.5 km east of the modern village of Korphos (Fig. 2.3). The site covers about 7.2 Ha on a small coastal promontory in Korphos Bay (Fig. 2.4). Because of its proximity to the ancient Mycenaean citadel at Mycenae (~30 km northwest) it is speculated that the site functioned as a trade harbour/naval base for the ancient city (Tartaron et al., in press).

Archaeological investigations have been ongoing at Kalamianos since 2007 as part of the Saronic Harbours Archaeological Research Project (SHARP). The site has a unique state of preservation, as the soil cover has largely been removed by erosion across the site revealing an extensive town with walls and foundation remains of Mycenaean construction, some of them monumental (Tartaron et al., in press). There are no standing structures remaining but building foundations and base blocks of walls are exposed and are well preserved. This unique context

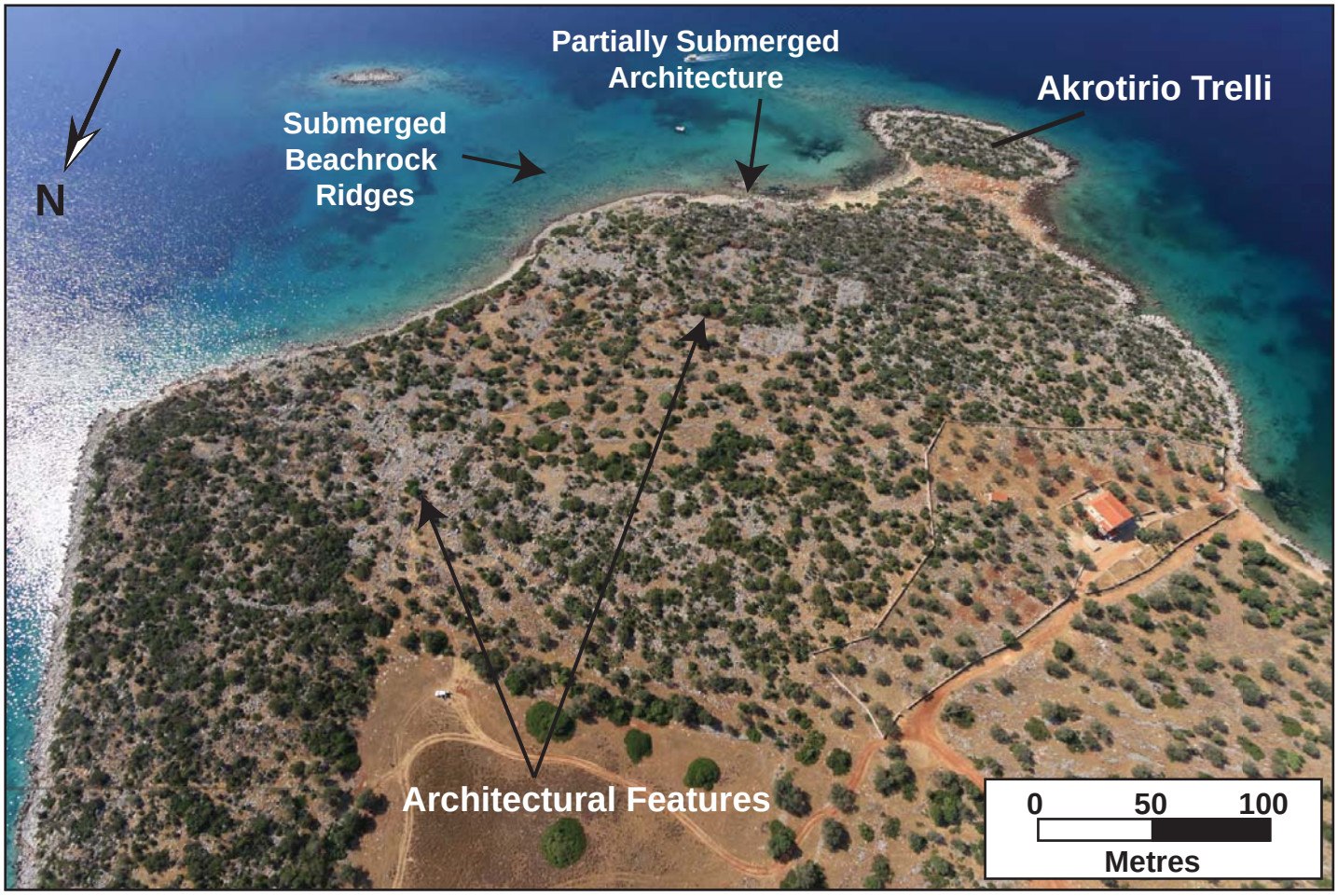


Figure 2.4: Aerial photograph of Kalamianos taken by kite-mounted camera (courtesy T. Tartaron). Note partially submerged architectural features on modern shoreline and submerged beach rock platforms in the shallow inshore area.

allowed for architectural surveys to document the urban layout of the Mycenaean settlement without the need of excavation, a topic that has been poorly addressed in the Aegean Bronze Age due to limited exposures at sites such as Tiryns and Mycenae (Maran, 2002-2003; French et al., 2003). An exposed site also presented a lack of datable sedimentary stratigraphy. Therefore, the age of architectural remains were constrained to be from the Mycenaean Late Helladic (LH) IIIB period (ca. 1300-1190 BC) from datable ceramics retrieved from buildings (Tartaron et al., in press). To date, architectural surveys have identified more than 50 structures and complexes and hundreds of walls adjacent to the modern coastline with some partially submerged architectural features close to the modern shoreline (Fig. 2.5) (Tartaron et al., in press). The paleoshoreline configuration during Mycenaean occupation and location of the ancient harbour basins at Kalamianos were unknown.

### 2.2.2. Geological Setting

The geography surrounding Kalamianos is rugged and rocky with a steep coastline and large cliffs providing natural fortification. The coastline along Korphos-Kalamianos has undergone Holocene co-seismic fault motions along northeast-southwest oriented normal and oblique-slip faults, resulting in a net regional subsidence (Nixon et al., 2009; Tartaron et al., in press). Investigations at Korphos Bay revealed a series of rapid sea level transgressions associated with up to five episodic seismic events (Nixon et al., 2009). The same study documented beachrock platforms located off the south-east shore at Kalamianos at depths of up to 6 m that were interpreted to record episodic subsidence.

The Late Holocene coastline along the Peloponnese, Greece, has not only been affected by global eustatic and glacio-hydro-isostatic RSL rise, it is also one of the most tectonically

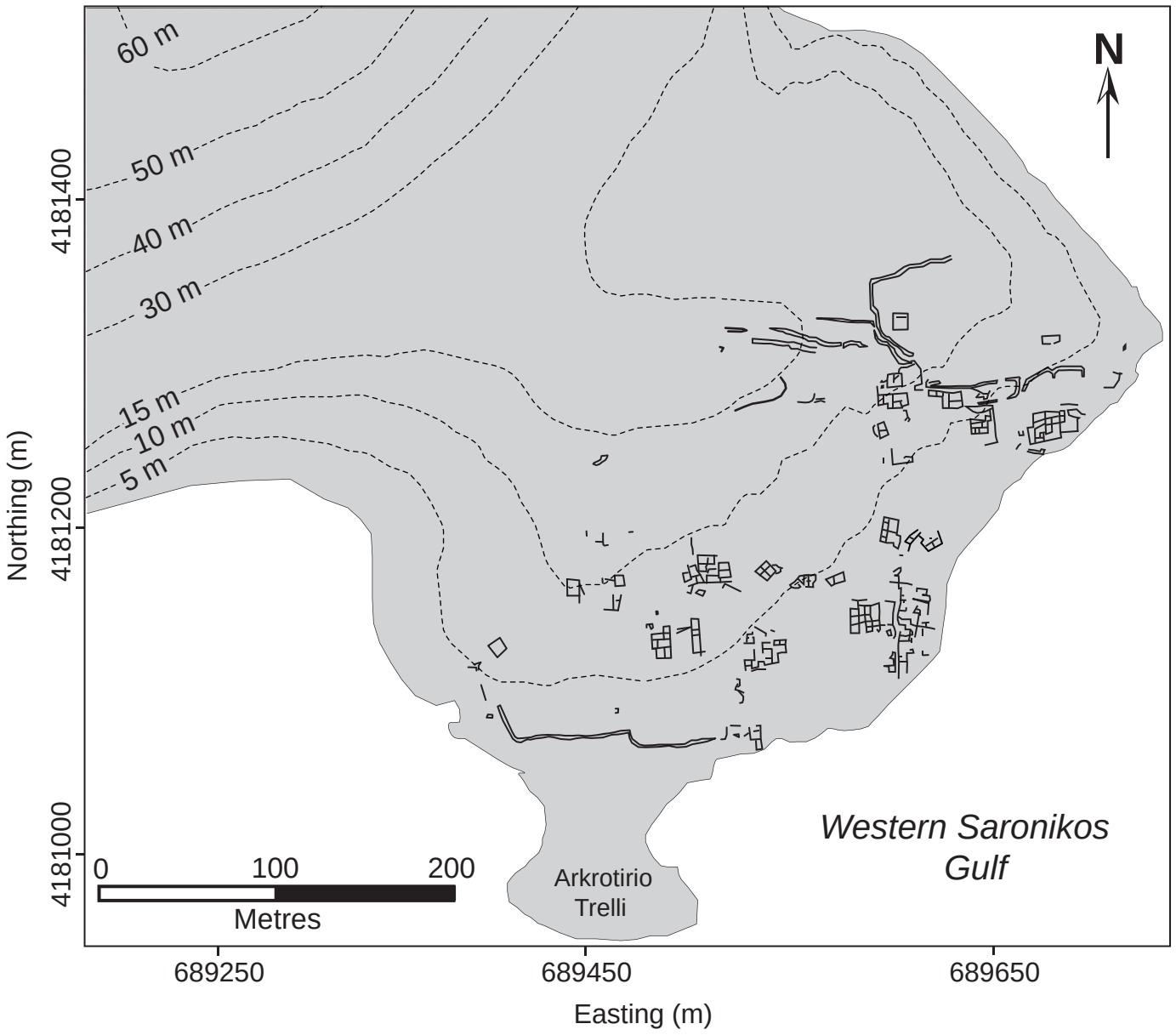


Figure 2.5: Mycenaean architectural features mapped at Kalamianos by Saronic Harbours Archaeological Project (from Tartaron et al., in press). Note some partially inundated architectural features on shoreline at southern end of site.

active regions on Earth under the influence of active crustal extension and significant normal faulting from a right-lateral shear system of the Hellenic Arc subduction zone (Armijo et al., 1992, 1996). Extensive northeast-southwest trending normal faults extending through the Mesozoic age limestone bedrock in southeastern Korinthia has caused significant localized subsidence of numerous fault blocks (Fig. 2.3A) (Armijo et al. 1996).

The town of Korphos is situated on a narrow strip of low hills and basins covering approximately 2 $km^2$ and adjacent to the Saronic Gulf of the Western Aegean Sea. It extends east along the coast of Korphos Bay towards and encompassing Kalamianos, located 2.5 km southeast of Korphos. The area is hemmed in on all sides by rugged hills and mountains of southeastern Korinthia and the Saronic Gulf (Fig. 2.3B). Vegetation cover, over colluvium and thin terra rosa soil, is relatively sparse, dominated by low shrubs and grass with some trees and appears to have been cleared for agricultural use in modern times.

The Mesozoic age limestone bedrock observed in the Korphos-Kalamianos region reveal a karstic landscape with visible paleo-karst and modern karren features on outcrops (Collins and Dunn, 2008). Two generations of fracture and joint sets were observed throughout the region. The older generation joint set, trending north-south and east-west, has been significantly eroded by groundwater flow with visible widening of fractures and cavern formation. These paleo-karst features were subsequently infilled by solution breccia from wall collapse, crystalline calcite and terra rosa soil and are now exposed at land surface. Currently, a younger generation of orthogonal joint sets overprint the older joints and has fractured the limestone into metre scale rectangular blocks. The east-west trending fractures of the older joints were reopened by the younger joint system to create conduits for groundwater flow from the mountains towards the west into Kalamianos and the Saronic Gulf (Miller and Dunn, 2009). The artesian springs

produced by this system provides potable water that is within United States drinking water standards.

## 2.3. Methods

### 2.3.1. Geophysical Survey

A systematic geophysical survey for the inshore and surrounding gulf near Kalamianos was conducted in 2009 to gather evidence for the location of the ancient shoreline, harbour, harbour basin and anchorage sites (Fig. 2.6). The survey area covered approximately 2 $km^2$ in which 170 line kilometre of bathymetry data were acquired. The broad regional survey was conducted using a Zodiac boat with NW-SE survey lines spaced at 20-30 m intervals and NE-SW tie lines spaced at 50 m intervals. A Knudsen 320 BP 200 kHz echosounder with the transducer mounted on a small catamaran was towed 10 m behind the survey vessel for data acquisition (Fig. 2.7A). A Trimble Ag132 sub-metre D-GPS was mounted on the catamaran for survey positioning and navigation. Higher resolution bathymetry for the inshore area southeast of Kalamianos was acquired separately using a Humminbird 200 kHz echosounder system mounted on a catamaran and pushed by snorkelers (Fig. 2.7B). Survey lines were oriented NW-SE, parallel to regional survey lines, but with a tighter spacing at 5-10 m intervals.

The acquired bathymetric data from both surveys was sorted and imported into a digital database on the Geosoft Oasis montaj software for processing. A correction was first applied to account for transducer depth in the water column. A non-linear filtering procedure was applied to the dataset to remove noise and spikes. Tie-line levelling and micro-levelling procedures were applied last to remove residual uncompensated systematic cross-line errors (Minty, 1991). The fully corrected bathymetric dataset was then gridded using with a cell spacing of 5 m using a

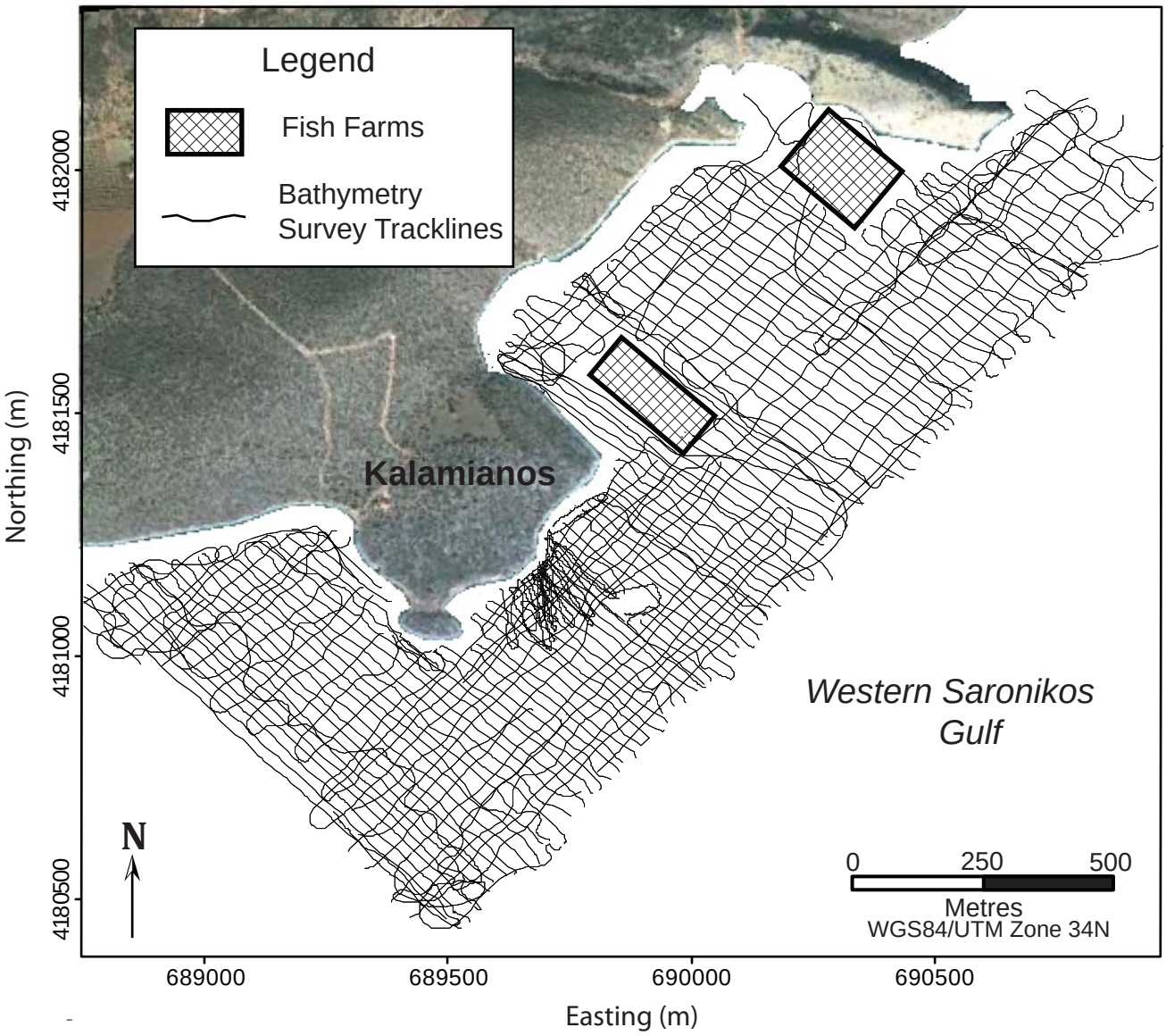


Figure 2.6: Survey area showing 200 kHz bathymetry survey track lines. Detailed survey over harbour basin (2-5 m line spacing) conducted with swimmer propelled catamaran.

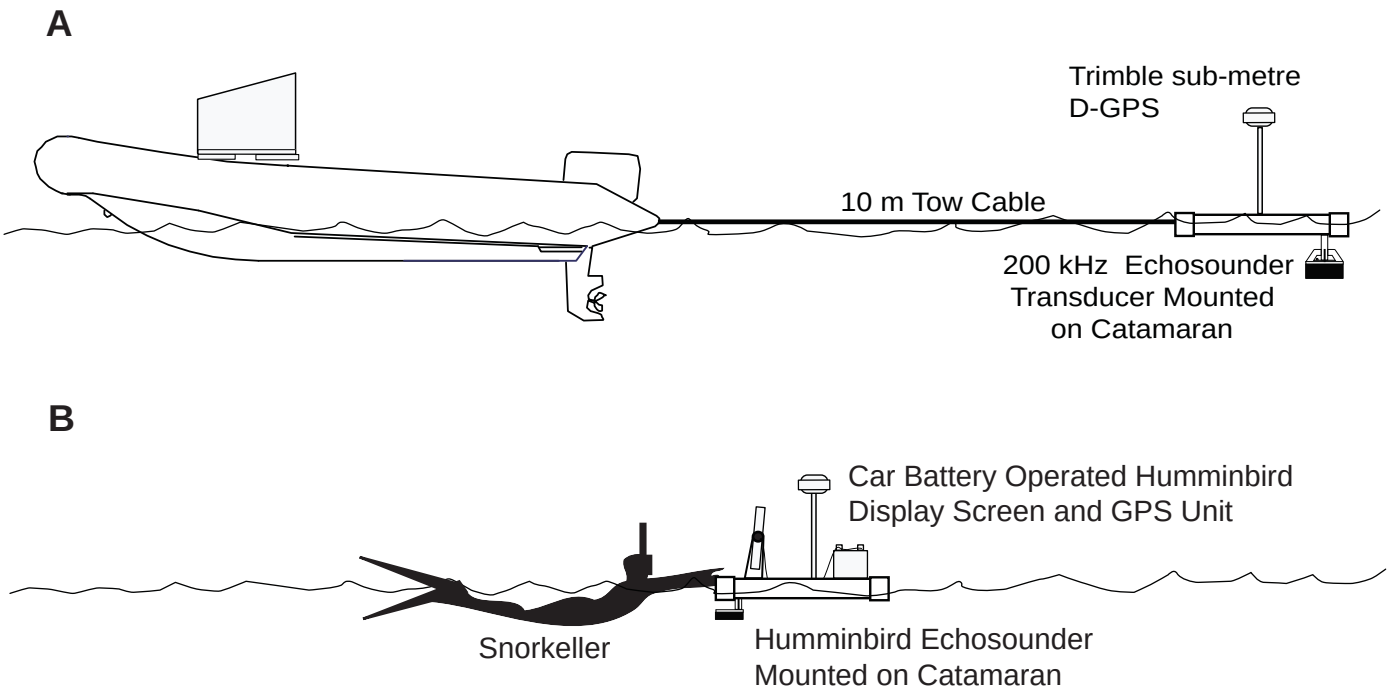


Figure 2.7: A) Equipment setup for regional bathymetric survey. B) Setup for high resolution shallow water bathymetric survey.

minimum curvature algorithm to generate the high resolution digital bathymetry model (DBM) of the inshore area adjacent to Kalamianos (Briggs, 1974). Using beachrock depths as constraints, various paleoshoreline configurations were generated using the DBM.

### 2.3.2. Diver Reconnaissance

A diver reconnaissance of the inshore area at Kalamianos was conducted using scuba equipment to investigate the submerged beachrock and other features of interest identified in the DBM. Samples of beachrock and pottery were collected from beachrock platforms at two different elevations (3.7 and 5.8 m.b.s.l.) and a full photographic documentation of submerged features was completed.

Beachrock samples collected at the 3.7 m.b.s.l. platform were discovered to contain large volumes of cemented clay pottery fragments and abundant charcoal fragments. The charcoal fragments were extracted and dated using AMS radiocarbon dating to date time of deposition of the beachrock sediments. Thin-sections of the beachrock samples were also produced for petrographic analysis.

## 2.4. Results

### 2.4.1. Bathymetry

Figures 2.8 and 2.9 show the results of detailed bathymetric mapping of the inshore area around Kalamianos. The water depth is less than 5 m across much of the inshore area and increases rapidly seaward, reaching a depth of more than 70 m within 300 m of the coast. The seabed relief is smooth with nearly continuous sediment cover, except in shallow water, where limestone bedrock and beachrock crop out in localized shoals. The bathymetry identified a

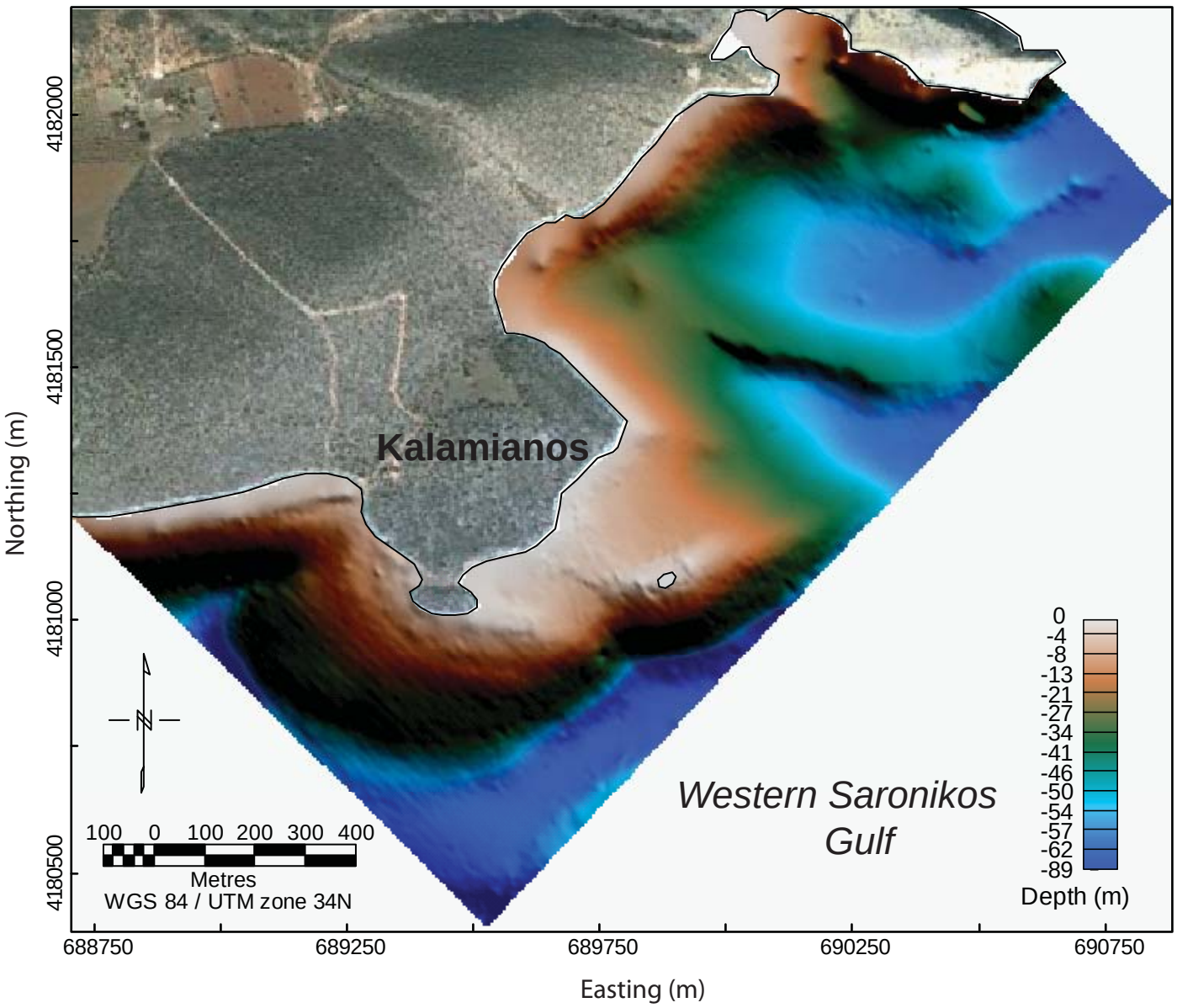


Figure 2.8: Regional colour-shaded digital bathymetry map at Kalamianos. Submerged isthmus identified southeast of Kalamianos. Note extension of normal faults visible in aerial photograph in bathymetric data.

submerged bedrock promontory on the east side of Akrotirio Trelli and a drowned isthmus that formerly connected the small island with the mainland coast. The submerged isthmus divides the inshore area into two separate lagoonal basins. Two distinct beachrock platforms (BR-1 and BR-2) were also identified in the bathymetry mapping and confirmed by underwater survey work (see description below).

In Figure 2.8, extending eastward from the coast at N 100˚ E, is the a northwest-southeast striking ridge that is consistent with the southeast-northwest normal faults of the Hellenic arc subduction zone. Of particular interest was the presence of a large and low gradient shallow region that was seen extending up to 400 m from the southeast shore of Kalamianos towards a small island. Water depth across this shallow inshore region near Kalamianos averaged 5 m and ranged from 0 m at the shoreline to a max depth of 10 m.

Several features of interest were identified within the shallow inshore region as seen from Figure 2.9 and Figure 2.10. Three concave inlets located adjacent to a pair of submerged promontories formed potential western, central and eastern anchorage basins (Fig. 2.9A). Two distinct platforms, BR-1 and BR-2, were apparent in the bathymetry at 3.7 and 5.8 m.b.s.l. respectively (Fig. 2.9 and Fig. 2.10). From Figure 2.9C, which models the shoreline at a lower sea level phase (5.8 m below modern), a 50-100 metre wide promontory was seen to connect mainland Kalamianos and the small island to form a small spit extending eastward into the gulf.

### 2.4.2. Beachrock

Two distinct beachrock platforms, BR-1 at 3.7 m and BR-2 at 5.8 m water depth, were identified in the shallows between the modern shoreline and the island outcrop (Fig. 2.9 and Fig. 2.10). Samples of BR-1 and BR-2 were collected through diver reconnaissance and analyzed by

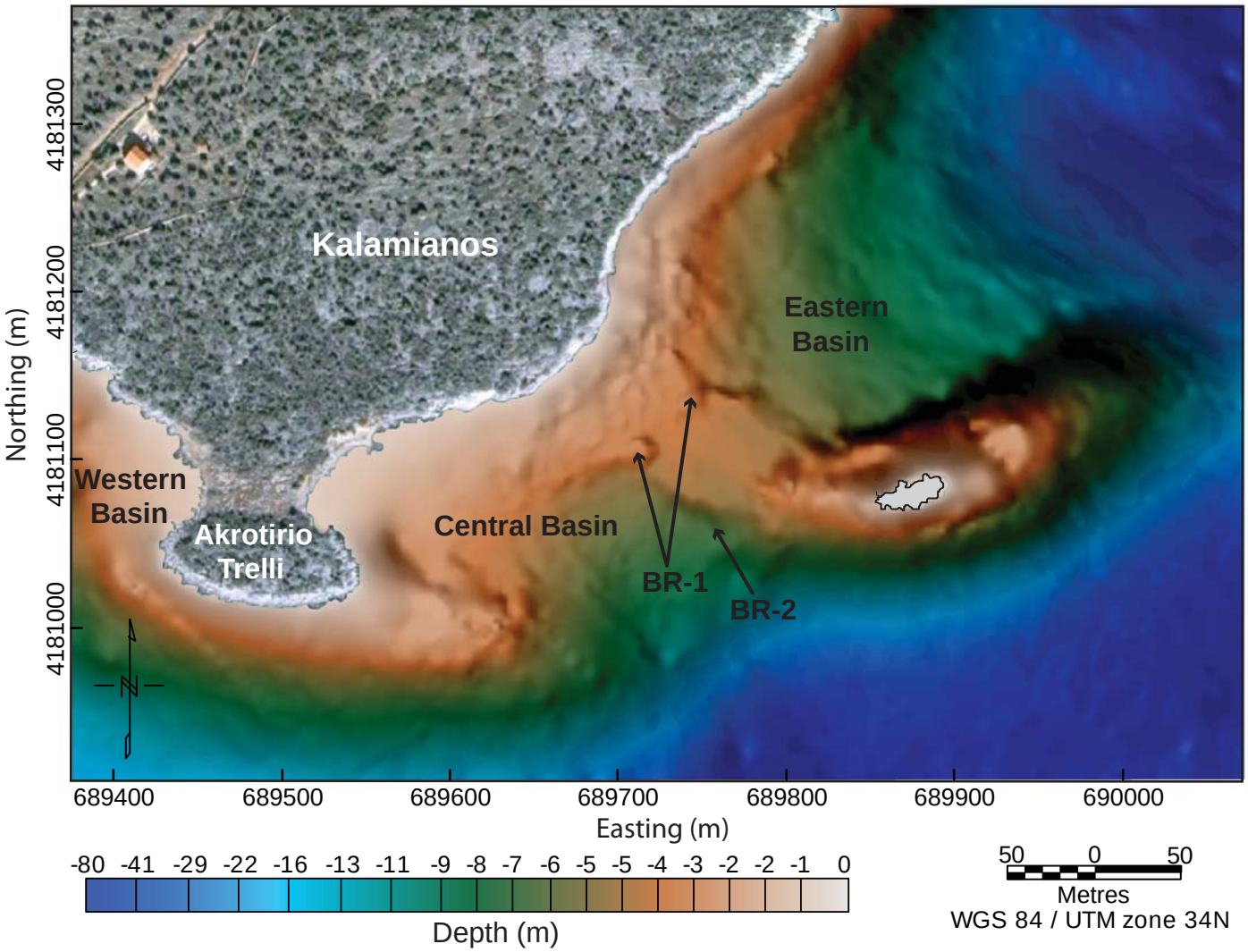


Figure 2.9A: Colour-shaded digital bathymetry map of the inshore area south of Kalamianos showing locations of beach rock ridges (BR-1, BR-2) and potential harbour basins.

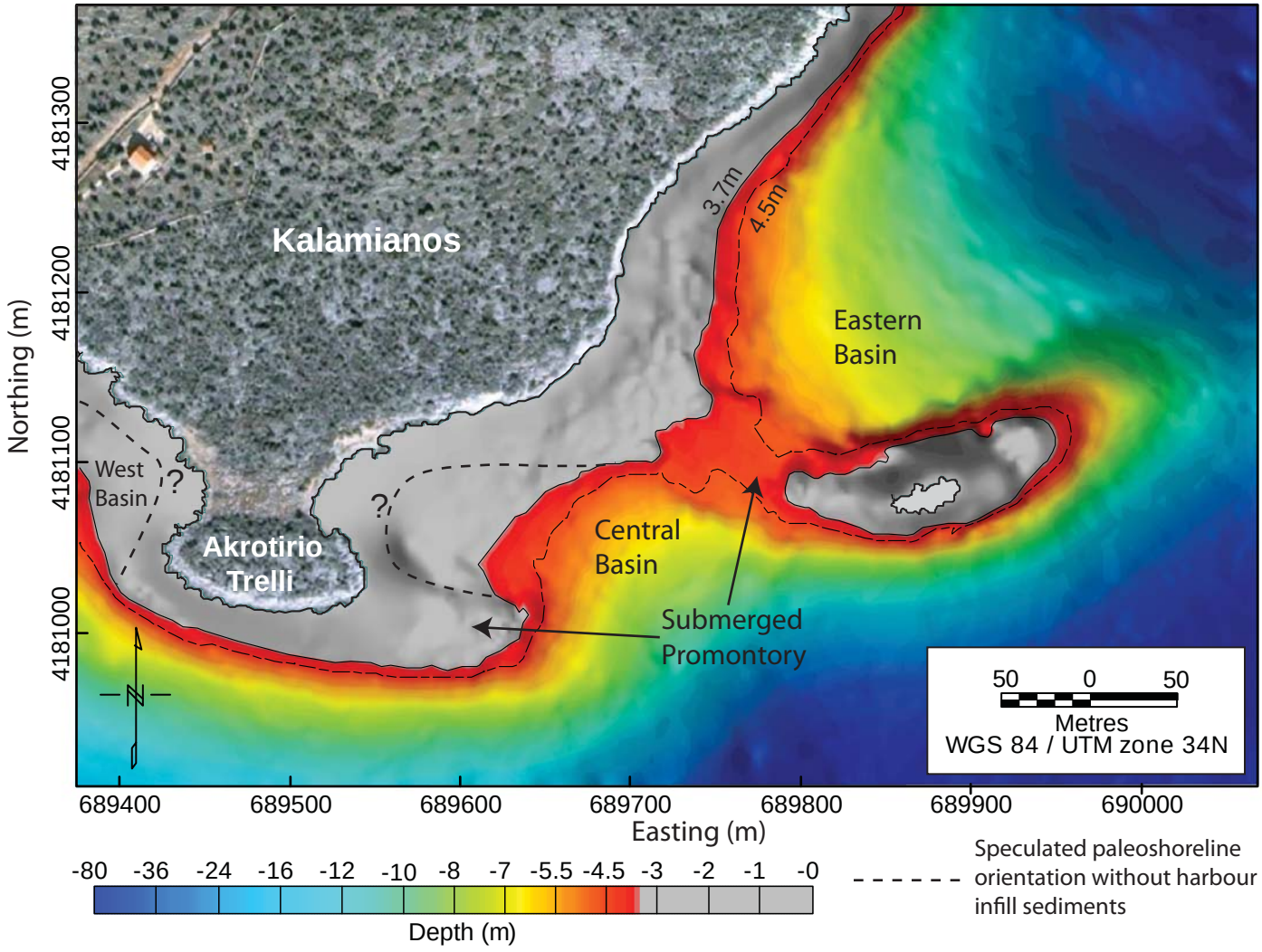


Figure 2.9B: Bathymetric model showing reconstructed paleoshoreline configuration during Mycenaean occupation (Late Helladic; 1300-1190 BC).

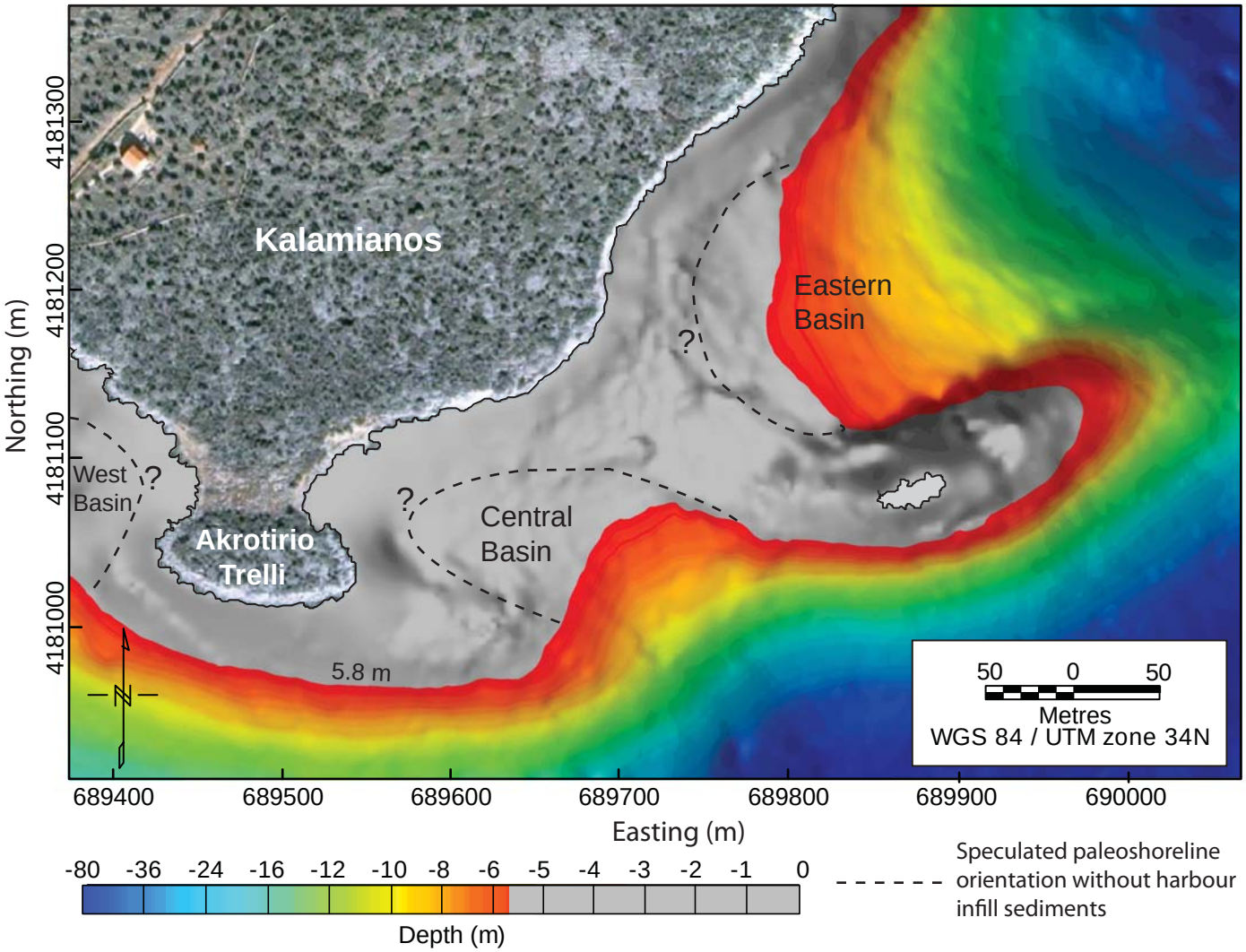


Figure 2.9C: Bathymetric model showing paleoshoreline configuration during Early Helladic (3100-2150 BC) occupation at Kalamianos.

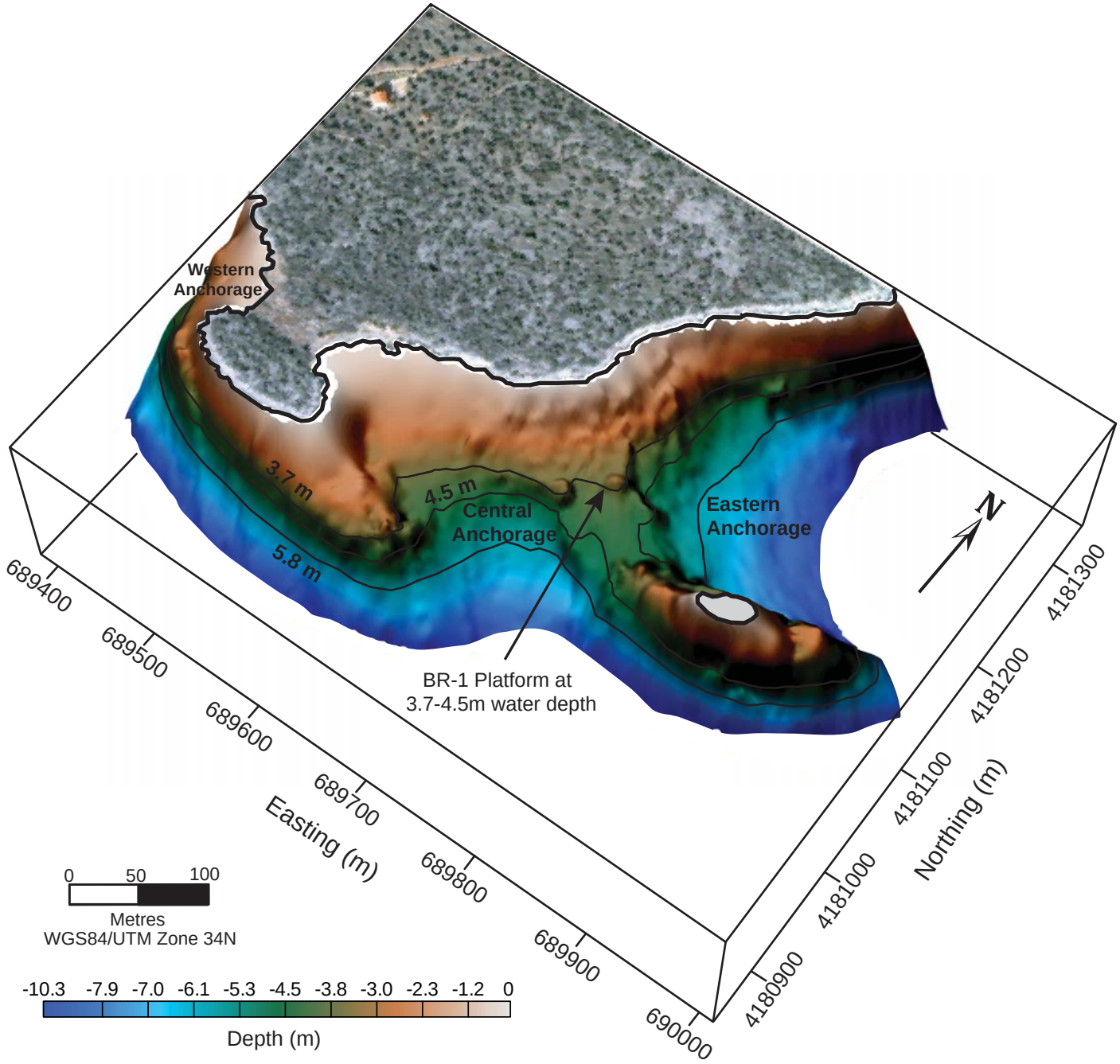


Figure 2.10: A 2.5-D colour-shaded digital bathymetric model of the inshore area at Kalamianos showing inundated promontory and potential anchorage sites during Late Helladic and Early Helladic lower phases of relative sea-level.

hand and in thin-section. The BR-1 beachrock is a calcarenite composed of approximately 20-40% pottery fragments and up to 40% carbonate shell material (Fig. 2.11A and Fig. 2.11B). The pottery fragments were identified to be of Mycenaean age, and dating to the LH IIIB period (1300-1190 BC)(Fig. 2.11C). AMS $^{14}C$ dating of wood charcoal yielded a 2-sigma calibrated age of 1616-1437 +/- 40 BC for BR-1 (Calib 6.0 software and the INTCAL09 database).(Fig. 2.11D). The charcoal appears to be a few hundred years older than that of the main Mycenaean Late Helladic IIIB phase of occupation (1300-1190 BC). The discrepancy may be attributed to the "old wood" effect or the wood fragments being remnants from a pre-Mycenaean phase of settlement, indicating that beachrock accumulation began just prior to the construction of the site.

Platform BR-2 yielded a beachrock with significantly different rock composition in comparison to BR-1. The beachrock BR-2 is a clast-rich bindstone with little matrix material. It comprises of <20% pottery fragments and ~65% carbonate shell material encrusted to a limestone bedrock spit and held together by a small amount of calcareous cement matrix (Fig. 2.12A). The encrusted pottery in BR-2 includes Early Helladic (ca. 3100-2150 BC) jars and bowls (corded ware) that provide a *terminus post quem* age for the formation of the BR-2 beachrock (Fig. 2.12B). The presence of Early Helladic pottery in BR-2 is consistent with pottery finds on the Akrotirio Trellis, which indicate an Early Bronze Age settlement phase at Kalamianos (Tartaron et al., in press).

Diver reconnaissance identified ballast stones scattered throughout the inshore area of Kalamianos. Several areas contain localized concentrations of ballast stones forming mounds consisting of andesitic and basaltic rocks with some Mycenaean pottery fragments and local limestone mixed within (Fig. 2.13).

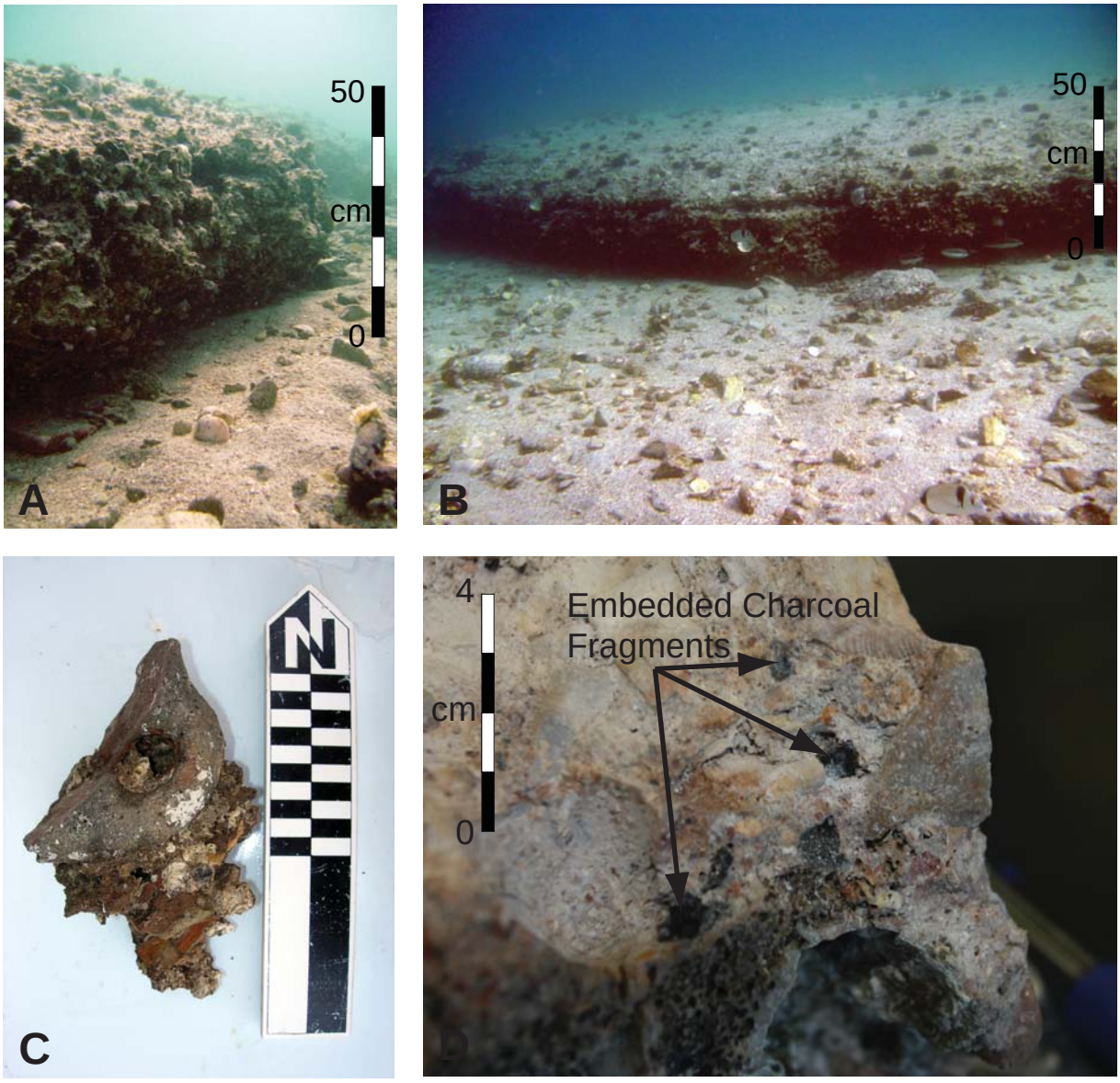


Figure 2.11: Underwater photographs of A) of beachrock platform BR-1 at 3.7-4.5 m water depth. B) Beachrock platform BR-2 at 5.8 m water depth. C) Mycenaean jug handle embedded and extracted from BR-1 beachrock. D) Charcoal fragments embedded within BR-1 beachrock.

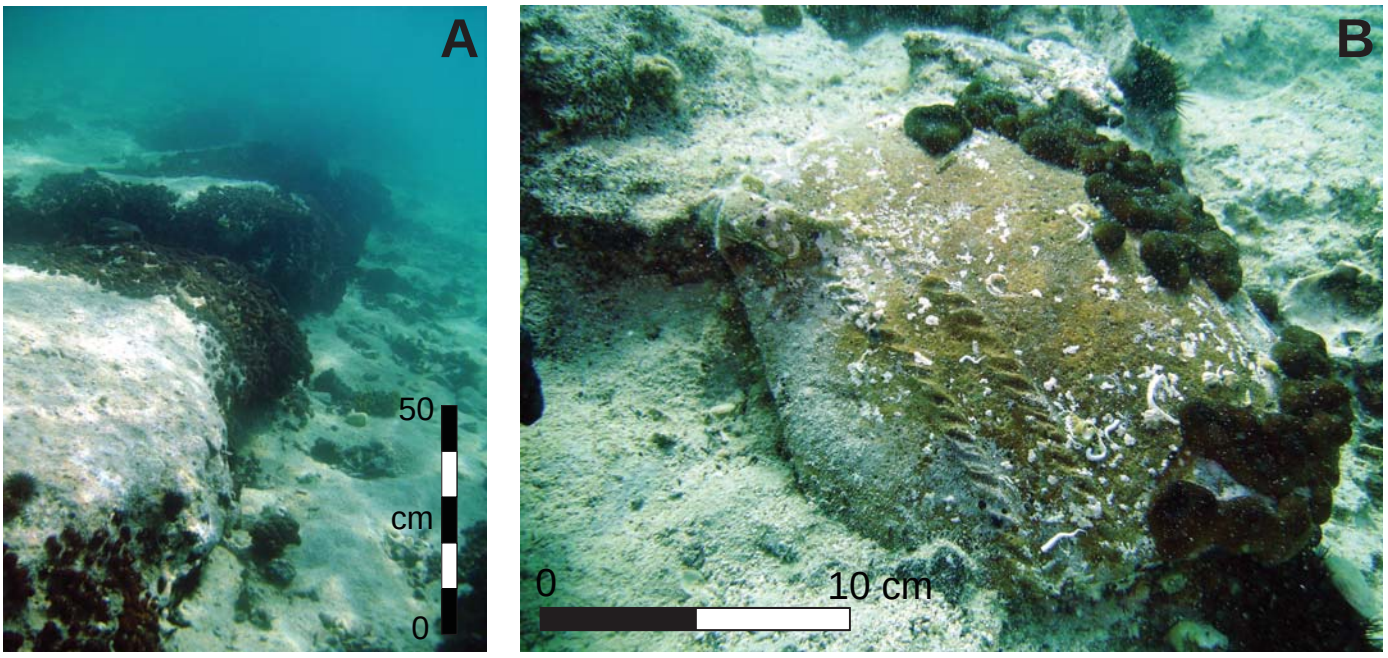


Figure 2.12: Underwater photographs of A) beachrock platform BR-2 in 5.8 m water depth. B) Well-preserved Early Helladic bowl fragment cemented in BR-2 beachrock.

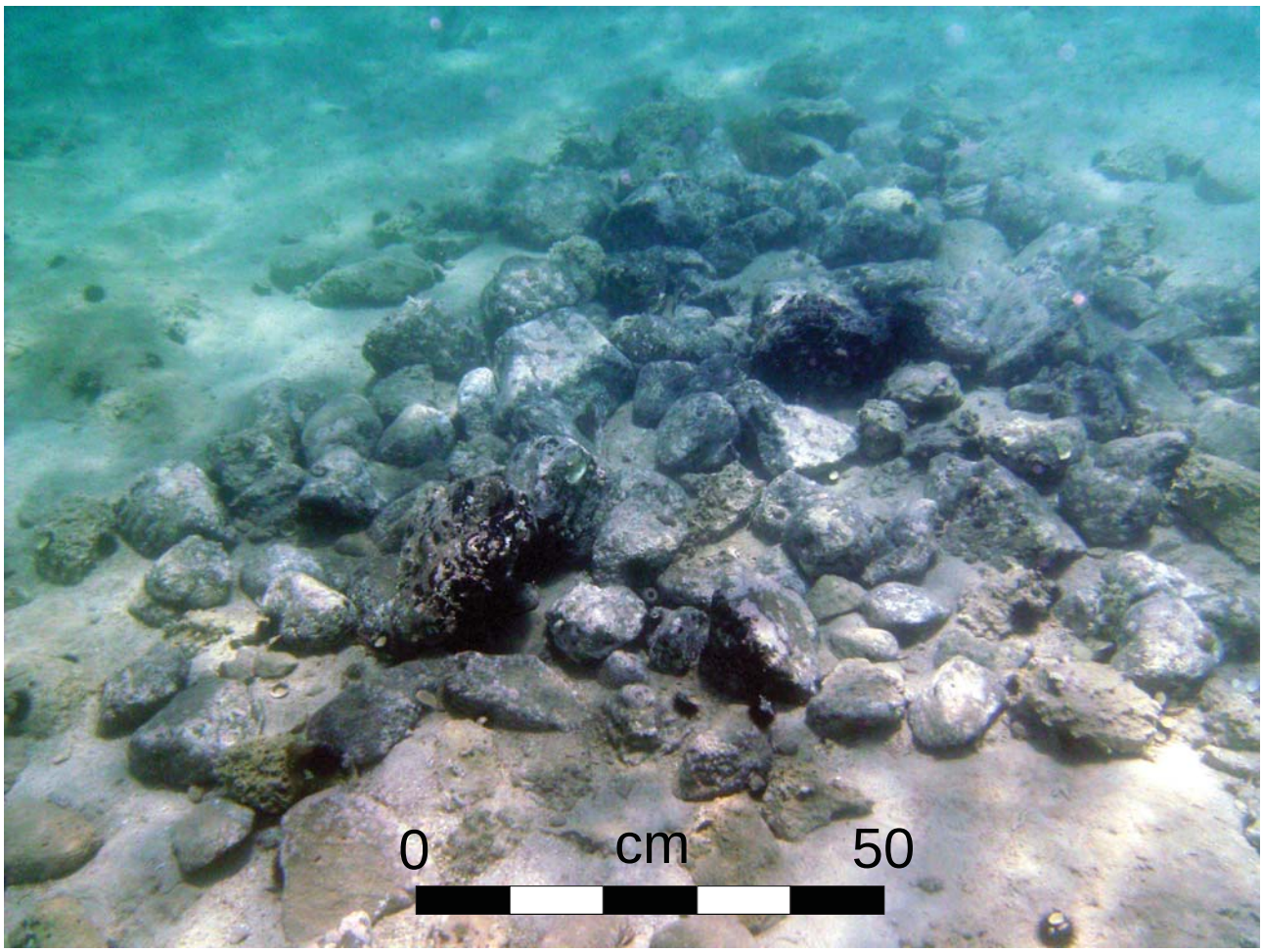


Figure 2.13: Underwater photograph of small ballast deposit consisting of limestone and andesitic cobbles and boulders.

### 2.4.3. Shoreline Reconstruction

BR-1 and BR-2 beachrock platforms and their estimated age ranges were used as a proxy for sea level at Kalamianos with each representing a separate phase of shoreline stabilization and beachrock formation. Radiocarbon dates obtained from BR-1 charcoal provided the estimated depositional age of BR-1. The age of BR-2 shoreline was estimated to approximately 2700 BC using the Early Helladic pottery as a proxy for age due to a lack of datable organic material. A sea-level curve was generated using the bathymetry and the top/bottom elevations of the dated beachrock in conjunction with sea level indicators of Nixon et al. (2009)(Fig. 2.14).

The Nixon et al. (2009) sea level curve, produced by dating organic matter in tidal notches in Korphos marsh, is slightly modified with the inclusion of BR-1 and BR-2 sea level points (Fig. 2.14). The RSL at Korphos and Kalamianos are compared with modeled eustatic and glacio-hydro-isostatic RSL curve for the Mediterranean by Lambeck and Purcell (2005). The curve at Kalamianos appears steeper, showing a higher rate of RSL rise at Kalamianos than at Korphos Bay and the rate suggested by the Lambeck and Purcell (2005) model from purely eustatic and isostatic effects. The differences in RSL can be attributed to tectonic effects and varying rates of localized coastal subsidence. The sea level curve was used in conjunction with the bathymetry data to generate two paleogeographic maps indicating the possible ancient coastline during the early Helladic settlement phase (Fig. 2.9C) and the main Mycenaean occupation period (Fig. 2.9B).

#### 2.4.3.1. Early Helladic Phase

The early Helladic coastline extends up to an extra 150 m into the Saronikos Gulf at a water depth of ~5.8 m relative to the modern shoreline. The promontory that was observed in the

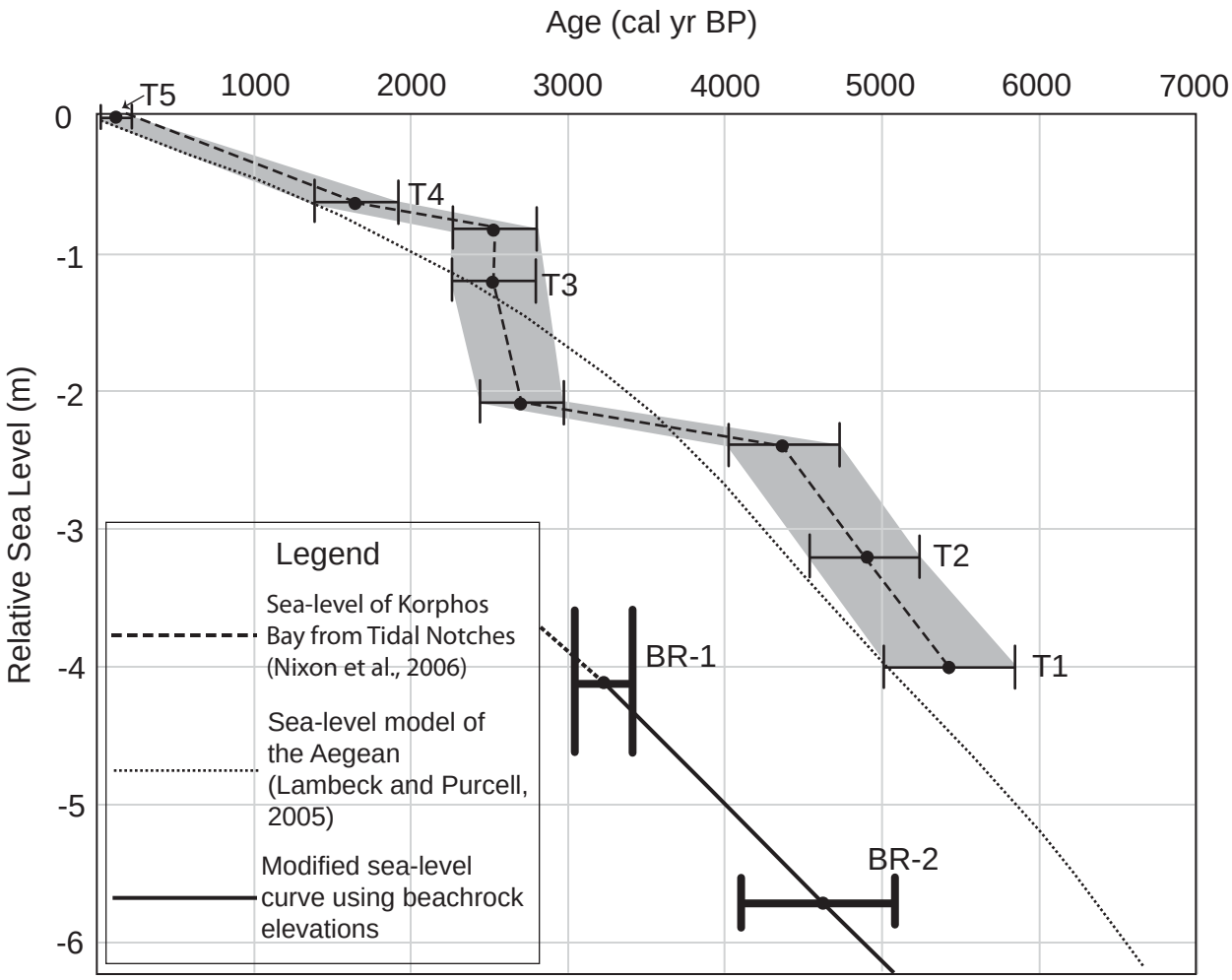


Figure 2.14: Sea-level curve for Korphos Bay from Nixon et al. (2009) with beachrock sea-level indicator from this study for comparison. Beachrock elevations lie well below the predicted RSL curve (Lambeck and Purcell, 2005) indicating active tectonic subsidence of the coastline at Kalamianos since the Early Helladic occupation.

bathymetry is seen above water and connects the island outcrop to the mainland forming a spit/tombolo with the potential to have been used as a natural harbour pier (Fig. 2.10). Also, beaches and shallow water to the east and west of the spit form small natural embayments.

#### 2.4.3.2. Mycenaean Phase

The coastline during Mycenaean occupation lies at a higher elevation than the early Helladic phase due to relative sea level rise but remains below the modern coastline. The coast extends up to 100 m from the modern shoreline at 3.7 m-4.5 m water depth (Fig. 2.10). The promontory observed at this time was submerged in very shallow water depths (< 1 m), disconnecting the island outcrop from the mainland but a much larger area of the island remained above water relative to modern day. However, the submerged promontory may have been within the intertidal zone and would be exposed above water at certain times of day.

## 2.5. Discussion

### 2.5.1. Coastal Subsidence

Preliminary field mapping of fault and fracture systems in the Korphos-Kalamianos region has identified several fault blocks. Kalamianos is located on a footwall block which displays evidence for recent downward movement relative to an adjacent block in the northeast. A large northwest-southeast trending fault scarp with well preserved slickensides at 85°-90° provide evidence for several metres of recent near vertical displacement (Fig. 2.15). The observed fault planes are part of the series of normal faults associated with crustal extension of the Aegean Plate from a right-lateral shear system imposed by the Hellenic Arc subduction zone (Fig. 2.3) (Armijo et al., 1996; Nixon et al., 2009). Regional faults of the Korphos-Kalamianos

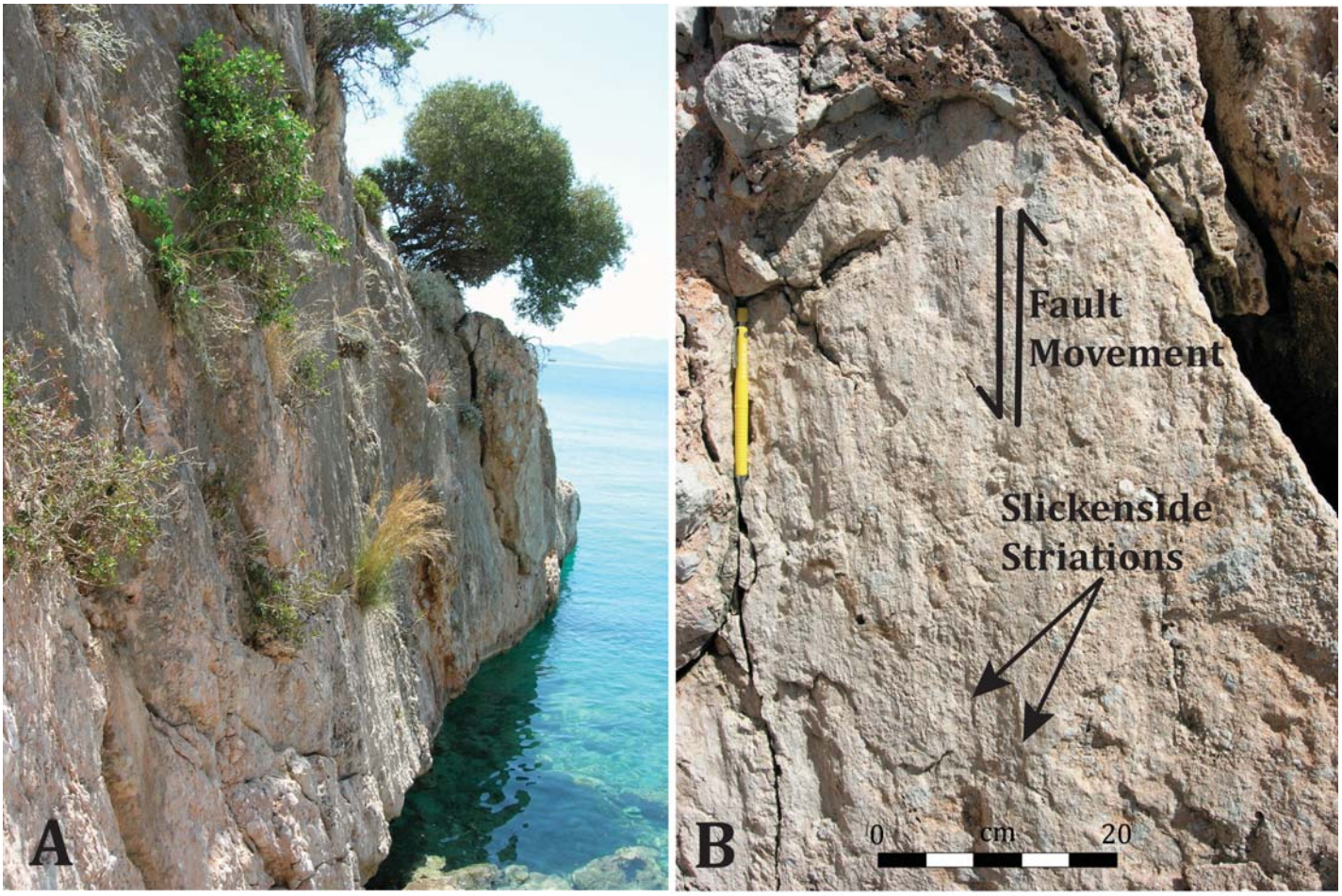


Figure 2.15: A) Steeply dipping fault scarp defining northeastern hanging wall block of normal fault to northeast of Kalamianos. B) Slickenside striations on fault plane pitching 83°, indicating oblique slip motions.

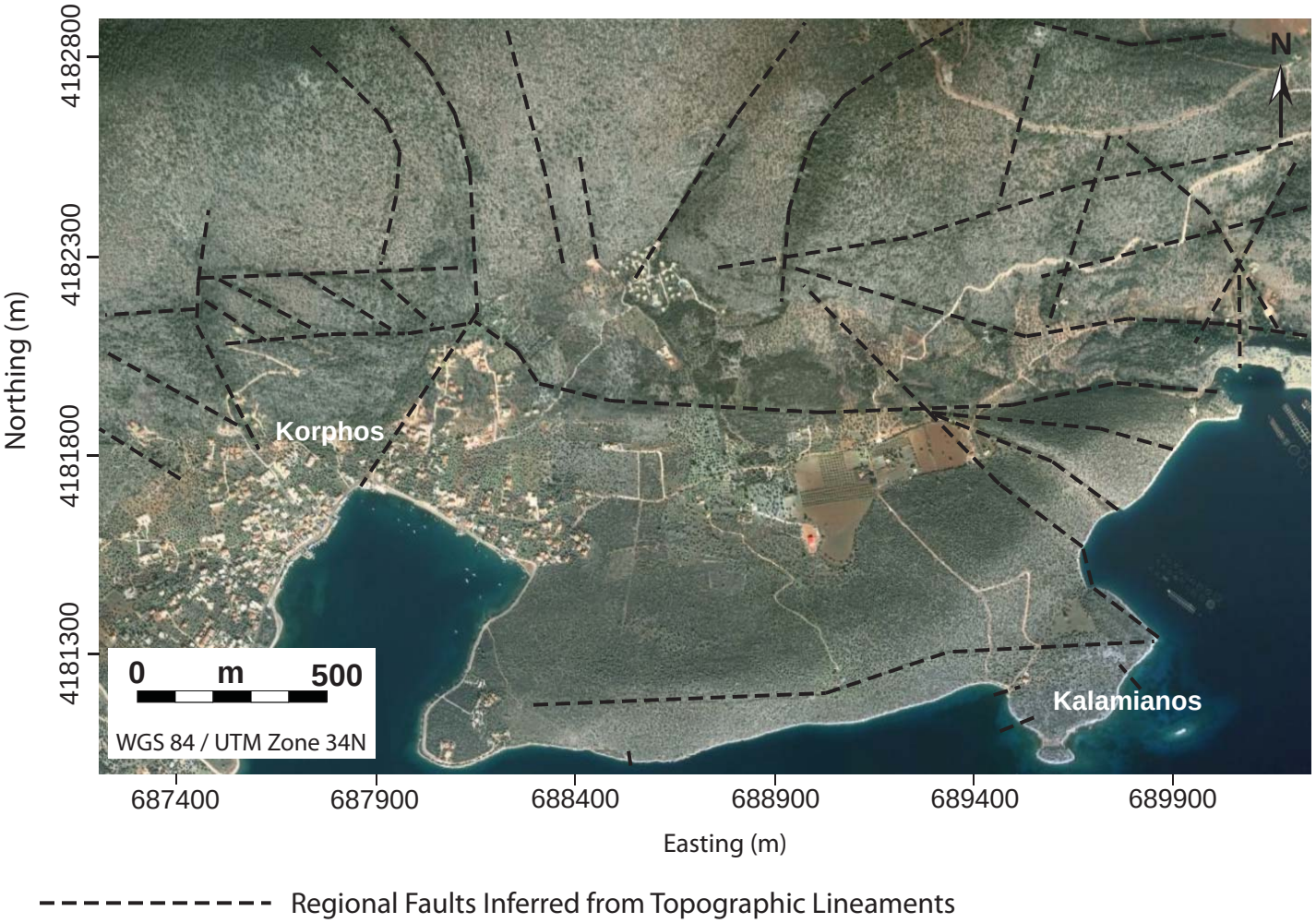


Figure 2.16: Aerial photo of the Korphos-Kalamianos region with inferred faults based on topographic lineaments.

region inferred using topographic relief observed from satellite imagery reveal a landscape dominated by fault systems (Fig. 2.16) (Google Earth Ltd., 2010). There is a significant risk of major earthquakes for the region surrounding Kalamianos, with known earthquake event in 1986 (Lyon-Caen et al., 1988). There remains a possibility that a major earthquake event resulted in the subsequent destruction and abandonment of Kalamianos during either the early Helladic and/or Mycenaean period.

Using the modern shoreline as a predictor to locate submerged harbour sites is a poor approach (Goodman et al. 2009). Effective reconstruction of submerged landscapes requires a detailed history of RSL for understanding the paleogeographic context of inundated areas and for modeling paleoshorelines. Available Late Holocene sea level models of the Mediterranean Sea are computed considering only eustatic and glacio-hydro-isostatic variables with a lack of tectonic variables (Lambeck and Purcell, 2005). Active neotectonics in the Korphos-Kalamianos region is an extra variable that must be considered for paleoshoreline reconstruction.

A previous study by Nixon et al. (2009) at a salt marsh nearby the town of Korphos, Greece, produced a sea level curve of Korphos Bay through examination of tidal notches and foraminifera/thecamoebians fossil assemblages in sediment cores. The addition of BR-1 and BR-2 radiocarbon dates and water depths from this study allowed for the modification of the sea level curve to represent relative change Kalamianos (Fig. 2.14). There was an observable difference in the rates of sea level rise between Korphos marsh and Kalamianos, with relative sea level rise occurring at a greater rate at Kalamianos, located a short 2.5 km to the west. A model of eustatic and glacio-hydro-isostatic RSL sea level change for the Mediterranean was included in Figure 2.14 for comparison (Lambeck and Purcell, 2005). The rate of RSL rise at Kalamianos is greater (BR-1 and BR-2 is ~2 m higher) than what is suggested by the Lambeck and Purcell

(2005) model. Any observable difference from the eustatic and glacio-hydro-isostatic RSL model must be attributed to other factors including tectonics. Known neotectonic activity of the Hellenic arc subduction zone and major normal fault systems through the region (Fig. 2.3A and 2.15) suggested differential subsidence caused by multiple active fault segments within the area encompassing Korphos Bay.

### 2.5.2. Anchorage Sites

The availability of well-protected natural harbours is known to be an important determinant for the location of Bronze Age coastal settlements in the Aegean (Shaw, 1990; Marriner et al., 2006; Marriner and Morhange, 2007; Papageorgiou, 2007; Tartaron et al., 2003). Many settlements were located on or adjacent to peninsulas or rocky headlands presumably because they provided sheltered embayments and protected beaches where ships could be moored safely or beached for the transfer of goods (Raban, 1999; Shaw, 2000; Marriner and Morhange, 2007). Settlement on peninsulas may have also afforded more defensible positions against attack by land (Shaw, 2000). Man-made harbour constructions, such as harbour breakwaters and moles, which are common in later Iron Age and later classical harbours, do not appear have been a feature of Bronze Age Aegean coastal settlements. Such constructions have been identified in eastern Mediterranean harbours; the best documented examples being the Bronze Age harbour quays constructed at Tel Dor (Raban, 1985) and boat slips excavated into bedrock at Sidon (Marinner et al., 2006).

Essential features for any harbour include having suitable anchorage/mooring sites nearby that would provide ships some means of protection from extreme weather while in dock. Reconstruction of the paleo-shoreline during the Mycenaean occupation and early Helladic

settlement (Fig. 2.9) has identified a shallow beach embayment east and west of two promontories (Fig. 2.10).

Water depth of the small embayments during the Late Bronze Age ranged up to 2 metres, an ample water depth for even the largest ships of that time period. The paleo-shoreline model indicated that the promontory itself at this time remained submerged but was within very shallow water (< 1 m) if we use the top of beachrock depth (3.7 m.b.s.l.) as a proxy for sea level (Fig. 2.9B). If this was the context during Mycenaean occupation, there exists the potential for a constructed boardwalk that would have connected Kalamianos to the island and would have provided a means for ships to moor and transfer cargo. Unfortunately, this theory is difficult to prove since any materials made from wood would have long been destroyed from exposure to the elements. However, we must also consider the accuracy of using beachrock as a proxy for sea level. The formation of beachrock in the intertidal zone suggests that the top of the beachrock platform would represent the upper limit of possible sea level and the bottom of the beachrock represents the lower limit. If we consider sea level from bottom of beachrock elevation at 4.5 m.b.s.l., the promontory appears exposed above water (Fig. 2.9B). During the EH period when RSL was lower than during the LH, the promontory is revealed to have been clearly above sea level.

BR-1 observed in the bathymetry represented the shoreline beach of Kalamianos during Mycenaean occupation in the Late Helladic. In particular, the section of BR-1 off the coast of Kalamianos represented the beach associated with the potential western and eastern anchorage sites and within this unit exist the highest concentration of Mycenaean pottery fragments. The large concentration of pottery provided evidence for significant activity along the beach and could have potentially originated as refuse dumped by ships while in harbour.

Diver reconnaissance identified the presence of ballast piles with concentrations of andesitic materials (Fig. 2.13). The andesitic rock, which was of volcanic origin, was not native to the region near Kalamianos and was likely derived from the volcanic Cycladic islands including Aegina, Santorini, Milos and Methana among others. This provided evidence that Kalamianos was a significant harbour town with active maritime trading.

A separate study by Dao et al. (*In Review*) using magnetic geophysical surveying methods also demonstrated the presence of extensive scattering of buried ballast stones and pottery fragments within the inshore area of Kalamianos, which support the suggested location of the harbour and anchorage sites seen in Figure 2.10.

### 2.5.3. Beachrock Origins

The submerged beachrock platforms at Kalamianos provide critical evidence for coastal subsidence in Korphos Bay and support previous study by Nixon et al., (2009). However, beachrock as a sea level indicator remain in debate due to gaps in knowledge about their exact process of formation (Kelletat, 2006; Knight, 2007). Preliminary petrographic examination of beachrock BR-1 indicated a composition that identified it to be that of a calcarenite with the presence of sparry calcite formation within pore spaces, which suggest formation in a supratidal nearshore environment along the coast from carbonate precipitation due to supersaturation of sediments and degassing of $CO_2$ (Hanor, 1978; Meyers, 1987; Omoto, 2004). The presence of charcoal fragments within samples of BR-1 also provides evidence that deposition and beachrock formation occurred in a supratidal environment where the charcoal would not be washed away by wave and tidal action. However, this suggests that sea level would be slightly lower than

actual beachrock elevations. One needs to consider that the paleoshorelines reconstructed using top of beachrock elevations are in actuality the extreme upper limit of possible RSL.

BR-2 was identified to be not a true beachrock but rather a bindstone composed of Early Helladic pottery fragments, shell fragments and limestone pebbles all cemented together by a small amount of calcareous matrix. This study assumed that the lithification process of BR-2 was similar to that of beachrock formation (BR-1), a product of cementation by carbonate precipitates. The issues with using BR-1 as a proxy for RSL apply to BR-2 as well. Also, the depositional environment and age of formation of the material was not as evident, which casts further doubt into its suitability as a marker for sea level. Deposition of the substrate materials could have occurred in a supratidal environment that was subsequently submerged rapidly due to faulting induced subsidence, or the pottery could have simply been deposited directly into already submerged sediments. The former theory would put BR-2 as a suitable indicator whereas the ladder would not.

Further work with BR-1 and BR-2 would include a detailed isotopic and petrographic analysis which may help reveal more evidence towards their depositional environment and formation and assess their suitability as a sea level indicator.

### 2.5.4 Archaeological Implications

The geological setting and extensive fault and fracture systems observed in the limestone bedrock of the Korphos-Kalamianos area act as conduits for groundwater flow. Extensive artesian springs could be seen along the coast near and at Kalamianos with significant flow volumes occurring even in modern day. An active fracture system connects mainland Kalamianos to the island outcrop towards the southeast and the presence of groundwater springs

can be seen extending towards the island itself along the fracture zone. Surficial freshwater in the Peloponnese is scarce and almost all ancient settlements relied on freshwater springs (e.g. Mycenae, Athens, Corinth). The abundance of freshwater springs would have made Kalamianos an attractive location for construction of a large settlement

Kalamianos was strategically advantageous for the militaristic Mycenaean civilization and positions itself well within the geography of Mycenaean Greece. A natural topography of steep cliffs and high mountains made Kalamianos a natural fortress. The high mountains along the coast also provide advantageous lookout points to monitor a large area of the Saronikos Gulf. Abundant freshwater springs in the region would also add to the attraction of the site. There were no evidence for a constructed harbour at Kalamianos but during the Early Helladic phase, the island was determined to have connected to the mainland to form a recurved spit, which would have acted as an ideal natural harbour configuration. Also, a rugged coastline and various natural embayments and inlets would have provided protection from the weather for ships thus eliminating the need to construct manmade breakwaters. Taking advantage of the natural geography, the site would have been near ideal for early settlers where minimal construction would be required to establish a fortified harbour town.

Situated a short 30 km northeast of Mycenae, 60 km southwest of Athens and facing southeast towards the Cycladic Islands along the Aegean, Kalamianos was well positioned within central Greek civilization. It may have played a significant role in Mycenaean maritime trade by acting as a central hub for people and goods travelling from western Mycenaean Greece (Mycenae, Argos, Tiryns) to eastern Mycenaean Greece (Athens and Thebes) and trade with the Cycladic Islands in the Aegean. This central location would have also made Kalamianos a strategic location for the anchorage of the Mycenaean Navy.

## 2.6. Summary

In this paper, we reconstruct the configuration of the Bronze Age coastline at Kalamianos using detailed digital bathymetric data and radiocarbon dating of submerged beachrock ridges. The results indicate that the coastline has undergone up to 6 m of relative sea level rise of which up to ~2 m could be attributed to co-seismic subsidence since the site was first occupied during the Early Helladic period and delineates the location of now potential anchorage/harbour sites. The relative sea level curve reconstructed for Kalamianos agrees well with previous work and indicates rapid, co-seismic subsidence of the coastline following the site occupation. Submerged archaeological sites are common around the Saronic Gulf and elsewhere in the Aegean and the methods reported here can be applied more broadly to reconstruction of the regional subsidence history, providing important baseline data for locating new underwater archaeological sites.

## 2.7. References

Armijo, R., Lyon-Caen, H., Papanastassiou, D., 1992. East-west extension and Holocene normal-fault scarps in the Hellenic arc. Geology 20(6), 491-494.

Armijo, R., Meyer, B., King, G.C.P., Rigo, A., Papanastassiou, D., 1996. Quaternary Evolution of the Corinth Rift and its Implications for the Late Cenozoic Evolution of the Aegean. Geophysical Journal International 126(1), 11-53.

Baika, K., 2008, Archaeological indicators of relative sea level changes in the Attico-Cycladic massif: preliminary results. Bulletin of the Geological Society of Greece 42, 33-48.

Bailey, G.N. and Flemming, N.C., 2008, Archaeology of the continental shelf: Marine resources, submerged landscapes and underwater archaeology. Quaternary Science Reviews, 27, 2153-2165.

Blackman, D.J., 1982a. Ancient harbours in the Mediterranean, part 1. International Journal of Nautical Archaeology 11, 79-104.

Blackman, D.J., 1982b. Ancient harbours in the Mediterranean, part 2. International Journal of Nautical Archaeology 11, 185-211.

Boyce, J.I., Reinhardt, E.G., Raban, A., Pozza, M.R., 2004. Marine magnetic survey of a submerged Roman harbour, Caesarea Maritima, Israel. International Journal of Nautical Archaeology 33(1), 122-136.

Boyce, J.I., Krezoski, G.M., Reinhardt, E.G., Goodman, B.N., Artzy, M., 2006. Marine Geophysical Mapping of Bronze-Age Harbor Structures, Liman Tepe, Turkey. Geological Society of America Abstracts with Programs 38(7), 150.

Boyce, J.I., Reinhardt, E.G., Goodman, B.N., 2009. Magnetic detection of ship ballast deposits and anchorage sites in King Herod's Roman harbour, Caesarea Maritima, Israel. Journal of Archaeological Science 36(7), 1516-1526.

Bracco, J.-P., 2005. Archaeological sites. In: Petit-Maire, N., Vrielinck, B. (Eds.), The Mediterranean Basin: The Last Two Climatic Cycles – Explanatory Notes of the Maps. Maison Méditerranéenne des Sciences de l'Homme, Aix-en-Provence, pp. 83-89.

Bricker, O.P., 1971. Introduction: beachrock and intertidal cement. In: Bricker, O.P. (Ed.), Carbonate Cements. Johns Hopkins Press, Baltimore, pp. 1–13.

Briggs, I. C., 1974. Machine contouring using minimum curvature. Geophysics, 39: 39–48.

Brun, J.P. and Dimitrios, S., 2010. 45 m.y. of Aegean crust and mantle flow driven by trench retreat, Geology, v. 38, p. 815-818.

Burchfiel B.C., Nakov R.,Tzankov T., 2003. Evidence from the Mesta half-graben, SW Bulgaria, for the Late Eocene beginning of Aegean extension in the Central Balkan Peninsula: Tectonophysics, v. 375, p. 61–76.

Cahoon, D.R., Reed, D.J., Day Jr., J.W., 1995. Estimating shallow subsidence in microtidal salt-marshes of the southeastern United States: Kaye and Barghoorn revisited. Marine Geology 128, 1–9.

Chivas, A., Chappell, J., Polach, H., Pillans, B., Flood, P., 1986. Radiocarbon evidence for the timing and rate of island development, beach-rock formation and hosphatization at Lady Elliot Island, Queensland, Australia. Mar. Geol. 69, 273–287.

Clift, P.D., Robertson, A.H.F., 1990. Deep-water basins within the Mesozoic carbonate platform of Argolis, Greece. Journal of the Geological Society 147, 825-836.

Collins, D., Dunn, R.K., 2008. Using Late Bronze Age Walls at Kalamianos, Greece, to Determine a Minimum Rate of Rillenkarren Formation. Geological Society of America Abstracts with Programs 40(2), 66.

Dao, P., Boyce, J., Koutsoumba, D., Tartaron, T., Pullen, D., In Review. Tri-axial Gradiometer Survey of Bronze Age Anchorage at Kalamianos (Korphos, Greece). Journal of Archaeological Science.

Erginal, A.E., Kiyak, N.G., Ozturk, B., 2010. Investigation of Beachrock Using Micoanalyses and OSL Dating: A Case Study from Bozcaada Island, Turkey. Journal of Coastal Research 26(2), 350-358.

Ersoy, Y., 1993. Clazomenae: The Archaic settlement. PhD Thesis, Bryn Mawr College, 320 p.

Fleury, P., Bakalowicz, M., Marsily, G. de, 2007. Submarine springs and coastal karst aquifers: A review. Journal of Hydrology 339, 79-92.

Flemming, N.C., 1999, Archaeological evidence for vertical movement on the continental shelf during the Palaeolithic, Neolithic and Bronze Age periods. Geological Society, London, Special Publications 1999, v. 146, p. 129-146.

Frankel, E., 1968. Rate of formation of beach rock. Earth Planet. Sci. Lett. 4, 439–440.

French, E. B., Iakovidis, S.E., Ioannides, C., Jansen, A., Lavery, J., Shelton, K., 2003. Archaeological Atlas of Mycenae. Archaeological Society at Athens Library 229, Athens.

Galili, E., Weinstein-Evron, M., Ronen, A., 1988. Holocene Sea level Changes Based on Submerged Archaeological Sites off the Northern Carmel Coast in Isreal. Quaternary Research 29, 36-42.

Galili, E., Weinstein-Evron, M., Hershkovitz, I., Gopher, A., Kislev, M., Lernau, O., Kolska-Horwitz, L., Lernau, H., 1993. Atlit-Yam: a prehistoric site on the sea floor off the Isreali coast. Journal of Field Archaeology 20, 133-157.

Goddio, F., Bernand, A., Bernand, E., Darwish, I., Kiss, Z., Yoyotte, J., 1998. Alexandria: The Submerged Royal Quarters. Periplus, London.

Goodman, B.N., Reinhardt, E.G., Dey, H.W., Boyce, J.I., Schwarcz, H.P., Sahoglu, V., Erkanal, H., Artzy, M., 2009. Multi-proxy geoarchaeological study redefines understanding of the paleocoastlines and ancient harbours of Liman Tepe (Iskele, Turkey). Terra Nova 21(2), 97-104.

Hanor, J.S., 1978. Precipitation of Beachrock Cements: Mixing of Marine and Meteoric Waters VS. $CO_2$-degassing. Journal of Sedimentary Petrology 48(2), 489-501.

Harding, A., Cadogan, G. and Howell, R., 1969, Pavlopetri, an underwater Bronze Age town in Laconia. Annual of the British School at Athens 64, 112-142.

Henderson, J.C., Gallou, C., Flemming, N.C. and Spondylis, E., in press, The Pavlopetri Underwater Archaeology Project: investigating an ancient submerged town, J. Benjamin and C. Bonsall, Eds. Oxbow Books, Oxford.

Jacobsen, T.W., Farrand, W.R., 1987. Franchthi Cave and Pralia: maps, plans and sections, in: Excavations at Franchthi Cave, Greece, Fascicle I. Indiana University Press, Bloomington, Indianapolis.

Kaye, C.A., Barghoorn, E.S., 1964. Late Quaternary sea level change and crustal rise at Boston, Massachusetts, with notes on the autocompaction of peat. Geological Society of America Bulletin 75, 63–80.

Kelletat, D., 2006. Beachrock as sea level indicator? Remarks from a geomorphological point of view. Journal of Coastal Research 22 (6), 1555–1564.

Knight, J., 2007. Beachrock Reconsidered. Discussion of: KELLETAT, D., 2006. Beachrock as Sea level Indicator? Remarks from a Geomorphological Point of View. Journal of Coastal Research, 22(6), 1558-1566. Journal of Coastal Research 23(4), 1074-1078.

Kraft, J.C., Kayan I., Erol, O., 1980. Geomorphic Reconstructions in the Environs of Ancient Troy. Science 209(4458), 776-782.

Lambeck, K., 1996. Sea level change and shore-line evolution in Aegean Greece since Upper Palaeolithic time. Antiquity 70, 588, 610.

Lambeck, K., and Purcell, A., 2005. Sea level change in the Mediterranean Sea since the LGM, model predictions for tectonically stable areas. Quaternary Science Reviews 24, 1969-1988.

Liritzis, I., Katsonopoulou, D., Soter, S., Galloway, R.B., 2001. In Search of Ancient Helike, Gulf of Corinth, Greece. Journal of Coastal Research 17(1), 118-123.

Lyon-Caen, H., Armijo R., Drakopoulos, J., Baskoutass, J., Delibassis, N., Gaulon, R., Kouskouna, V., Latoussakis, J., Makropoulos, K., Papadimitriou, P, Papanastassiou, D., Pedotti, G., 1988. The 1986 (South Peloponnesus) Earthquake: Detailed Study of a Normal Fault, Evidence for East-West Extension in the Hellenic Arc. Journal of Geophysical Research 93(12), 14967-15000.

Mahon, I., Pizarro, O., Johnson-Roberson, J., Friedman, A., Williams, S.B., Henderson, J.C., 2011. Reconstructing Pavlopetri: Mapping the World's Oldest Submerged Town using Stereo-vision. IEEE International Conference on Robotics Automation 9-13 May 2011, 2315-2321.

Maran, J., 2002-03. The Town of Tiryns after the Fall of the Palace: Some New Insights. BICS 46, 223-224.

Marriner, N., Morhange, C., Boudagher-Fadel, M., Bourcier, M., Carbonel, P., 2005. Geoarchaeology of Tyre's ancient northern harbour, Pheonicia. Journal of Archaeological Sciences 32, 1302-1327.

Marriner, N., Morhange, C., Doumet-Serhal, C., 2006. Geoarchaeology of Sidon's ancient harbours, Phoenicia. Journal of Archaeological Science 33(11), 1514-1535.

Marriner, N., Morhange C., 2007. Geoscience of ancient Mediterranean harbours. Earth-Science Reviews 80, 137-194.

Marriner, N., Morhange, C., Goiran, J.P., 2010. Coastal and ancient harbour geoarchaeology. Geology Today 26(1), 21-27.

Meyers, J.H., 1987. Marine Vadose Beachrock Cementation by Cryptocrystalline Magnesian Calcite - Maui, Hawaii. Journal of Sedimentary Petrology 57(3), 558-570.

Miller, G., Dunn., R.K., 2009. Brittle Fracture Analysis and Identification of Bronze Age Water Resources at Kalamianos, Eastern Peloponnese, Greece. Geological Society of America Abstracts with Programs 41(3), 96.

Minor, R., Grant, W.C., 1996. Earthquake-induced Subsidence and Burial of Late Holocene Archaeological Sites, Northern Oregon Coast. American Antiquity, 61(4), 772-781.

Minty, B.R.S., 1991. Simple Mirco-Levelling for Aeromagnetic Data. Exploration Geophysics 22, 591-592.

Nixon, F.C., Reinhardt, E.G., Rothaus, R., 2009. Foraminifera and tidal notches: Dating Neotectonic events at Korphos, Greece. Marine Geology 257, 41-53.

Noller, J.,Wells, L., Reinhardt, E.G., Rothaus, R., 1997. Subsidence of the Harbor at Kenchreai, Saronic Gulf, Greece, during the Earthquakes of a.d. 400 and a.d. 1928. Eos 78, 636

Omoto, K., 2004. Radiocarbon ages and isotope fractionations of beachrock samples collected from the Nansei islands, southwestern Japan. *Radiocarbon,* 46, 539–550.

Paoletti, V., Secomandi, M., Piromallo, M., Giordano, F., Fedi, M., Rapolla, A., 2005. Magnetic Survey at the Submerged Archaeological Site of Baia, Naples, Southern Italy. Archaeological Prospection 12, 51-59.

Papageorgiou, S., Arnold, M., Laborel, J., Stiros, S.C., 1993. Seismic uplift of the harbour of ancient Aigeira, Central Greece. International Journal of Nautical Archaeology 22, 275-281.

Papageorgiou, D., 2008. The marine environment and its influence on seafaring and marine routes in the Prehistoric Aegean. European Journal of Archaeology 11, 199-222.

Papanikolaou, D., Lykousis, V., Chronis, G., Pavlakis, P., 1988. A comparative study of Neotectonic basins across the Hellenic arc: the Messiniakos, Argolikos, Saronikos and Southern Evoikos Gulfs. Basin Research 1(3), 167-176.

Peltier, W.R., 2002. On eustatic sea level history, Last Glacial Maximum to Holocene. Quaternary Science Reviews 21, 377-396.

Pirazzoli, P.A., Stiros, S.C., Arnold, M., Laborel, J., Laborel-Deguen, F., Papageorgiou, 1994. Episodic uplift deduced from Holocene shorelines in the Perachora Peninsula, Corinth area, Greece. Tectonophysics 229(3-4), 201-209.

Pullen, D.J., Tartaron, T.F., N.D., *In Press*. Where's the Palace? The Absence of State Formation in the late Bronze Corinthia, Rethinking the Mycenaean Palaces, 2nd ed. Michael Galaty and William Parkinson. UCLA/Cotsen Institute of Archaeology, Los Angeles, pp. 146-158.

Raban, A., 1985. Caesarea Maritima 1983-1984. International Journal of Nautical Archaeology 14(2), 155-177.

Reinhardt, E.G., Patterson, R.T., Schröder-Adams, C.J., 1994. Geoarchaeology of the ancient harbor site of Caesarea Maritima, Israel: evidence from sedimentology and paleoecology of benthic foraminifera. Journal of Foraminiferal Research 24, 37-48.

Reinhardt, E.G., Patterson, R.T., Blenkinsop, J., Raban, A., 1998. Paleoenvironmental evolution of the inner basin of the ancient harbor at Caesarea Maritima, Israel: foraminiferal and Sr isotopic evidence. Revue de Paleobiologie 17, 1-21.

Reinhardt, E.G., Raban, A., 1999. Destruction of Herod the Great's harbor at Caesarea Maritima, Isreal – Geoarchaeological evidence. Geology 27(9), 811-814.

Rothaus, R., Reinhardt E.G., and Noller, J., 2008. Earthquakes and subsidence at Kenchreai: using recent earthquakes to reconsider the archaeological and literary evidence. Archaeology and History in Medieval and Post-Medieval Greece, Carraher, W. Hall, L., Moore Aldershot, R.S. (eds) Ashgate Publishing, UK., 53-66.

Schwarzer, K., Diesing, M., Larson, M., Niedermeyer, R.O., Schumacher, W., Furmanczyk, K., 2003. Coastline evolution at different time scales – examples from the Pomeranian Bight, southern Baltic Sea. Marine Geology 194, 79-101.

Shackleton, J.C., van Andel, T.H., Runnels, C.N., 1984. Coastal Paleogeography of the Central and Western Mediterranean during the Last 125,000 Years and its Archaeological Implications. Journal of Field Archaeology 11(3), 307-314.

Shaw, J.W., 1990. Bronze Age Aegean Harboursides. Tbera and the Aegean World III (D.A. Hardy, ed.), Vol. I, 420-436.

Shepard, F.P., 1964. Sea level changes in the past 6000 years: possible archaeological significance. Science 143, 574-576.

Sonnenburg, E.P., and Boyce, J.I., 2008. Data-Fused Digital Bathymetry and Side-Scan Sonar as a Base for Archaeological Inventory of Submerged Landscapes in the Rideau Canal, Ontario, Canada. Geoarchaeology 23, 654-674.

Soter, S., 1998. Holocene uplift and subsidence of the Helike Delta, Gulf of Corinth, Greece. Geological Society, London, Special Publications 146, 41-56.

Tartaron, T.F., Gregory, T.E., Pullen, D.J., Noller, J.S., Rothaus, R.M., Rifle, J.L., Tzortzopoulou-Gregory, L., Schon, R., Caraher, W.R., Pettegrew, D.K., Nakassis, D., 2006. The Eastern Korinthia Archaeological Survey - Integrated Methods for a Dynamic Landscape. Hesperia 75, 453-523.

Tartaron T.F., Pullen, D.J., and Noller, J.S., 2006. Rillenkaren at Vayia: Geomorphology and a New Class of Earth Bronze Age Fortified Settlement in Southern Greece. Antiquity, 80: 145-160.

Tartaron, T.F., Pullen, D.J., Dunn, R.K., Dill., A. and Boyce, J.I., 2011. The Saronic Harbors Archaeological Research Project (SHARP): Investigations at Mycenaean Kalamianos, 2007-2009. Hesperia.

Tatsumi, S.H., Kowata, E.A., Gozzi, G., Kassab, L.R.P., Suguio, K., Barreto, A.M.F., Bezerra, F.H.R., 2003. Optical dating results of beachrock, eolic dunes and sediments applied to sea level changes study. J. Lumin. 102–103, 562–565.

van Andel, T., 1989. Late Quaternary sea level and archaeology. Antiquity 63, 733-745.

van Andel, T., Shackleton, J.C., 1982. Late Paleolithic and Mesolithic Coastlines of Greece and the Aegean. Journal of Field Archaeology 9, 445-454.

Vousdoukas, M.I., Velegrakis, A.F., Plomaritis, T.A., 2007. Beachrock occurance, characteristics, formation mechanism and impacts. Earth-Science Reviews 85, 23-46.

# CHAPTER 3: TRI-AXIAL GRADIOMETER SURVEY OF BRONZE AGE ANCHORAGE AT KALAMIANOS (KORPHOS, GREECE)


## Abstract

Magnetic survey methods are employed widely in land-based archaeology for detecting low amplitude magnetic anomalies associated with small scale cultural artifacts but few submerged ancient harbours and archaeological sites have been documented using marine geophysical methods. In particular, magnetic gradient methods have not been applied in archaeological settings. A marine magnetic gradient survey using a tri-axial gradiometer system (SeaQuest$^{TM}$) was conducted at Kalamianos to locate concentrations of cultural material, which helped to identify and map the natural Bronze Age harbour and anchorages during Mycenaean occupation. More than 150-line km of magnetic gradient data was acquired in 2009 within a 10-km$^2$ area and was integrated with a detailed digital bathymetry model (DBM) for interpretation. Kalamianos is a recently discovered Late Helladic (ca. 1300-1190 BC) Mycenaean coastal settlement located near the modern village of Korphos, Greece on the Western Saronic Gulf. The coastal context and site plan suggested its function as a port but the location and construction of the harbour basin was unclear. The local coastline has experienced > 6 m of shoreline transgression since the Early Helladic (ca. 3100-2150 BC) and has partially inundated Kalamianos, including the harbour basin.

The gradiometer survey revealed evidence for accumulation of buried cultural artefacts over an inundated limestone platform. High magnetic gradients were observed over known outcrops of pottery rich beachrock platforms BR-1 at 3.7 m depth, BR-2 at 5.8 m depth and over two submerged promontories. Evidence of possible ballast deposits were observed in sheltered

central and eastern embayments adjacent to a pair of promontories which would have functioned as a natural breakwater, and suggested potential locations for harbour anchorages. No evidence of formal constructed harbour structures were observed.

## 3.1. Introduction

Submerged harbour basins are a common feature along the coasts of the Mediterranean (Marriner and Morhange, 2007). Of the few ancient harbours that have been discovered and well documented, many have been inundated as a result of relative sea level (RSL) rise and coastal transgression (Lambeck and Purcell, 2005), tectonically influenced subsidence (e.g. Kenchreai; Noller et al., 1997) and/or sediment compaction (e.g. Alexandria; Stanley and Bernasconi, 2006). There is a lack of empirical knowledge on Bronze Age Aegean harbours due in part to reliance on modern geomorphology for exploration of ancient harbours. Bronze Age harbours that have been discovered (i.e. Ayia Irini on Kea Island, Vayia in Eastern Korinthia,) all share a common trait of being modified natural harbours with no evidence for any major constructed harbour structures (Tartaron et al., 2003). Natural (i.e. eustatic sea level fluctuations, tectonism, erosion, sedimentation) and anthropogenic processes could drastically alter coastal geomorphology in relatively short temporal scales and render once ideal natural harbours useless when observed in modern day. The lack of "visibility" becomes a significant challenge for mapping and discovery and is particularly true for harbours from the prehistoric or Bronze Age periods which exploit natural geomorphically suitable locations (i.e. promontories, narrow isthmus, river deltas with wide protected bays) with a lack of easily distinguishable formal constructed harbour structures (i.e. stone or concrete piers, moles, quays and seawalls).

The application of remote sensing geophysical techniques to archaeological exploration is not a new concept and has been applied to various land based archaeological sites, including the use of ground penetrating radar and magnetic methods as a non-destructive tool for site evaluation and guiding excavation programs (Young and Droege, 1986; Basile et al., 2000; Neubauer et al., 2002; Nuzzo et al., 2002). The usage of non-invasive remote sensing technology for preliminary mapping of submerged archaeological sites have been few but have recently been demonstrated to be effective from the use of magnetic methods to map submerged coastal settlements and harbour basins with good success at Baia, Naples (Paoletti et al., 2005), Caesarea Maritima, Isreal (Boyce et al., 2004; Boyce et al., 2009) and Liman Tepe, Turkey (Boyce et al, 2006). Structural remains containing high concentrations of cultural materials (i.e. clay pottery, stone walls and foundations, kilns and fire hearths) generate magnetic anomalies through contrasting magnetic susceptibilities and remnant magnetizations with surrounding rock and sediments (Gibson, 1986; Boyce et al., 2009). At Caesarea, Boyce et al. (2004) demonstrated the effectiveness of using magnetic methods for high resolution mapping of the locations of submerged ancient harbour moles due to the magnetic properties of hydraulic concrete that the Romans used for construction. Further studies at Caesarea by Boyce et al., (2009) demonstrated that magnetic methods have potential for mapping ancient ship ballast deposits, which may provide insights for understanding anchorage sites and trade activity of ancient harbours. Through high resolution magnetic surveying, processing and interpretation of magnetic data, significant information on local geology and site archaeology could potentially be extracted.

The harbour of Kalamianos, a Late Helladic IIIB (LH; ca. 1300-1190 BC) Mycenaean coastal settlement located near the modern village of Korphos, Greece, has undergone inundation through coastal co-seismic subsidence (Nixon et al., 2009; Tartaron et al. in press). The potential

for constructed harbour structures from this period is unlikely and was presented as a low "visibility" problem for researchers interested in the harbour location and layout. In this study we demonstrated the effectiveness of using a tri-axial gradiometer system and magnetic gradient data processing methods as a tool for the exploration and delineation of a previously undiscovered harbour basin and anchorages of unknown size, location and construction through locating the distribution of buried cultural material and ballast deposits. While magnetic gradient equipment methods have been increasing in popularity for usage in airborne and land-based mineral exploration and marine pipe or ferrous target detection, it has yet to be applied to archaeological studies. Unlike standard single sensor magnetometer systems utilized in previous submerged harbour studies at Baia and Caesarea (Paoletti et al., 2005; Boyce et al., 2004; Boyce et al., 2009) that measure the total magnetic intensity, gradiometers measure the change in magnetic field intensity with respect to vertical or horizontal distances and have several advantages over single (total field) magnetometers: 1) they are immune to time-varying shifts in the geomagnetic field strength and do not require diurnal corrections, 2) they have a much greater sensitivity for detection of small magnetic anomalies, 3) gradient measurement acts as a low-pass spatial filter, rejecting contributions from deep magnetic source bodies. A gradiometer thus has the ability to resolve much smaller near-surface magnetic targets (e.g. pottery deposits, ballast mounds).

## 3.2. Study Site and Archaeology

### 3.2.1 Study area and Archaeology

Kalamianos is located on a peninsula on the northwestern shore of the Western Saronikos Gulf, about 2.5 km southeast of the modern village of Korphos, Greece, 25 km southeast of Corinth, Greece and 30 km northeast of the ancient city of Mycenae (Fig. 3.1). The peninsula is currently undeveloped, uninhabited and does not to appear to have been occupied since the Mycenaean in the Late Helladic (ca. 1300-1190 BC). The vegetation cover is sparse, dominated by low shrubs and grass with a few trees. First discovered in 2001 by the Eastern Corinthian Archaeological Survey (EKAS), the site layout and archaeology has been well documented by the Saronic Harbour Archaeological Project (SHARP) but has been limited to outcrops above modern sea level (Tartaron et al. 2006; Tartaron et al., in press). The site location and context suggested a coastal harbour settlement but the location and layout of the ancient harbour at Kalamianos was unknown and undocumented prior to this study.

SHARP completed a full archaeological inventory of Kalamianos from 2006-2009, which revealed an extensive fortified settlement of the Mycenaean Palatial Period covering over 7.2 hectares with more than 50 structures and complexes and hundreds of walls that have been documented to date (Tartaron et al. in press). Diver reconnaissance discovered Early Helladic (EH) (ca. 3100-2150 BC) pottery encrusted to a bedrock platform at ~5.8 metres water depth over the inshore region southeast of Kalamianos, suggesting a previous phase of occupation and abandonment prior to the Mycenaean settlement. An extensive beachrock platform containing high concentrations of Mycenaean pottery fragments was also discovered at 3.7-4.5 m depth. Mounds of ballast stones consisting of limestone and andesite were also documented across the inshore region (Fig 3.12).

### 3.2.2 Geological Setting

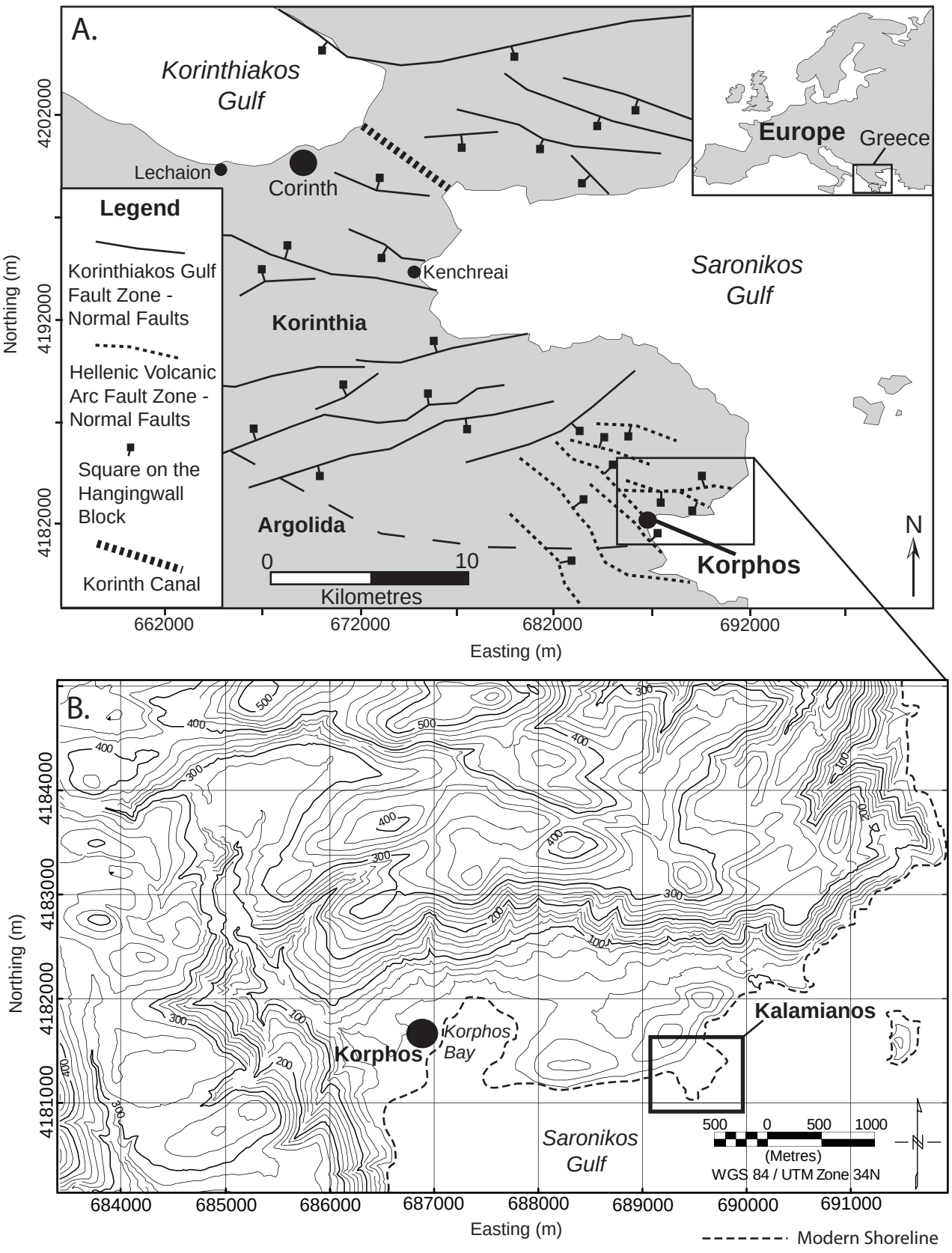


Figure 3.1: A) Location of Kalamianos in north-eastern Peloponnesus with mapped regional faults, modified from Nixon et al. (2009). B) Contoured topographic map of the Korphos-Kalamianos region (contour interval 20m).

The settlement at Kalamianos was constructed upon ~1 km thick Mesozoic age limestone bedrock which dominates southeastern Korinthia, Peloponnesus (Clift and Robertson, 1990). The Korphos-Kalamianos region is characterized by north-dipping alternating beds of bivalve bearing crystalline limestone and thin granular weathered limestone. Neotectonic north-south crustal extension of the Aegean plate has produced significant recent normal faulting with some oblique motion of the bedrock (Armijo et al., 1996). The region consists of several fault blocks which have undergone differential movement over time with evidence of recent near vertical displacement (post Bronze Age) of the block on which Kalamianos rests, observed from a well developed fault scarp northeast of Kalamianos and inundated beachrock horizons from the EH and LH period. Extensive east-west faulting has produced associated fracture patterns and natural stair-step topography at Kalamianos.

The Korphos-Kalamianos region is rugged and rocky with a steep coastline and large cliffs that provide natural fortification. The modern village of Korphos and Kalamianos are located on a narrow strip of low hills and basins covering approximately 2 $km^2$ adjacent to the Western Saronic Gulf and are hemmed in on all sides by the rugged slopes and mountains of southeastern Korinthia (Fig. 3.1B). The hills are stony, dominated by colluvium eroded from the surrounding slopes and a thin terra rosa soil cover. The landscape is predominately karstic with visible paleo-karst and modern karren features on bedrock outcrops (Collins and Dunn, 2008). Two generations of joint sets were observed throughout the region. The older generation of joints trend north-south and east-west and has been eroded by groundwater flow with visible widening of fractures and cavern formation. It has since been infilled by solution breccia from wall collapse, crystalline calcite and terra rosa soil, and now remain exposed at land surface. A younger generation of joints occur in three orthogonal sets and overprinted the older sets, which

has resulted in the fracturing of the limestone at Kalamianos into metre scale blocks (Miller and Dunn, 2009). Exposed fractures at surface were observed to have been infilled with terra rosa soil and colluvium (Fig. 3.10**)**

From the DBM, the inshore region adjacent to Kalamianos is a narrow platform with low relief, shallow (<15 m depth) and gently slopes outwards until a steep drop-off into deeper waters of the Saronikos Gulf at ca.100-250 m from the modern shoreline (Fig. 3.2). Two natural submerged isthmuses are also observed protruding from the southeast shore of Kalamianos with flanking shallow water basins (Dao et al., 2011). Diver reconnaissance revealed deposits of ballast stones and two beachrock platforms at 3.7-4.5 m and ~5.8 m depth which contain concentrations of Mycenaean and EH pottery respectively (Dao et al., 2011).

## 3.3. Methods

### 3.3.1 Marine Geophysical Survey

A systematic marine magnetic survey was conducted over a 2 $km^2$ area of the inshore region surrounding Kalamianos (Fig. 3.3). Over 150 line kilometres of magnetic gradient data was acquired using a Marine Magnetics SeaQuest$^{TM}$ tri-axial gradiometer system in NW-SE survey lines spaced at 20-30 m intervals and perpendicular NE-SW tie lines spaced at 50 m intervals. The gradiometer was towed 40 m behind a Zodiac boat at an average speed of 10 km/h, at a depth of 0-1 m below water surface and continuously sampled at a rate of 2 Hz for the duration of data acquisition (Fig. 3.4A). Navigation and survey positioning was provided onboard by a Trimble RTK sub-metre D-GPS unit which provided real time differential corrections through reception of correction data from an onshore receiver.

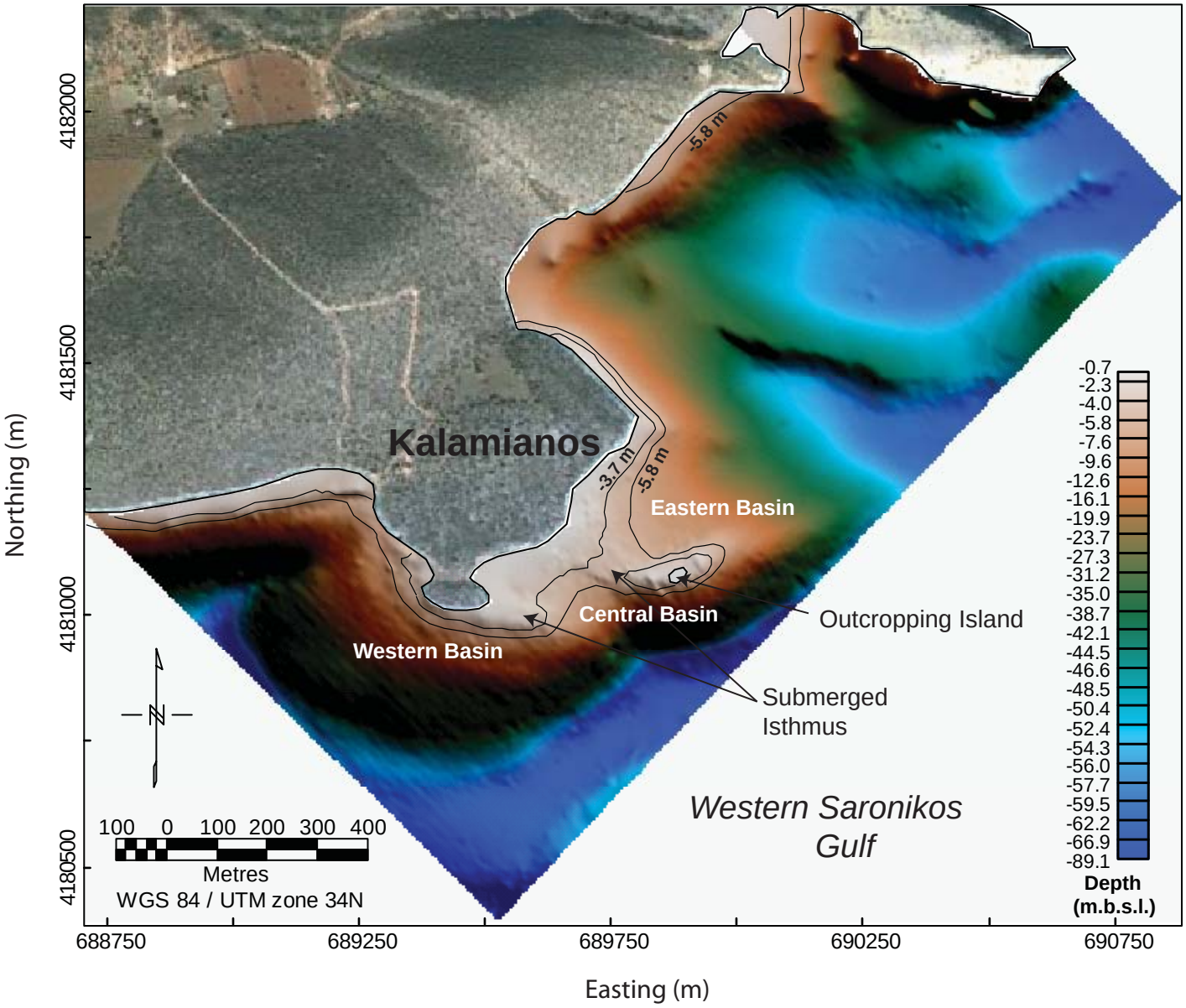


Figure 3.2: Colour-shaded digital bathymetric map of the coastal region adjacent to Kalamianos. Contours at 3.7 m and 5.8 m below modern sea level show paleoshoreline configuration during the Mycenaean (Late Helladic; ca. 1300-1190 BC) and Early Helladic (ca. 3100-2150 BC) occupation respectively.

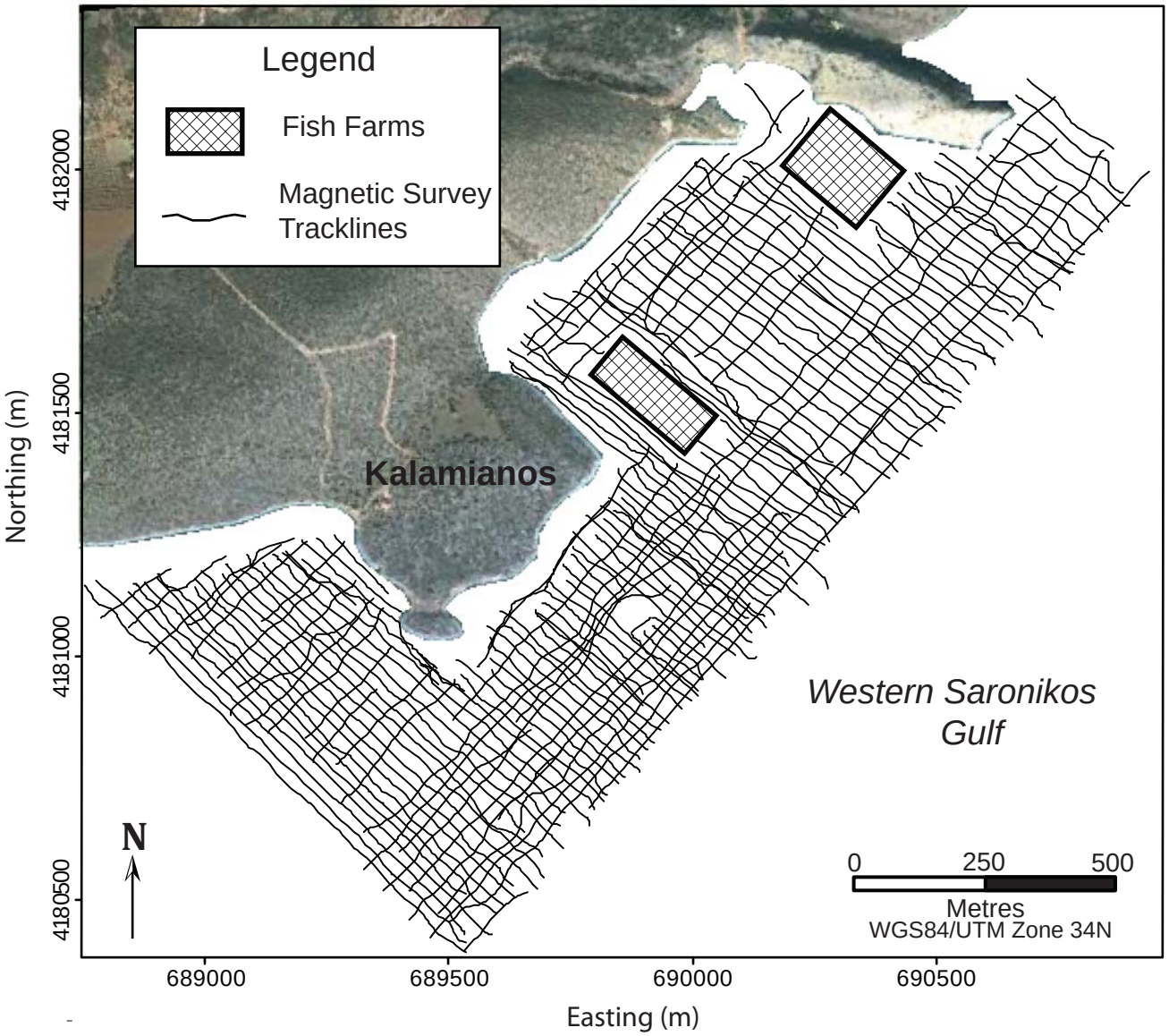


Figure 3.3: Survey area showing magnetic gradient survey track lines.

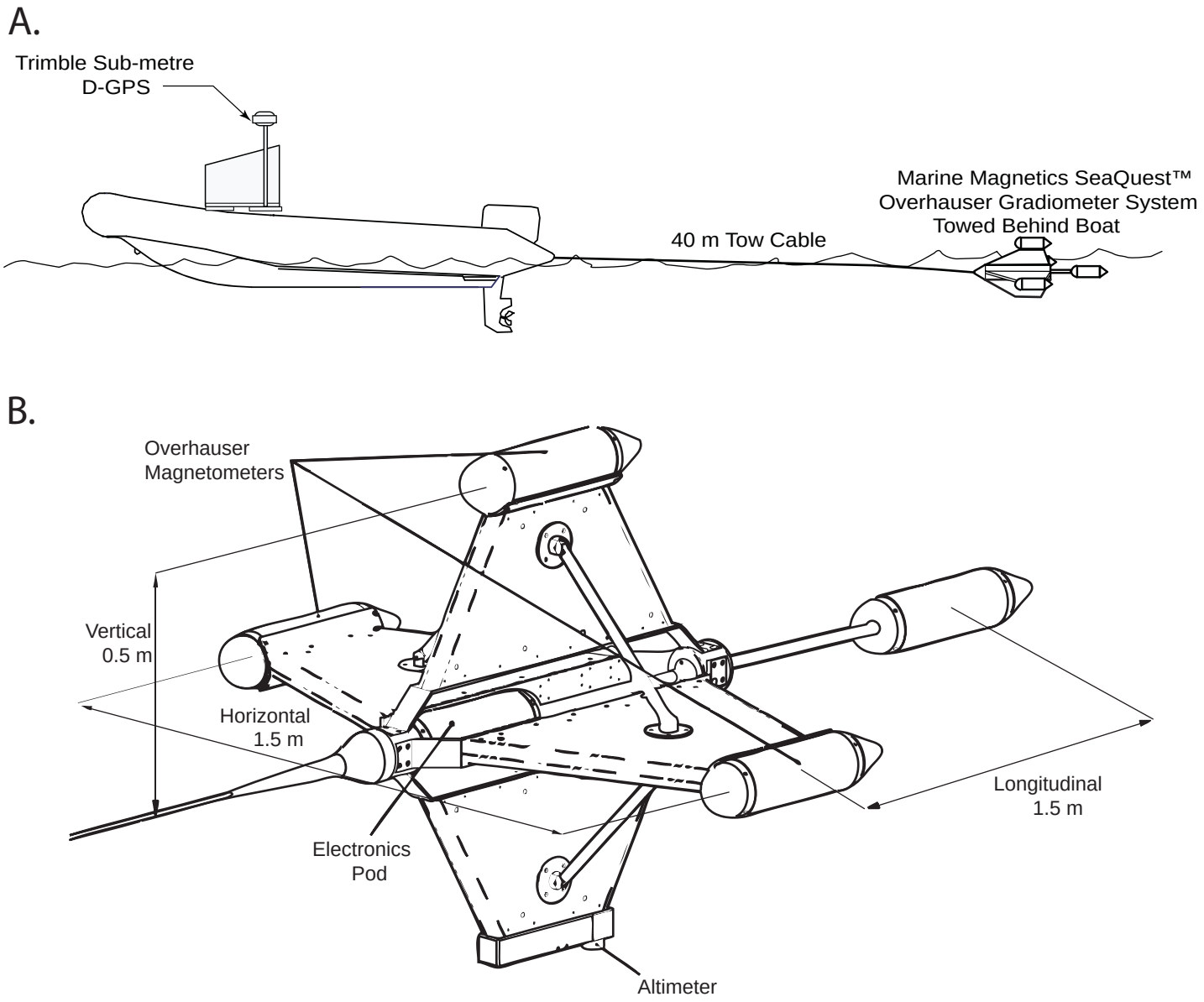


Figure 3.4: A) Survey boat and equipment configuration. B) Schematic of the SeaQuestTM magnetic gradiometer system. Total magnetic fields are measured by 4 Overhauser sensors and gradients calculated along three axes.

Recent studies on submerged ancient harbours have employed the usage of total field magnetic methods for detection of constructed formal harbour architecture (i.e. moles, seawall, piers) and ballast deposits (Boyce et al., 2004; 2006; 2009) but marine magnetic gradient methods were untested for such an application. Four Overhauser magnetometers attached in fixed distances on the SeaQuest$^{TM}$ collected real magnetic gradients in the vertical, horizontal and longitudinal directions which allowed for the calculation of the total gradient or analytic signal during post survey processing (Fig. 3.4B). Overhauser sensors are a newer generation of scalar quantum magnetometers which are advantageous over other designs for marine archaeological surveys due to: 1) high sensitivity (up to 0.01 nT), 2) continuous sampling (1-4 Hz for SeaQuest$^{TM}$), 3) omnidirectional sensors with no dead zones, heading errors and warm-up time. Also, gradiometers, which measure the change in magnetic field intensity with respect to vertical or horizontal distance (units $nTm^{-1}$), have several advantages over single (total field) magnetometers in archaeological applications: 1) they have a much greater sensitivity for detection of small magnetic anomalies, 2) gradient measurement acts as a low-pass spatial filter, rejecting contributions from deep magnetic source bodies, 3) analytic signal processing reduces data to single magnetic peaks which improve edge and target detection.

### 3.3.2. Geophysical Data Processing

A significant advantage of the SeaQuest$^{TM}$ tri-axial gradiometer system over standard single sensor magnetometers is the measurement of real vertical, horizontal and longitudinal magnetic gradients and allows for the direct measurement and computation of the total gradient (3-D analytic signal). The absolute value of the amplitude of the 3-D analytic signal (AAS) or total gradient at (x,y) is derived from the three orthogonal gradients of the total magnetic field:

$$|A(x,y)| = \sqrt{\left(\partial M/\partial x\right)^2 + \left(\partial M/\partial y\right)^2 + \left(\partial M/\partial z\right)^2} \qquad \text{Equation 3.3.1}$$

where $|A(x,y)|$ =the absolute value of the 3-D analytic signal ($nTm^{-1}$), and *M*= ambient magnetic field strength (nT) (Roest et al. 1992). The computation of analytic signal from single sensor magnetometer data could be achieved through computation of spatial derivatives from a total magnetic intensity grid but the procedure enhances gridding artifacts, track corrugation errors, overall noise and has difficulty in accurately calculating the horizontal derivatives of small anomalies oriented perpendicular to flight-line directions (Roest et al., 1992). A tri-axial gradiometer collects real magnetic gradients and effectively eliminates processing errors introduced by spatial derivatives of gridded data.

Post-survey correction of the marine magnetic gradient data included lag and diurnal corrections, IGRF removal and tie-line levelling of the total field measurements from each of the four fixed Overhauser sensors onboard the SeaQuest™ (Boyce et al. 2009). The corrected measurements were used to compute real vertical, horizontal and longitudinal magnetic gradients and subsequently the total gradient (analytic signal, Equation 3.3.1) in nanoteslas per meter (nT/m). The analytic signal computation reduces dipole signals to single anomalies with peaks over the contacts of contrasting magnetic source bodies and was developed as an alternative to reduction-to-pole corrections for delineating edges of magnetic anomalies in geologic materials with unknown remnant magnetization (Roest et al. 1992; MacLeod et al., 1993). This correction provides a significant advantage in near surface feature delineations in archaeological

applications where the remnant magnetizations of cultural materials are often random and unknown.

Total magnetic intensity data from a single Overhauser sensor was processed separately to produce a total magnetic intensity grid for interpretation and comparison with magnetic gradient and analytic signal grids. An aggressive magnetic regional residual separation using a 1.5 m upward continuation was applied on the magnetic total field grids to discriminate against deep magnetic source bodies and enhance near surface representation (Jacobsen, 1987).

As an aid for magnetic source modeling and the interpretation of magnetic survey data, magnetic susceptibility measurements were obtained from beachrock, pottery and andesitic ballast stone samples retrieved through diver reconnaissance. The beachrocks (BR-1 and BR-2) were grinded into sand sized particles and 9-10 g samples were placed into cubettes for volume magnetic susceptibility measurements ($\kappa$) using a Bartington MS2-B susceptibility meter. Five samples of each beachrock were measured to provide a mean magnetic susceptibility value. Volume susceptibility measurements were also performed on whole ballast stones, pottery shards and limestone bedrock fragments using a Bartington MS2-E1 surface measurement probe. Three individual ballast stones were measured with three surface measurements each to provide a mean susceptibility. Two EH and two LH pottery shards were measured three times each for mean susceptibility. A forward magnetic model was generated to simulate the degree of impact on the magnetic field intensity in response to the presence of ballast mounds and horizontally extensive units of beachrock and sediment containing concentrations of broken pottery. The GM-Sys software was used to generate the model with the measured mean magnetic susceptibility values from collected samples of rock and pottery.

## 3.4. Results

### 3.4.1. Magnetic and bathymetry data

The bathymetry map of the inshore area and surrounding region at Kalamianos is shown as a colour-shaded image in Figure 3.2. As seen in the bathymetry data, the inshore region surrounding Kalamianos is characterized by a downward sloping shallow platform (<15 m) that extends outwards for 100-250 m along the length of the rugged and rocky modern shoreline. Water depth steeply increases to >60 m beyond the edge of the platform. A small island outcrops ~200 m from the southeast shore of Kalamianos and is connected to mainland Kalamianos by a submerged isthmus 50-100 m wide. An underwater valley trending N 100$^{o}$ E off the northeast coast of Kalamianos was also clearly seen in the bathymetry and is believed to be a continuation of a large regional normal fault that extends out into the Saronikos Gulf.

The magnetic total field map (Fig. 3.5), vertical, horizontal, longitudinal gradients maps (Fig. 3.6A, 3.6B, 3.6C) and analytic signal map (Fig. 3.7) are shown as colour shaded grids. The total field map displays data collected from a single sensor onboard the SeaQuest$^{TM}$ gradiometer platform and represents the variation in the Earth's magnetic field intensity (in nanoteslas; nT) over the region due to changes in magnetic susceptibility ($\kappa$) of the underlying sediment, bedrock and cultural materials. Contrasting magnetic susceptibilities generate variations in observed ambient field strength and appear as anomalies on a grid of magnetic intensity. From Figure 3.5, relative high magnetic intensity regions could be seen off the southeast and southwest shores of Kalamianos. The variation in magnetic intensity had a normal distribution that ranged up to 126 nT throughout the surveyed area in the most extreme limits but the majority of the region had a magnetic intensity variation of only ca. 10 nT. A region of high magnetic intensity northeast of Kalamianos was associated with a modern fish farm and the ferrous construction materials.

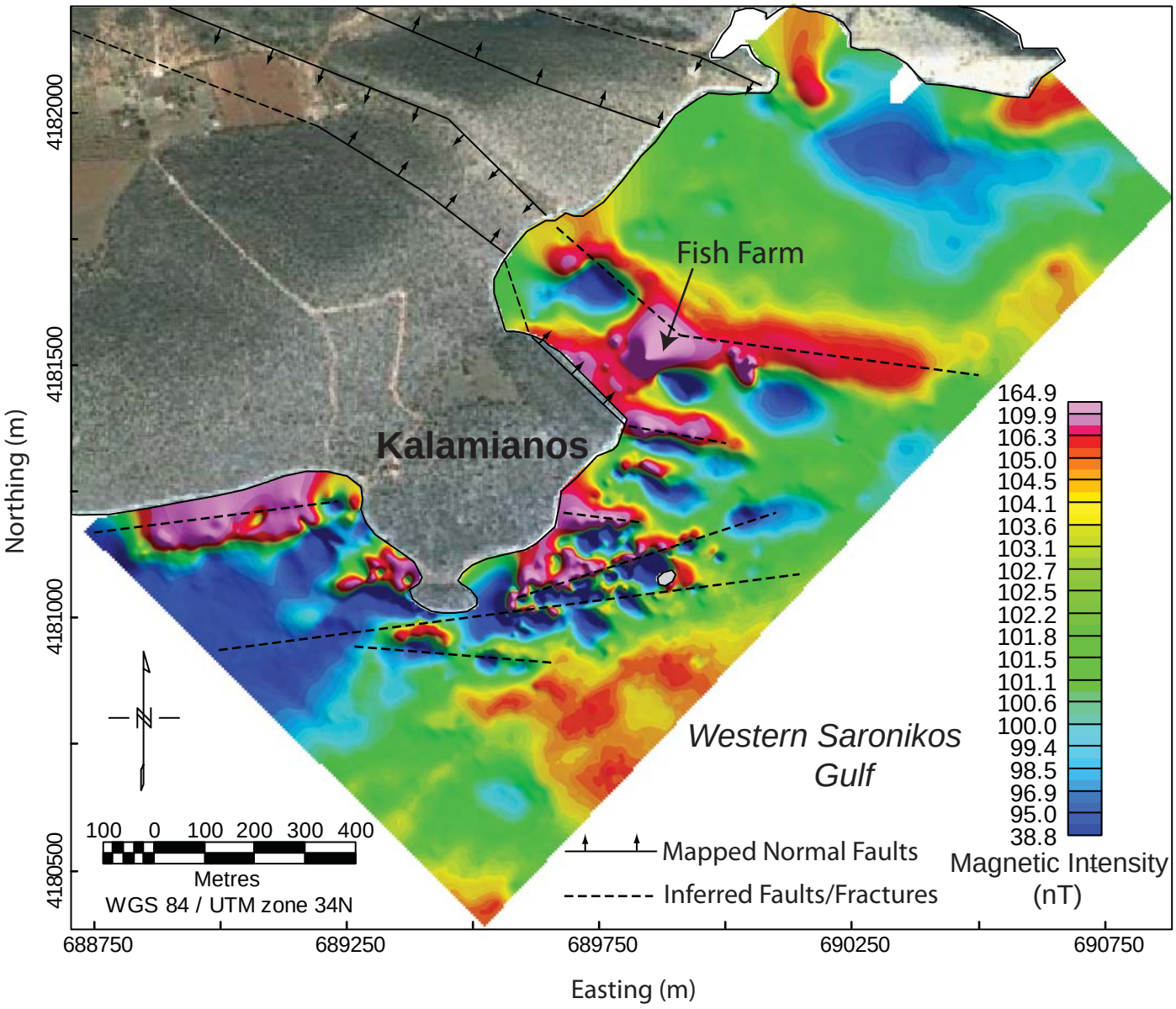


Figure 3.5: Colour-shaded total magnetic intensity map obtained with single sensor. Northwest-southeast and west-east linear magnetic anomalies are interpreted as fault planes and fracture zones. Note southeastward extension of normal faults into small embayment to east of Kalamianos.

A.

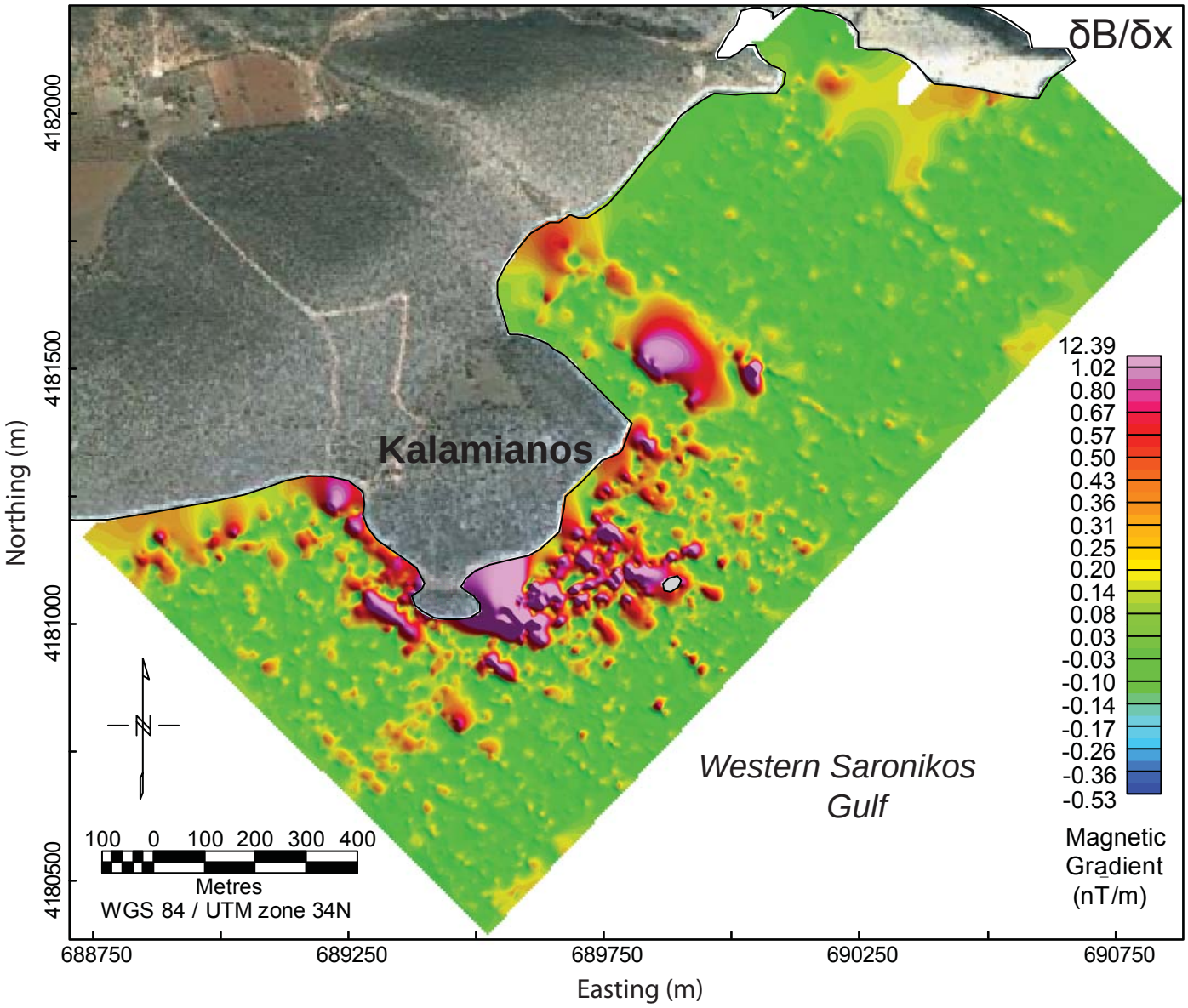


Figure 3.6A: Colour-shaded horizontal (x) magnetic gradient map at Kalamianos.

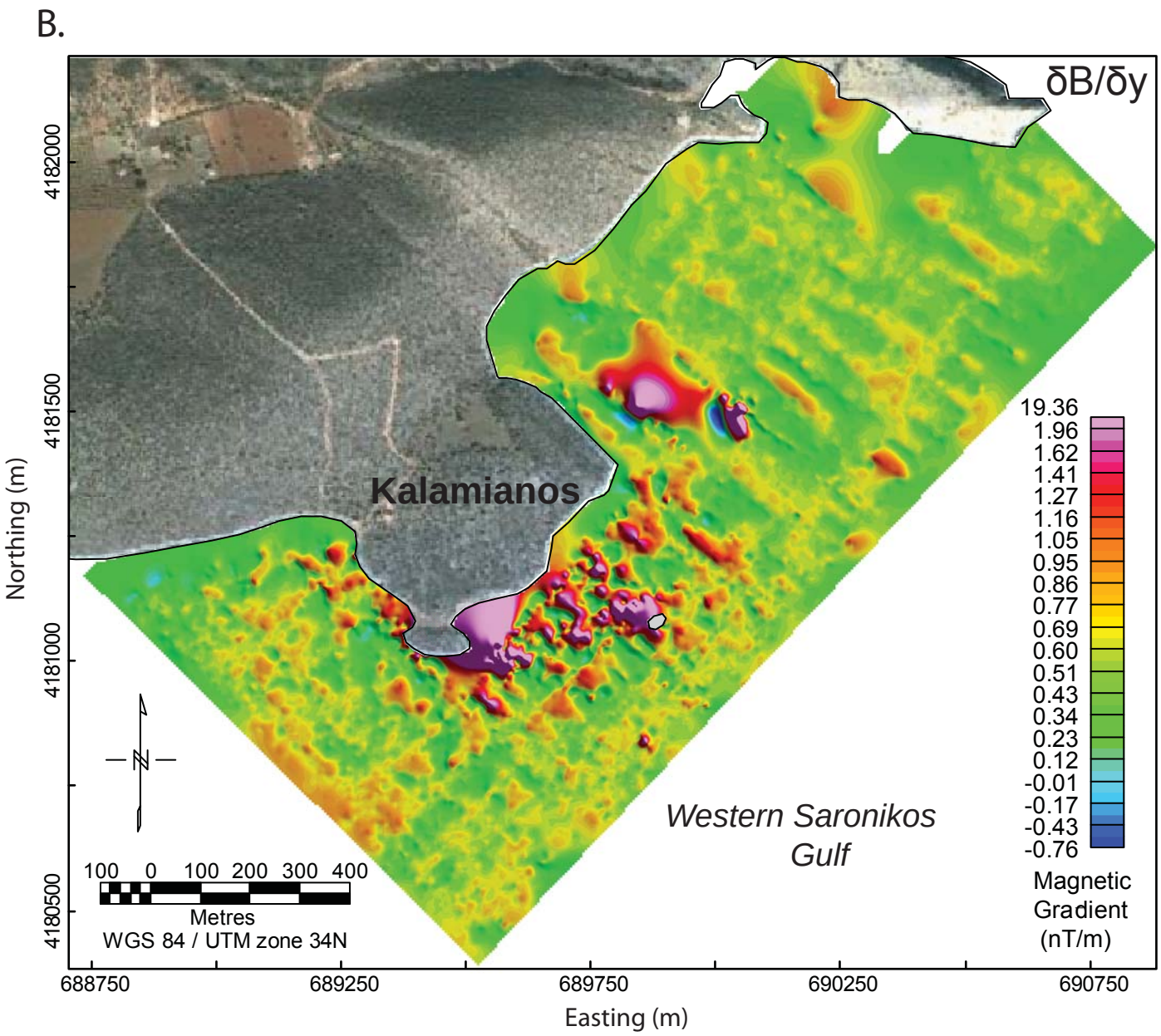


Figure 3.6B: Colour-shaded longitudinal (y) magnetic gradient map at Kalamianos.

C.

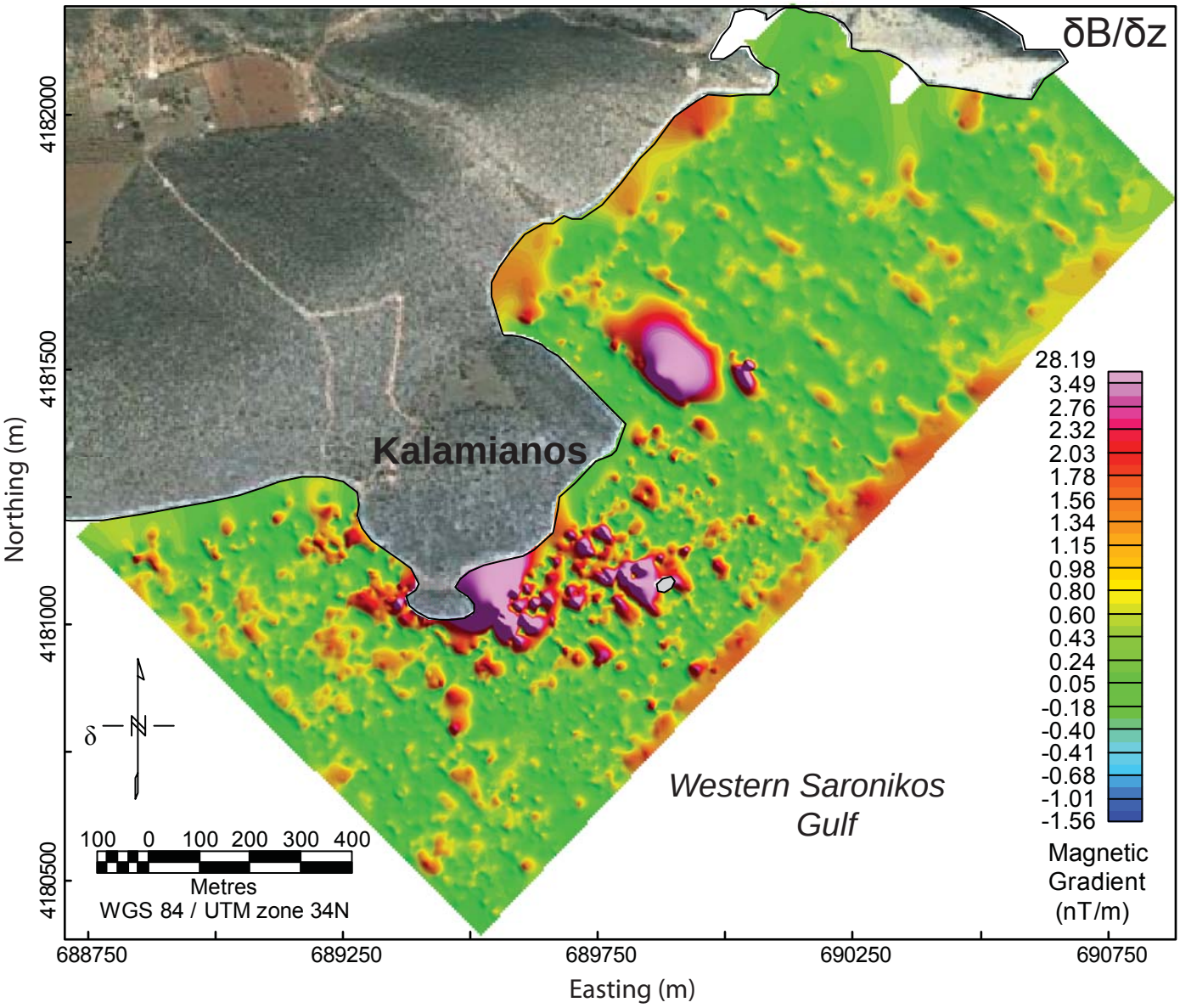


Figure 3.6C: Colour-shaded vertical (z) magnetic gradient map at Kalamianos.

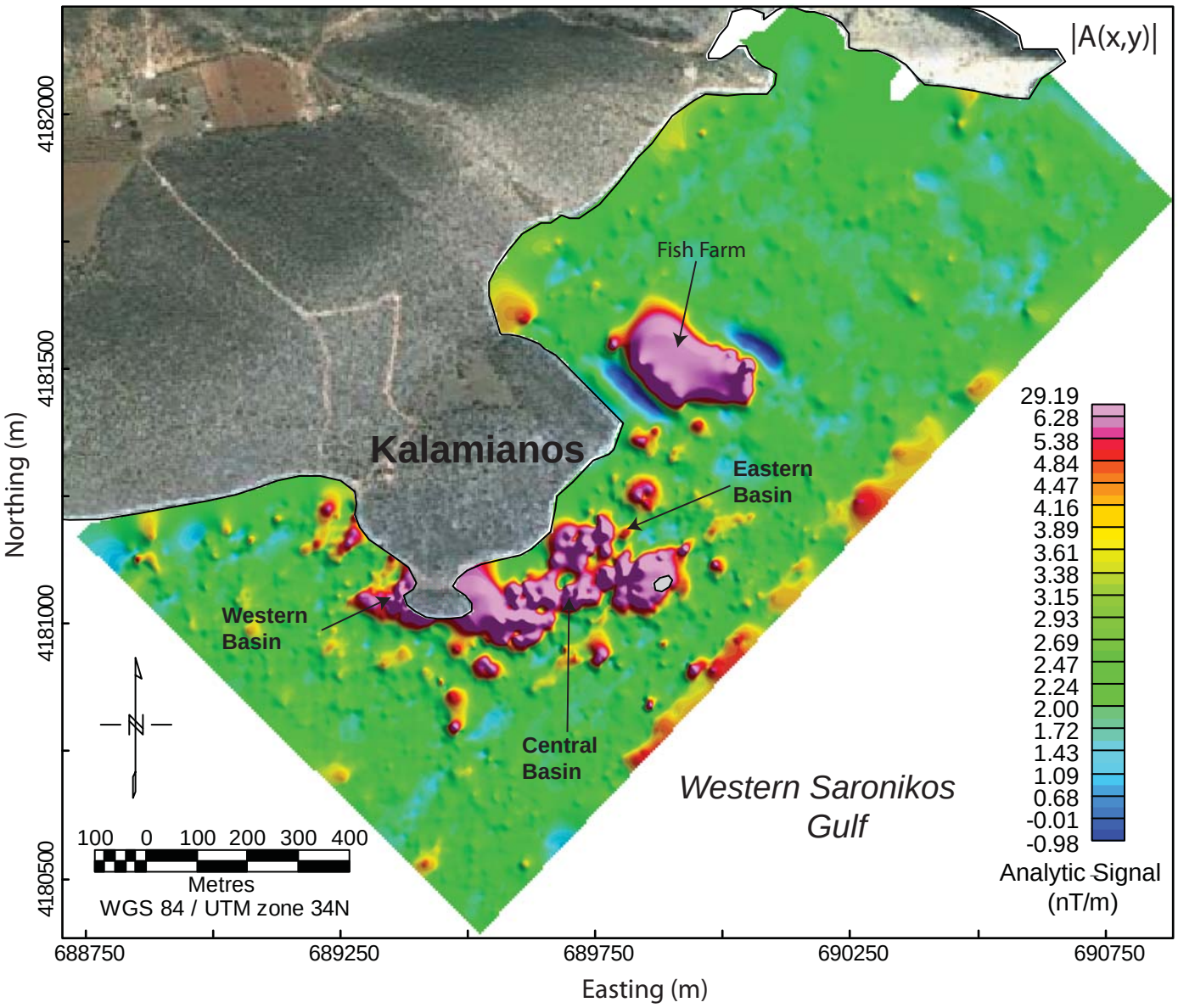


Figure 3.7: Colour-shaded analytic signal (total gradient) map. Note clustering of magnetic anomalies in shallow embayments to south of Kalamianos landsite. Magnetic anomaly around fish farm is due to ferrometallic debris and dock infrastructure.

However, underlying the fish farm region, a linear magnetic anomaly was seen to extend outwards at N 100$^{o}$ E, coinciding with the underwater valley observed in the bathymetry. Linear trending anomalies were observed south of Kalamianos and crosscut a portion of the submerged inshore region from the total magnetic intensity and residual magnetic maps (Fig. 3.5 and 8B). South of Kalamianos, 200-300 m beyond the shallow inshore platform, a region with relatively higher magnetic intensity could be observed over deep water.

The magnetic gradient maps (Fig. 3.6) display a significantly different representation. Long wavelength anomalies associated with large regional geologic heterogeneity are not well represented by magnetic gradients but near surface, short wavelength anomalies are enhanced. Many small magnetic anomalies appear more distinctly with a large concentration observed southeast of Kalamianos in the central harbour basin. The magnetic anomalies represented vary between the vertical, horizontal and longitudinal gradient maps since they each represent a different vector of change within the total field. The magnitude of the magnetic gradients range up to 20-30 nT/m in the most extreme limits and are believed to be from modern day ferrous targets (fish farm, anchors, boat engine etc.) and not archaeological or geological. However, the majority of surveyed region show magnetic anomalies with < 1 nT/m variation. Anomalies over the inshore area southeast of Kalamianos display 2-3 nT/m variability. The computation of the analytic signal effectively combined the three magnetic gradient maps into a single total gradient map and further improved edge clarity (Fig. 3.7). A large proportion of magnetic anomalies overlap with known areas of beachrock BR-1 and BR-2 outcrops, the submerged promontories and adjacent shallow western, central and eastern basins (Fig. 3.8A). From Fig. 3.8A, the anomalies with the highest magnetic gradients (5-8 nT/m) are concentrated over both submerged isthmus and the western and eastern basins that flank it. Many smaller magnetic targets observed

in the individual gradient maps are no longer visible once integrated into the total gradient. The area east and west of Akrotirio Trelli has the highest observed magnetic gradients and the extent of the anomaly is seen to trend along the Late Helladic shoreline at 3.7 m depth. A ridge seen in the DBM over the western basin at 13 m depth displayed an associated magnetic response which is speculated to be associated with a paleoshoreline at Kalamianos predating the Early Helladic (Fig. 3.8A).

### 3.4.2. Magnetic Susceptibility

The magnetic susceptibility (κ) of the collected geological and archaeological samples is summarized in Table 3.1. The region is underlain by low magnetic susceptibility limestone bedrock but the cultural overburden is highly susceptible, which is responsible for the high magnetic relief over the inshore area. The LH pottery shards are revealed to have ~500% higher magnetic susceptibility than their EH counterparts. This result was consistent with the LH pottery rich BR-1 having ~400% higher magnetic susceptibility than its counterpart, the EH pottery rich BR-2. The magnetic susceptibility of andesite ballast stones were found to be up to ~450% higher than that of the pottery rich beachrock and are similar to that of pure pottery.

## 3.5. Discussion

The magnetic gradient survey, digital bathymetry model (DBM) and diver reconnaissance at Kalamianos has identified accumulations of LH and EH pottery and ballast mounds off the southeast shore of Kalamianos including two submerged beachrock platforms (BR-1, BR-2) paralleling the modern shoreline and a submerged isthmus connecting the mainland to a small island 200 m offshore. The concentration of LH and EH pottery are located

| Sample | Material | n | Mean Magnetic Susceptibility (κ) (x$10^{-6}$ SI) |
|---|---|---|---|
| BR-1 | Calcarenite | 5 | 133.3 |
| BR-2 | Beachrock | 5 | 38.9 |
| Ballast 1 | Andesite | 3 | 228 |
| Ballast 2 | Andesite | 3 | 701.3 |
| Ballast 3 | Andesite | 3 | 256.1 |
| EH Pottery | Clay | 6 | 151.2 |
| LH Pottery | Clay | 6 | 726.2 |
| Bedrock | Limestone | 6 | 23.5 |

Table 3.1: Results of volume magnetic susceptibility measurements of beachrock, ballast stones, pottery and limestone bedrock.

within their respective beachrock platforms BR-1 (3.7-4.5 m depth) and BR-2 (5.8 m depth). The disparity in platform depth and lack of mixing between the pottery shards of different ages suggest two separate phases of occupation at Kalamianos prior to its abandonment. The pottery showed little reworking and bioencrustation which suggest lithification with local sediments into beachrock on a low energy beach which subsequently experienced rapid burial possibly due to sudden co-seismic subsidence of the coastline. These results have important archaeological implications for understanding the role, structure and operation of the Kalamianos harbour in antiquity.

### 3.5.1. Magnetic Anomalies at Kalamianos

The magnetic gradient method and 3-D analytic signal processing (total gradient) (Figs. 3.6, 3.7, 3.8) provides a different aspect of the magnetic field, rate of change, as opposed to standard total field intensity methods (Fig. 3.5), which has been proven to be more effective in delineating edges of source bodies (Roest et al. 1992; MacLeod et al., 1993). In this study, it was shown that the computation of magnetic gradients resulted in the enhancement and improved delineation of small near surface magnetic source bodies (cultural material) and the suppression of deeper and longer wavelength signal from a geologic source (Figs. 3.7 and 3.8A).

Long linear trending magnetic anomalies observed in the total field map (Fig. 3.5), which are thought to be associated with large regional fault planes and terra rosa soil infilled fractures and grikes, are suppressed in the magnetic gradients and analytic signal (Figs. 3.6 and 3.7). The high amplitude (> 3 nT) linear magnetic anomalies observed in the residual field map (Figs. 3.8B and 3.8C) are suspected to be geologic background signal associated with near-surface grikes infilled with relatively high magnetic susceptibility terra rosa soil (Figs. 3.8D and 3.9). A land

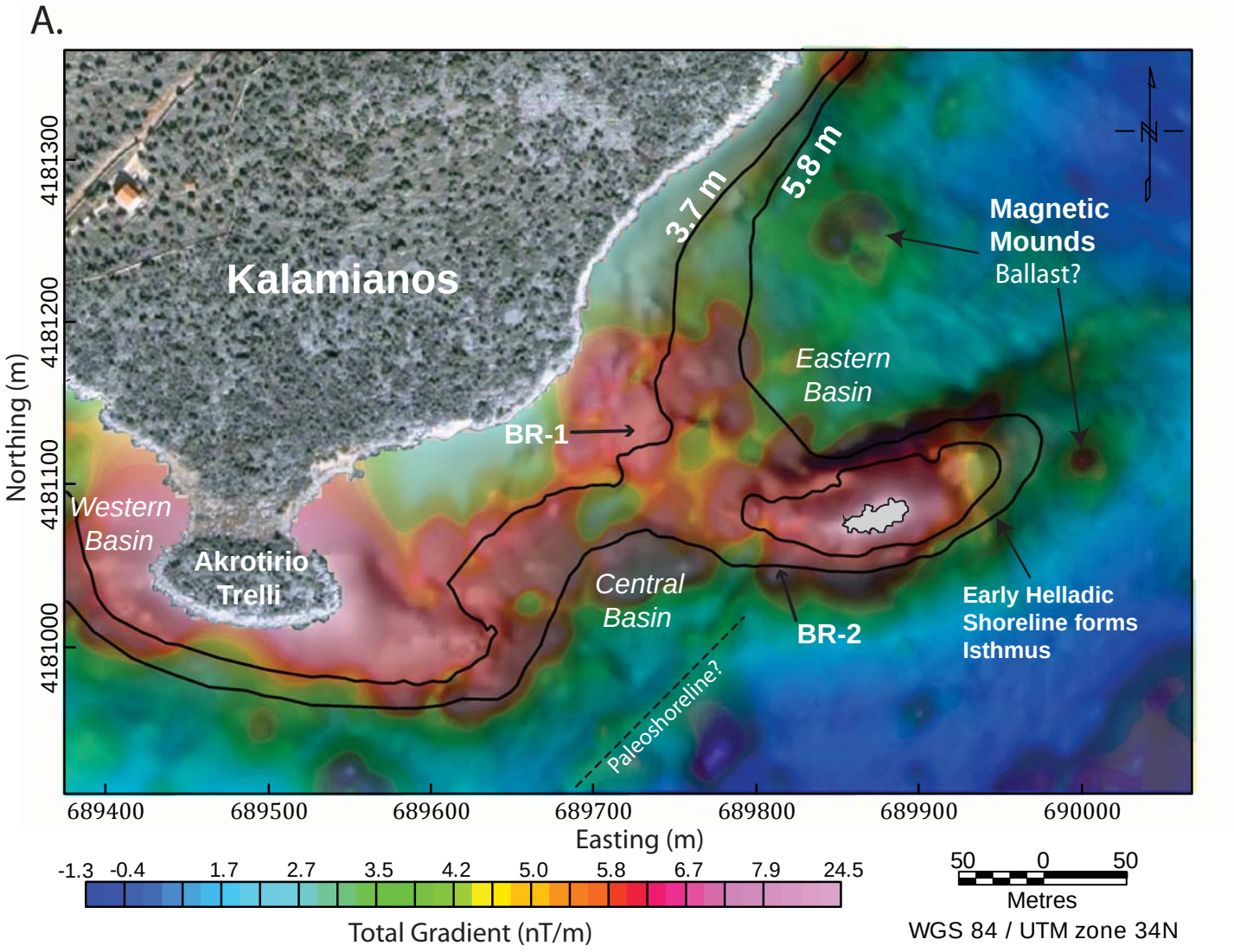


Figure 3.8A: Semi-transparent overlay of the analytic signal map on the digital bathymetry model of the inshore harbour basin at Kalamianos. Location of the Early Helladic paleoshoreline (5.8 m) and Late Helladic paleoshoreline (3.7 m) also shown. The submerged promontory connecting the island to mainland was emergent during the Early Helladic period, providing two well-sheltered anchorage areas.

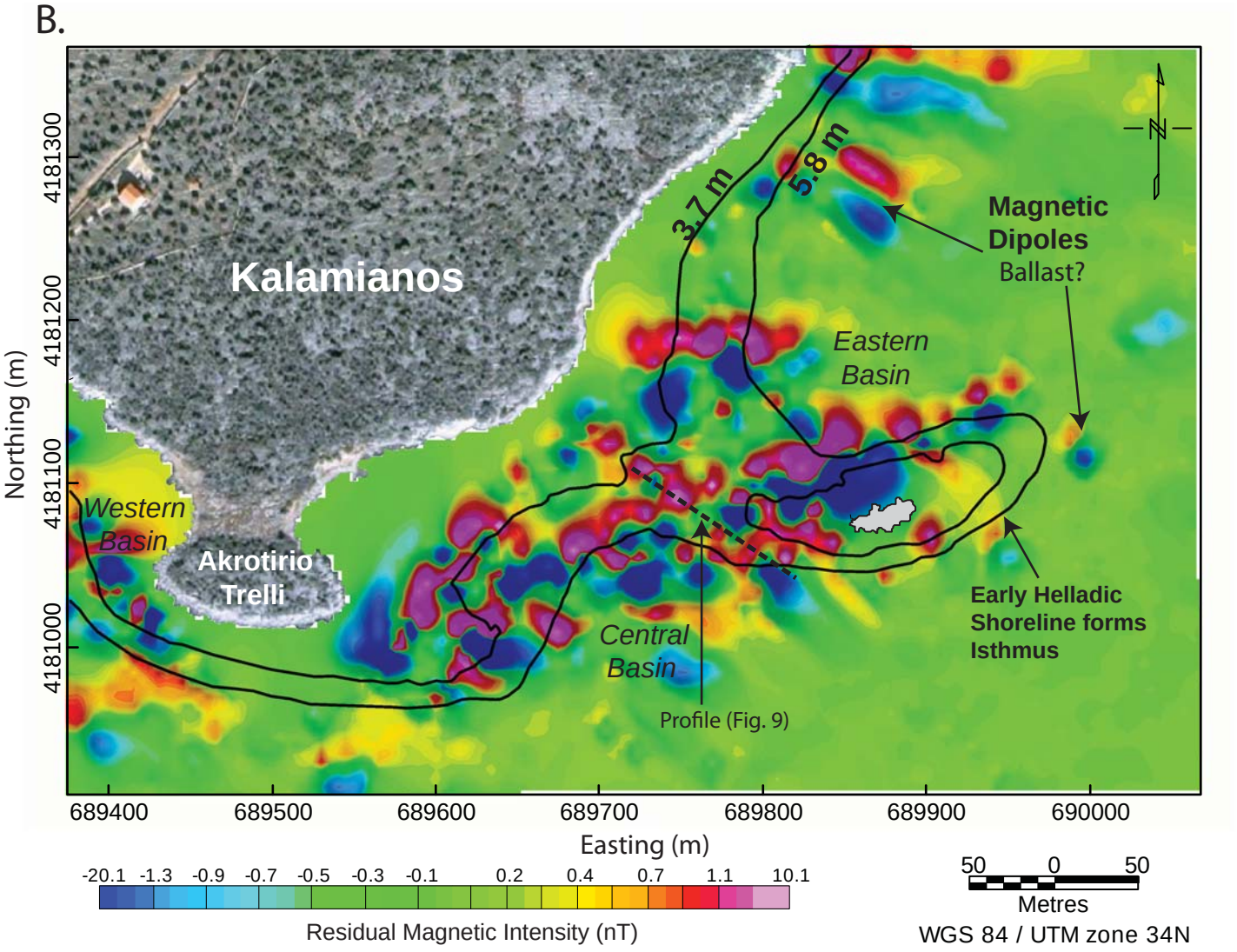


Figure 3.8B: Colour-shaded residual magnetic intensity map of the harbour area. Note west-east magnetic lineaments indicating presence of fractures in limestone bedrock underlying harbour areas. Isolated dipole anomalies are likely the result of ballast mounds.

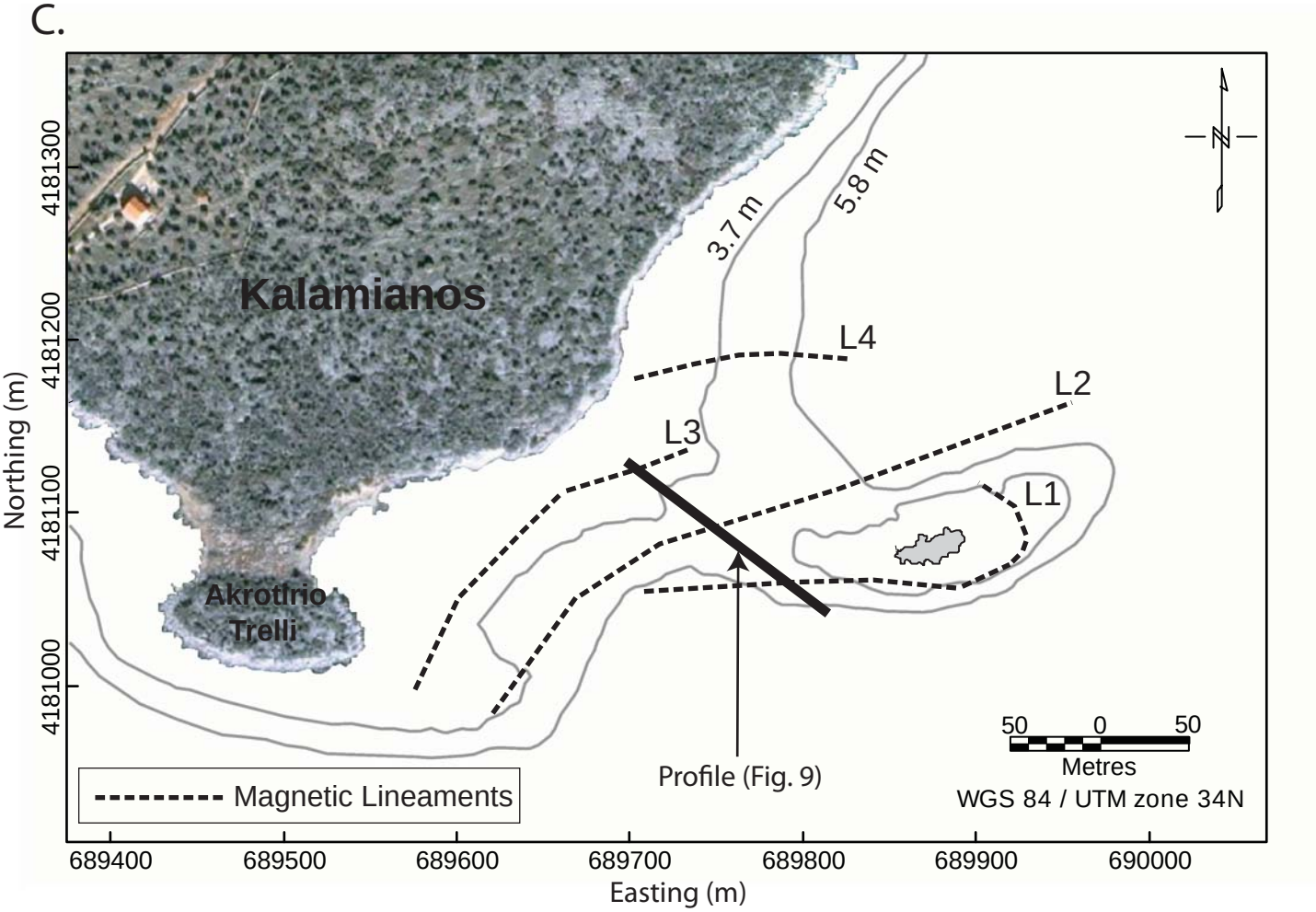


Figure 3.8C: Map showing interpreted magnetic lineaments.

D.

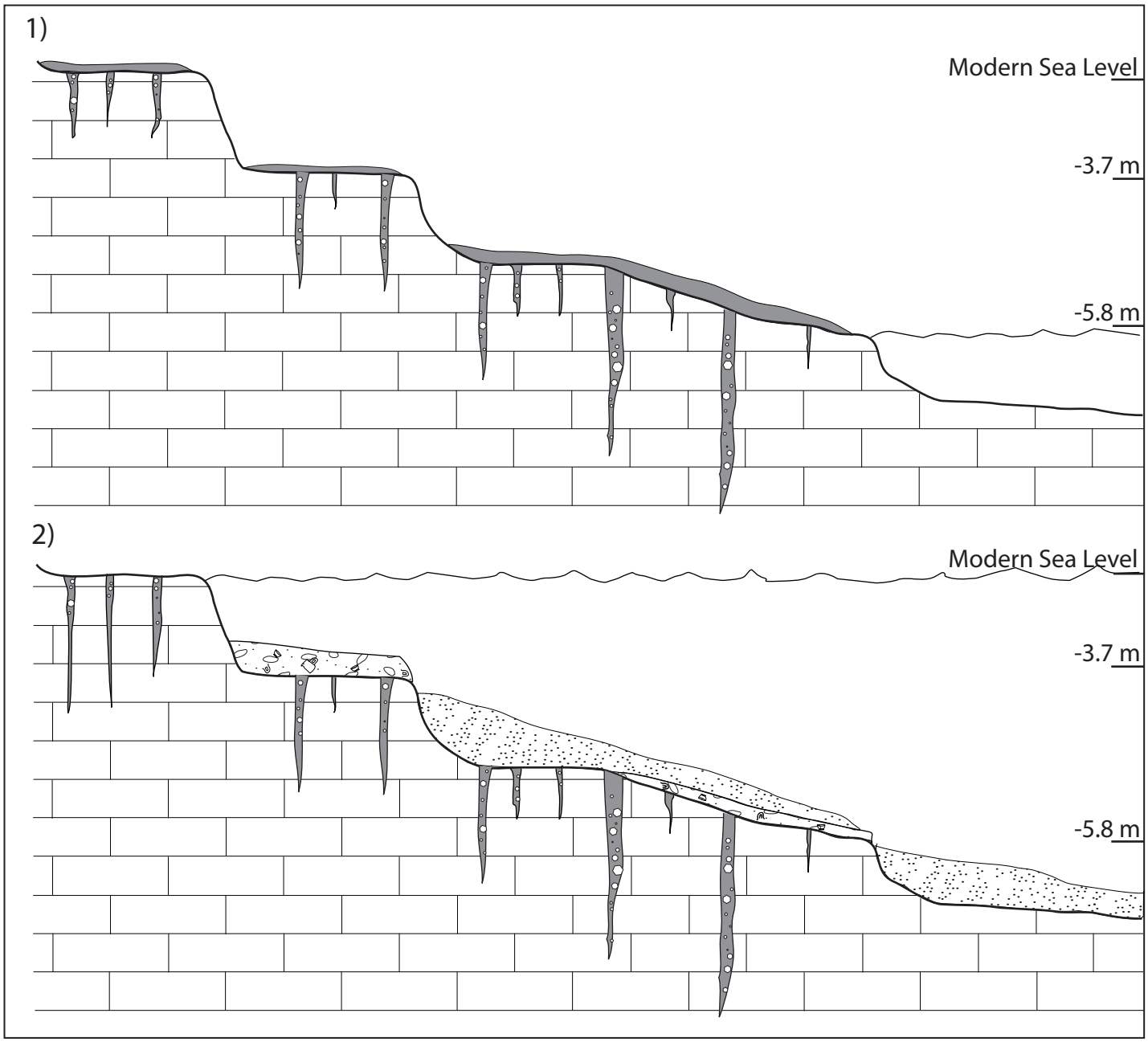


Figure 3.8D: 1) 1) Conceptual model for formation of beachrock and fracture system at Kalamianos. During phase of lowered sea level (-5.8 m) solutionally widened fractures (grikes) are sub-aerially exposed and infilled with high magnetic susceptibility terra rosa soil. 2) During subsequent shoreline transgression, infilled grikes are inundated and beachrock and marine sediments are deposited over submerged terrestrial surface. Infilled grikes have a much greater magnetic susceptibility than the surrounding bedrock and are responsible for observed west-east magnetic lineaments in Figure 3.8B.

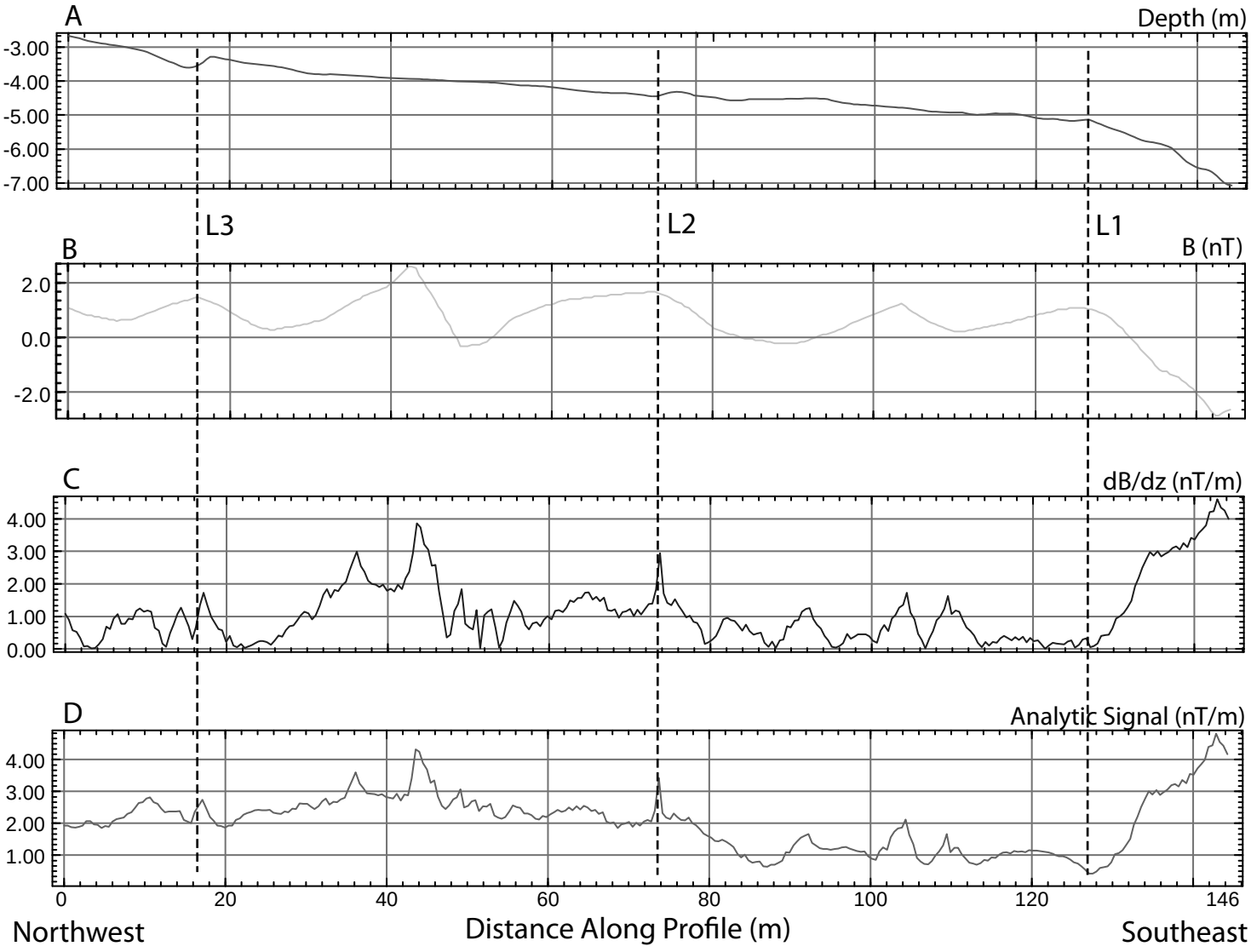


Figure 3.9: Bathymetry and magnetic profiles across inshore area (location on Fig. 3.8B). A) Water depth. B) Total magnetic intensity. C) Vertical gradient. D) Analytic signal. High-frequency magnetic anomalies in C and D are related to local concentrations of pottery and ballast materials.

based parallel was drawn from large fractures and grikes infilled with terra rosa observed along the coastline above modern mean sea level (Fig. 3.10). Observed from ca. 300-600 m southeast of Kalamianos, the increase in total magnetic intensity was speculated to be associated with a plume of terra rosa soil that had been eroded from adjacent slopes at Kalamianos and deposited as basin fill sediments (Fig. 3.5).

The extensive geologic background signal from near surface grikes, fractures and basin sediments are of greater amplitude (> 3 nT) relative to signal amplitudes (< 2 nT) generated by cultural material as demonstrated by a forward magnetic model (Fig. 3.11). Interference of cultural material signal by the geologic background in the total magnetic intensity map hinders observations. Reduction of the total field grid to residual magnetic field with an aggressive 1.5 m upward continued regional residual separation proved ineffective in removing the geologic background signal. However, this geologic background signal is not pronounced in the magnetic gradients and analytic signal.

The pattern of magnetic anomalies observed in the total field (Fig. 3.5A) and residual magnetic field (Fig. 3.8B) is complex and cannot be explained by pottery or beachrock alone. From the residual total magnetic field map (Fig. 3.8B) the shore-parallel linear magnetic anomalies have amplitude variations of 1-2 nT, far greater than could be achieved by the observed unit of pottery rich beachrock, ballast deposits or basin fill sediments as simulated in the magnetic model (Fig. 3.11). This feature appears restricted to the shallow basin southeast of Kalamianos and do not occur elsewhere within the study area. We believe that these magnetic lineaments are infilled paleokarstic landforms (dissolution widened fractures and grikes) associated with two generations of limestone joint sets observed in the Korphos-Kalamianos region (Fig. 3.10). During a lower phase of sea level or prior to co-seismic subsidence of the


Figure 3.10: A) Solutionally-widened fracture (grike) on shoreline at Kalamianos. B) Terra rosa soil and limestone breccia, formed by collapse in filling of fractures. C) Terra rosa soil with brecciated clast in 1 m wide grike.

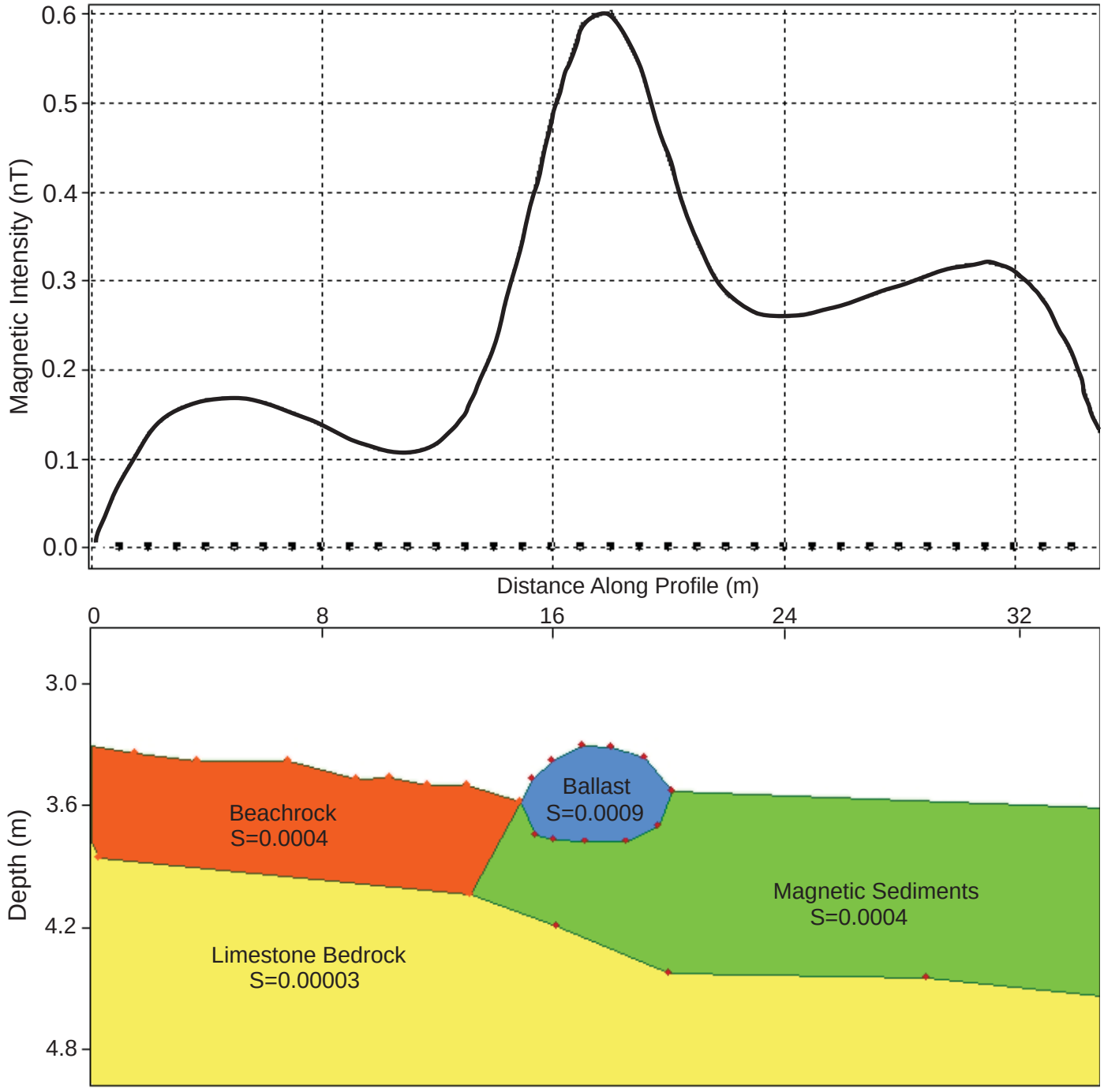


Figure 3.11: GM-SYS forward magnetic model showing hypothetical total field anomaly generated by various cultural materials (ballast, pottery rich beachrock).

shoreline, the shallow limestone bedrock platform southeast of Kalamianos would have outcropped well above water level and subject to karstic weathering with subsequent infilling of grikes with high magnetic susceptibility terra rosa soil (Fig. 3.8D). Shoreline transgression has since inundated these infilled grikes. Restricted occurrence appears related local coastal geomorphology. The majority of the inshore area along the Korphos-Kalamianos coast is narrow and steeply plunges into much greater depths which would have been akin to large cliffs when exposed during periods of lower RSL. It is not an ideal environment for extensive limestone dissolution and sediment deposition relative to the low relief topography at Kalamianos.

The bathymetric and magnetic variability over the inshore area southeast of Kalamianos is displayed in Figure 3.9 and a clear transition between BR-1 and BR-2 is visible through a decrease in mean magnetic intensity at ca. 80 m along profile. Three peaks observed along the profiles of the total field, vertical gradient and analytic signal are associated with the location of the magnetic lineaments observed in the residual magnetic map (Fig. 3.8C and Fig. 3.9). A simple magnetic model was generated to simulate the resultant anomalies due to ballast mounds, pottery rich beachrock and magnetic basin fill sediment to aid interpretation (Fig. 3.11). Magnetic susceptibility values used in the model approximate true susceptibilities measured from samples (Table 3.1) and unit thickness approximated from observed outcrop thickness (Fig. 3.12). It was observed that a 50 cm thick unit of pottery rich beachrock results in a relatively long wavelength anomaly with a 0.17 nT maximum amplitude. A 5 m long and 25 cm thick beachrock pile results in a shorter wavelength anomaly with a 0.6 nT amplitude. No samples of the basin sediment had been collected thus it was modelled using the same magnetic susceptibility as the beachrock, with the assumption of a similar composition (limestone and terra rosa sediment mixed with pottery), but with a greater vertical extent. The resultant anomaly

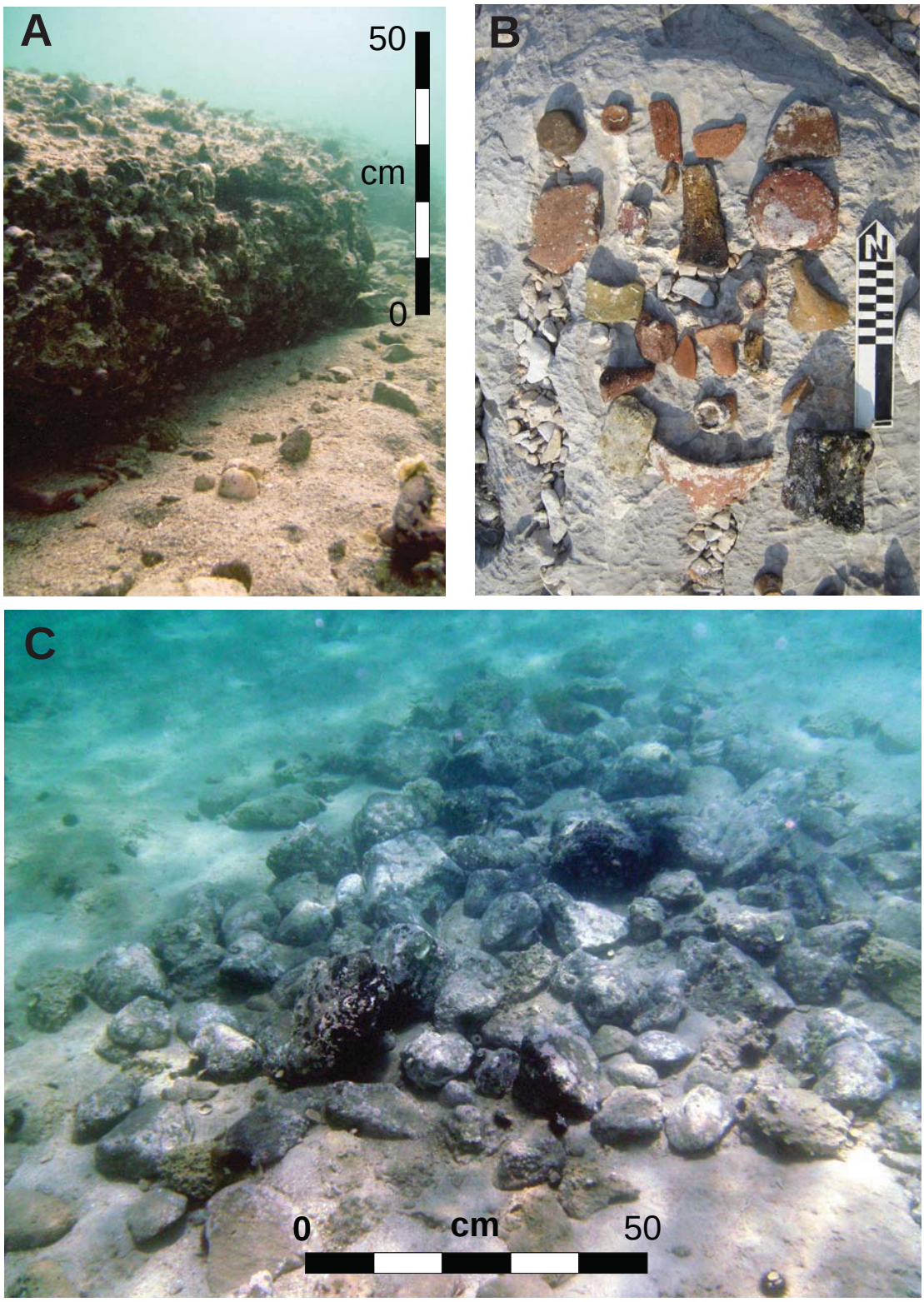


Figure 3.12: Underwater photographs showing A) Beachrock platform BR-1 at 3.7-4.5 m water depth. B) Mycenaean pottery sherds extracted from BR-1 beachrock samples. C) Small ballast deposit containing limestone and andesite cobbles.

from a 70 cm thick sedimentary deposit displayed an expected longer wavelength anomaly with amplitude of 0.3 nT. The modelled values suggest that the magnitude of the anomalies generated by the beachrock and sediment (0.1 nT and 0.25 nT respectively) are too small to account for the higher intensity/amplitude variations observed in the residual magnetic intensity, which indicate that the contribution of the beachrock to the overall magnetic variability over the inshore area was minimal and would be difficult discern from total field data alone. However, analytic signal processing of magnetic gradient data appear successful for suppressing the geologic background signal. Small dipoles and magnetic anomalies coinciding with beachrock platforms became visible and suggest that the observed signal has more significant contributions from cultural material rather than geologic material (Fig. 3.7 and 3.8A).

### 3.5.2. Archaeological Implications

A major difficulty faced by researchers exploring for Aegean Bronze Age harbours is the lack of "visibility" due to the modification of specific natural geomorphic landforms, exploited by Bronze Age civilizations for harbour placement, through tectonics (i.e. subsidence, uplift), eustatic sea level rise and erosion (Tartaron et al., 2003). With a lack of large constructed harbour structures (i.e. piers, breakwaters, seawalls), inundated or buried harbour basins are difficult to detect. Results from the magnetic gradient survey revealed no evidence for constructed harbour structures in the form of magnetic anomalies. Using magnetic gradient methods, small and shallowly buried magnetically susceptible cultural materials were detected and used as a proxy for evidence of human occupation and activity. This supported the idea that Bronze Age civilizations, including the Mycenaean, exploited natural geomorphic structures for coastal settlement and harbour placement, unlike succeeding civilizations (i.e. post Bronze Age

Greeks, Romans, modern) who constructed engineered harbours at strategic locations without limitation by geomorphology.

The DBM revealed two submerged isthmus with the eastern promontory connecting the mainland to a small island 200 m southeast of Kalamianos (Fig. 3.2). Well preserved EH pottery within beachrock at 5.8 m depth provides evidence which suggest that the paleoshoreline during the Early Helladic was approximately 5.8 m lower than the modern shoreline. During this period, a promontory could be seen to connect the island to the mainland to form a recurved spit. Akrotirio Trelli during this period extended further eastward to form the second promontory observed from the paleocoastlines reconstructed at Kalamianos. East and west of both promontories, shallow water depths form large natural sheltered embayments which are speculated to have functioned as natural harbours and anchorage areas for Kalamianos. The size of these basins were extensive with the central basin having covered ca. 10,000 square metres and the eastern basin having covered ca. 20,000 square metres. This is supported by the magnetic gradiometer results, which reveal anomalies concentrated around the island but also within the speculated eastern, central and eastern anchorage basins. Several mound like magnetic anomalies were observed further out into both the central and eastern basins and are speculated be ballast deposits from anchored ships (Fig. 3.8A).

During Mycenaean occupation, the mean sea level has risen to ~3.7-4.5 m below modern sea level, estimated using LH pottery rich beachrock unit BR-1 as a reference (Dao et al., 2011). From the DBM, the promontory would have been submerged in very shallow water (< 1 m) during this period but evidence of additional constructed harbour structures connecting to this island has not been discovered. The existence of a constructed pier is probable but there is no clear evidence for its former existence. The natural building material for structures in

Kalamianos, as observed from the ruins still remaining above sea level, are limestone blocks quarried from the abundant local limestone bedrock and are thus indistinguishable from the local geology visually or through magnetic methods. Wooden building materials have low preservation potential in exposed ruins and have left no evidence. Further submergence of the promontory post Mycenaean occupation due to tectonic induced subsidence would have exposed a constructed pier to significant erosion and bioencrustation which makes differentiation between structure and natural limestone bedrock improbable. The availability of two natural isthmus provided Kalamianos with natural breakwaters with sheltered basins to the east or west dependant on wind direction and a well sheltered central basin for all weather conditions.

Evidence of marine trade activity at Kalamianos could be observed from the presence of probable ballast deposits which consist partially of high magnetic susceptibility volcanic rocks (andesite) sourced from the volcanic islands of the Hellenic arc located in the Aegean Sea. Ballast material was discovered by diver reconnaissance to be widely distributed across the inshore area. Magnetic gradient results support this with magnetic anomalies concentrated over the central and eastern basins.

### 3.6. Summary

This study demonstrated the advantage in the utility of magnetic gradient methods in comparison to standard single sensor magnetic methods for mapping submerged features in a marine archaeological setting. The high quality analytic signal data acquired from a marine gradiometer system successfully improved discrimination against deep magnetic source bodies to simplify magnetic data processing and interpretation of near surface cultural material deposits. Results have provided insight into the construct and layout of the harbour at Kalamianos. High

magnetic susceptibility cultural material including pottery and volcanic ballast material are ideal targets for magnetic detection.

The magnetic gradient and DBM results revealed no evidence for a constructed harbour but instead characterized two submerged isthmuses that would have functioned as a natural breakwater, sheltering adjacent eastern or western shallow anchorage basins dependant on wind direction. Magnetic anomalies concentrate over the suggested central and eastern basins, adjacent to the isthmuses, which provided evidence for the presence of a significant concentration of buried cultural material. Marine activity at Kalamianos was thus concluded to have concentrated around the region adjacent to the isthmuses, the location of the ancient harbour. Further diver reconnaissance and excavations are required to groundtruth the geophysical results.

### 3.7. References

Armijo, R., Lyon-Caen, H., Papanastassiou, D., 1992. East-west extension and Holocene normal-fault scarps in the Hellenic arc. Geology 20(6), 491-494.

Basile, V., Carrozzo, M.T., Negri, S., Nuzzo, L., Quarta, T., Villani, A.V., 2000. A ground-penetrating radar survey for archaeological investigations in an urban area (Leece, Italy). Journal of Applied Geophysics 44(1), 15-32.

Boyce, J.I., Reinhardt, E.G., Raban, A., Pozza, M.R., 2004. Marine magnetic survey of a submerged Roman harbour, Caesarea Maritima, Israel. International Journal of Nautical Archaeology 33(1), 122-136.

Boyce, J.I., Krezoski, G.M., Reinhardt, E.G., Goodman, B.N., Artzy, M., 2006. Marine Geophysical Mapping of Bronze-Age Harbor Structures, Liman Tepe, Turkey. Geological Society of America Abstracts with Programs 38(7), 150.

Boyce, J.I., Reinhardt, E.G., Goodman, B.N., 2009. Magnetic detection of ship ballast deposits and anchorage sites in King Herod's Roman harbour, Caesarea Maritima, Israel. Journal of Archaeological Science 36(7), 1516-1526.

Clift, P.D., Alastair, H.F.R., 1990. Deep-water basins within the Mesozoic carbonate platform of Argolis, Greeece. Journal of the Geological Society 147, 825-836.

Collins, D., Dunn, R.K., 2008. Using Late Bronze Age Walls at Kalamianos, Greece, to Determine a Minimum Rate of Rillenkarren Formation. Geological Society of America Abstracts with Programs 40(2), 66.

Dao, P., Boyce, J.I., Koutsoumba, D., Pullen, D., Tartaron, T., Rothaus, R., 2011. Reconstruction of Late Bronze-Age Coastal Environments and Anchorage Sites at Kalamianos (Korphos, Greece). GAC-MAC Annual Meeting, Ottawa, Abstracts.

Franco, L., 1996. Ancient Mediterranean harbours: a heritage to preserve. Ocean & Coastal Management 30(2-3), 115-151.

Gibson TH. 1986. Magnetic prospection on prehistoric sites in western Canada. Geophysics 51, 553–560.

Jacobsen, B.H., 1987. A case for upward continuation as a standard separation filter for potential-field maps. Geophysics 52(8), 1138-1148).

Lambeck, K., and Purcell, A., 2005. Sea level change in the Mediterranean Sea since the LGM, model predictions for tectonically stable areas. Quaternary Science Reviews 24, 1969-1988.

Luyendyk, A.P.J., 1997. Processing of airborne magnetic data: Journal of Australian Geology & Geophysics 17(2), 31-38.

MacLeod, I.N., Jones, K., Dai, T.F., 1993. 3-D Analytic Signal in the Interpretation of Total Magnetic Field Data at Low Magnetic Latitudes: Exploration Geophysics 24, 679-688.

Marriner, N., Morhange C., 2007. Geoscience of ancient Mediterranean harbours. Earth-Science Reviews 80, 137-194.

Miller, G., Dunn., R.K., 2009. Brittle Fracture Analysis and Identification of Bronze Age Water Resources at Kalamianos, Eastern Peloponnese, Greece. Geological Society of America Abstracts with Programs 41(3), 96.

Minor, R., Grant, W.C., 1996. Earthquake-induced Subsidence and Burial of Late Holocene Archaeological Sites, Northern Oregon Coast. American Antiquity, 61(4), 772-781.

Minty, B.R.S., 1991. Simple Micro-Levelling for Aeromagnetic Data: Exploration Geophysics 22, 591-592.

Neubauer, W., Eder-Hinterleitner, A., Seren, S., Melichar, P., 2002. Georader in the Roman civil town Carnuntum, Austria: an approach for archaeological interpretation of GPR data. Archaeological Prospection 9(3), 135-156.

Nixon, F.C., Reinhardt, E.G., Rothaus, R., 2009. Foraminifera and tidal notches: Dating Neotectonic events at Korphos, Greece. Marine Geology 257, 41-53.

Noller, J.,Wells, L., Reinhardt, E.G., Rothaus, R., 1997. Subsidence of the Harbor at Kenchreai, Saronic Gulf, Greece, during the Earthquakes of a.d. 400 and a.d. 1928. Eos 78, 636

Nuzzo, L., Leucci, G., Negri, S., Carrozzo, M.T., Quarta, T., 2002. Application of 3D visualization techniques in the analysis of GPR data for archaeology. Annals of Geophysics 45(2), 321-337.

Paoletti, V., Secomandi, M., Piromallo., M., Giordano, F., Fedi, M., Rapolla, A., 2005. Magnetic Survey at the Submerged Archaeological Site of Baia, Naples, Southern Italy. Archaeological Prospection 12, 51-59

Papanikolaou, D., Lykousis, V., Chronis, G., Pavlakis, P., 1988. A comparative study of Neotectonic basins across the Hellenic arc: the Messiniakos, Argolikos, Saronikos and Southern Evoikos Gulfs. Basin Research 1(3), 167-176.

Pullen, D.J., Tartaron, T.F., N.D., *In Press*. Where's the Palace? The Absence of State Formation in the late Bronze Corinthia, Rethinking the Mycenaean Palaces, 2nd ed. Michael Galaty and William Parkinson. UCLA/Cotsen Institute of Archaeology, Los Angeles, pp. 146-158.

Reinhardt, E.G., Raban, A., 1999. Destruction of Herod the Great's harbor at Caesarea Maritima, Isreal – Geoarchaeological evidence. Geology 27(9), 811-814.

Roest, W.R., Verhoef, J., Pilkington, M., 1992. Magnetic interpretation using the 3-D analytic signal. Geophysics 57 (1), 116-125.

Stanley, D.J., Bernasconi, M.P., 2006. Holocene depositional patterns and evolution at Alexandria's Eastern Harbor, Egypt. Journal of Coastal Research 22, 283-297.

Tartaron, T.F., Rothaus, R.M., Pullen, D.J., 2003. Searching for Prehistoric Aegean Harbors with GIS, Geomorphology, and Archaeology. Athena Review 3(4), 27-36.

Tartaron, T.F., Gregory, T.E., Pullen, D.J., Noller, J.S., Rothaus, R.M., Rifle, J.L., Tzortzopoulou-Gregory, L., Schon, R., Caraher, W.R., Pettegrew, D.K., Nakassis, D., 2006. The Eastern Korinthia Archaeological Survey - Integrated Methods for a Dynamic Landscape. Hesperia 75, 453-523.

Tartaron T.F., Pullen, D.J., and Noller, J.S., 2006. Rillenkaren at Vayia: Geomorphology and a New Class of Earth Bronze Age Fortified Settlement in Southern Greece. Antiquity, 80: 145-160.

Tartaron, T.F., Pullen, D.J., Dunn, R.K., Dill., A. and Boyce, J.I., 2011. The Saronic Harbors Archaeological Research Project (SHARP): Investigations at Mycenaean Kalamianos, 2007-2009. Hesperia.

Young, C.T., Droege, D.R., 1986. Archaeological applications of resistivity and magnetic methods at Fort Wilkins State Park, Michigan. Geophysics 51(3), 568-575.

# CHAPTER 4: SUMMARY/CONCLUSIONS

The overall objective of this thesis was to reconstruct changes in the Bronze Age coastline at Kalamianos by integrating detailed bathymetric data with sea level indicators. The results were presented as two separate papers for publication (Chapters 2, 3). The research findings and their implications for understanding the archaeology and coastal evolution of Kalamianos are summarized in the following sections.

## 4.1. Research Findings and Archaeological Implications

Chapter 2 focused on paleogeographic reconstruction of the Bronze Age coastline to predict harbour basins and anchorage locations at Kalamianos. The Early Helladic and Late Helladic coastline configurations were reconstructed using detailed digital bathymetric data and radiocarbon dating of submerged beachrock ridges. It was revealed that up to 6 m of relative sea level rise, of which approximately 2 m was contributed by tectonic subsidence, has occurred since Early Helladic occupation of Kalamianos. From significant erosion observed at Kalamianos, it is likely that the reconstructed coastal configurations for the Early and Late Helladic shorelines are not as laterally extensive as was suggested by the Digital Bathymetry Model (DBM). Harbour infill sediments may have been extensive and buried portions of the paleoshoreline. Two submerged promontories were identified in the DBM with flanking shallow water basins. During the Early Helladic and Mycenaean occupation, the promontory would have been above sea level and connected with a small modern day island to form a narrow isthmus. Akrotirio Trelli located ca. 200 m west of the submerged promontory could also be classified as another natural promontory which extends from Kalamianos into the Saronic Gulf. Bronze Age

harbours depicted on ancient frescos at Akrotiri and known Bronze Age harbours at Aia Irini on Kea Island and at Vayia in eastern Korinthia all share a common configuration. The harbours were constructed using natural geomorphic features with a promontory situated between two adjacent natural harbours. The existence of two promontories at Kalamianos with shallow flanking basins conform to the general agreement on Bronze Age harbour configurations and suggests a high potential for the harbour location. The western harbour basin situated between Akrotirio Trelli and the submerged promontory would have been a well sheltered harbour regardless of wind direction from the north, east or west. The eastern harbour basin would have been a favourable harbour during periods with winds from the north and west.

The second paper (Chapter 3) applied the usage of high resolution magnetic gradient surveying to identify and delineate small (< 2 nT) near-surface magnetic targets associated with cultural material (pottery shards, volcanic ballast stones) at Kalamianos for locating potential anchorages and harbour basins. The analytic signal processing from magnetic gradient data successfully discriminated small near-surface targets and rejected long wavelength geologic background signal. Numerous magnetic anomalies, speculated to be associated with cultural material (volcanic ballast stones and pottery shards) in beachrock and harbour infill sediments, were identified southeast of Kalamianos in western and eastern basins adjacent to the submerged promontory. Shore-parallel high intensity magnetic lineaments were identified from residual magnetic intensity processing of total field data and are speculated to be associated with dissolution widened fractures (grikes) infilled with high magnetic susceptibility terra rosa soils. No constructed structural features were identifiable from the DBM or magnetic mapping. Results support the idea of a natural harbour at Kalamianos during Early Helladic and Late Helladic occupations as was suggested in Chapter 2.

Overall, this thesis succeeded in: 1) paleogeographical reconstruction of the positions of the Early Helladic and Late Helladic shorelines at Kalamianos, 2) identification of potential harbour and anchorage sites at Kalamianos, 3) demonstrated the potential of paleogeographic reconstruction in submerged ancient harbour archaeological exploration, and 4) demonstrated the potential of magnetic gradient imaging for submerged ancient harbour exploration.

### 4.2. Improvements to Geophysical Survey Methods

The geophysical techniques (digital bathymetry and magnetic gradients) applied are remote sensing methods and interpreted with limited geologic control (i.e. beachrock samples, underwater photographs of geomorphology and sediments). A systematic vibra-coring program or underwater grab sampling of harbour fill sediments located over magnetic anomalies is necessary to provide important geologic control for interpretation and ground-truthing of the conclusions proposed. Anomalous magnetic features, particularly the magnetic lineaments speculated to be infilled grikes, require proper ground-truthing to support its validity. Lithified subterranean structures (i.e. grikes) require detailed seismic reflection profiling to discern its structure. A detailed forward magnetic model of the harbour basin could be generated using the additional information suggest above. The magnetic model with appropriate geologic control would support the interpretations if the modeled results appear similar to observed values.

The resolutions of the geophysical maps are constrained by survey design and survey equipment. The survey parameters for this study were designed for mapping of beachrock and potential architecture larger than the line spacing. Cultural artefact mapping, often small targets (< 1 m), require much higher inline and cross-line survey density to produce high resolution magnetic maps (grid cell size ca. 1-2 m) to be able to accurately define targets of interests of

comparable size. In practice, the maximum grid cell size should not be less than one quarter line spacing due to issues of aliasing, distortion of the signal, which occur during interpolation of lower resolution data to a higher resolution and is therefore dependant on inline and cross-line spacing during data acquisition. The inline resolution could be improved through the usage of higher frequency (> 20 Hz) magnetometers or decreased vessel velocity during data acquisition. Cross-line resolution could be improved with tighter line separations (5-10 m spacing) for small target detection.

The nature of working in shallow marine environments present challenges in access and navigation which makes geophysical surveying at resolutions that could be achieved on land prohibitively difficult. Near-shore regions with very shallow (< 2 m) water depths impeded magnetic data acquisition and are poorly represented. The usage of relatively smaller remotely operated vehicles (ROV) could achieve much higher cross-line resolution (< 5 m) but the cost of the technology is currently prohibitively high.

The use of only two beachrock platforms, BR-1 and BR-2, as a sea level indicator at Kalamianos restricted constructed sea level histories to the Early Helladic and Late Helladic periods. Further studies using other proxies are required to reproduce then relative sea level curve since Mycenaean occupation and will provide further insight into the coastal evolution and inundation of Kalamianos.

### 4.3. Future Work

This thesis has provided important baseline information for understanding changes in the coastline at Kalamianos and for predicting the location of harbours and anchorage sites. These

data provide a basis for more focussed studies of the harbour basin sediments and their archaeological potential as outlined below.

### 4.3.1 Harbour Basin Sediments

Coring through basin sediments would yield a record of environmental change that has been recorded in the sedimentary/environmental facies and biofacies. This recorded sequence allow for generating a model on coastal change through a multi-proxy geoarchaeological analysis as described by Goodman et al. (2009). Because of the high abundance, high preservation potential and the unique niches of individual species, the analysis of skeletal remains of foraminifera collected from sediment cores would provide insight into the environmental evolution at Kalamianos harbour over time due to possible anthropogenic activity or sea level changes. The variations on species and abundances of marine to brackish water foraminifera assemblages could be directly correlated to changing coastal environmental conditions. The sedimentary/environmental facies of basin sediments (i.e. grain size, sorting, grading, cultural material distribution) would have recorded coastal environmental conditions and anthropogenic activity overtime. $C^{14}$ radiocarbon dating of foraminifera assemblages in respective environmental facies would aid in reconstructing coastal evolution since pre-Mycenaean occupation at Kalamianos.

### 4.3.2 Magnetic Mapping of Anchorages

Geologic background signal was significant relative to anomalies generated by cultural material and are speculated to be sourced from basin infill sediments consisting of a large proportion of high magnetic susceptibility terra rosa soil that have been eroded from adjacent

slopes. Significant soil erosion observed at Kalamianos supports the idea of large terra rosa sediment plumes deposited in the adjacent basins. The collection and analysis of terra rosa for magnetic susceptibility would provide important geologic control for the refinement of the hypothetical forward magnetic model of the inshore region.

### 4.3.2 Beachrock Origin

Beachrock from this study was observed to have significant potential for the preservation of archaeological material for regions inundated by sea level transgression. There exists good potential for beachrock elsewhere along the Aegean coastlines to contain preserved archaeological material associated with inundated archaeological sites. This study also used beachrock elevations as the main indicator for paleosea-level but the assumption of beachrock formation near sea level has been debated in recent literature (Knight, 2007). Further studies on beachrock origin and process of formation at Kalamianos along with paleoenvironmental reconstruction from sediment cores would reveal the suitability of using beachrock as a sea level indicator for paleocoastal reconstruction.

Geochemical properties of calcite cement in beachrock pores spaces are the key to revealing formational conditions. The $O^{18}/O^{16}$ isotopic ratios of calcite cements are good indicators for primary cementation environments due to discernable variations between marine and fresh water. Oxygen isotope analysis on calcite cements of beachrock samples would provide evidence of their depositional environment.

Detailed examination of sediment grains structure on thin-sections of beachrock BR-1 and BR-2 samples would reveal information on porosity and initial conditions of sediment

during lithification. In combination with $O^{18}/O^{16}$ isotopic ratios, it would reveal information on the conditions and rate of beachrock formation in the Aegean.